UNIVERSITÀ DEGLI STUDI DI PADOVA

SEDE AMMINISTRATIVA: UNIVERSITÀ DEGLI STUDI DI PADOVA
DIPARTIMENTO DI FARMACIA
DIPARTIMENTO DI BIOLOGIA

SCUOLA DI DOTTORATO DI RICERCA IN
BIOLOGIA E MEDICINA DELLA RIGENERAZIONE
INDIRIZZO: INGEGNERIA DEI TESSUTI E DEI TRAPIANTI
CICLO: XXI

STUDY OF ROLE OF Aβ PEPTIDES ON ANGIOGENESIS RELATED TO ALZHEIMER'S DISEASE

DIRETTORE DELLA SCUOLA: CH.MO PROF. PIERPAOLO PARNIGOTTO
SUPERVISORE: CH.MO PROF. MARCELLA FOLIN

DOTTORANDA: FIORAVANZO LARA

02 FEBBRAIO 2009

To all the people and animals of my life

Index

Sommario ..... **ix**

Summary ..... **xv**

Abbreviations ..... **xix**

1 Introduction **1**

1.1. Angiogenesis 2
1.1.1. Angiogenic phases 3
1.1.2. Cell types involved in angiogenesis 6
1.1.3. Pro-angiogenic factors 10
1.1.4. Endogenous inhibitors of angiogenesis 25
1.1.5. Methods for assessing angiogenesis 27
1.2. The Blood Brain Barrier 32
1.2.1. Anatomical composition of the BBB 35
1.2.2. BBB in neurologic disorders 40
1.3. The β-Amyloid peptide 42
1.3.1. Aβ formation 43
1.3.2. Aβ aggregation 45
1.3.3. Aβ effects 48
1.4. Angiogenesis and AD 54

2 Material and methods **57**

2.1. Cell cultures 57
2.1.1. Human Cerebral Endothelial Cells (HCECs) 57
2.1.2. Rat Cerebral Endothelial Cells (RCECs) 60
2.1.3. Rat Hippocampal Astrocytes (RHAs) 62
2.1.4. Cell culture mediums 63

2.2. Experimentation with $A\beta_{1-40}$ and $A\beta_{1-42}$ peptides 64
2.2.1. Preparation of peptides 64
2.2.2. Angiogenic activity *in vivo*. Chorio-Allantoic Membrane (CAM) assay 64
2.2.3. Angiogenic activity *ex-vivo*. Aortic-ring assay 65
2.2.4. Angiogenic activity *in vitro* on HCECs and RCECs 66
2.2.4.1. Proliferation 66
2.2.4.2. Migration 67
2.2.4.3. Morphogenesis on Matrigel 67
2.2.5. EC viability 68
2.3. Experimentation with $A\beta_{1-42}$ peptide on RCECs and RHAs 69
2.3.1. VEGF-A release in RCEC and RHA culture mediums 69
2.3.2. Expression of VEGF-A mRNA in RCECs and RHAs 70
2.3.3. RHA viability 74
2.4. Experimentation with treated RHA culture medium on RCECs 75
2.4.1. Preparation of samples 75
2.4.2. Proliferation 75
2.4.3. Migration 76
2.4.4. Morphogenesis on Matrigel 76
2.4.5. Determination of cytokines in culture mediums 77
2.4.6. RCEC Viability 79
2.5. Experimentation with $A\beta_{1-42}$ peptide in absence and in presence of $hVEGF_{165}$ on RCECs 80
2.5.1. Preparation of human Vascular Endothelial Growth Factor ($hVEGF_{165}$) 80
2.5.2. RCEC viability and proliferation with increasing concentration of $hVEGF_{165}$ 80
2.5.3. Aggregation kinetics 81
2.5.4. RCEC viability 81
2.5.5. Morphogenesis on Matrigel 81
2.6. Statistical analysis 82

3 Results 83

3.1. Characterization of cell cultures 83

3.1.1. Characterization of cerebral endothelial cells (CECs) 83
3.1.2. Characterization of rat hippocampus astrocytes (RHAs) 85
3.2. Experimentation with $A\beta_{1-40}$ and $A\beta_{1-42}$ peptides 86
3.2.1. Angiogenic activity *in vivo*. Chorio-Allantoic Membrane (CAM) assay . 86
3.2.2. Angiogenic activity *ex-vivo*. Aortic-ring assay 87
3.2.3. Angiogenic activity *in vitro* on HCECs and RCECs 88
3.2.3.1. Proliferation 88
3.2.3.2. Migration 89
3.2.3.3. Morphogenesis on Matrigel 90
3.2.4. Endothelial cells viability 93
3.3. Experimentation with $A\beta_{1-42}$ peptide on RCECs and RHAs 95
3.3.1. VEGF-A release in RCEC and RHA cell culture mediums 95
3.3.2. Expression of VEGF-A mRNA in RCECs and RHAs 95
3.3.3. RHA viability 99
3.4. Experimentation with treated RHA culture medium on RCECs 99
3.4.1. Proliferation 99
3.4.2. Migration 100
3.4.3. Morphogenesis on Matrigel 101
3.4.4. Determination of cytokines in culture mediums 103
3.4.5. Viability 105
3.5. Experimentation with $A\beta_{1-42}$ peptide in absence and in presence of $hVEGF_{165}$ on RCECs 106
3.5.1. RCEC viability and proliferation with increasing concentration of $hVEGF_{165}$ 106
3.5.2. Aggregation kinetics 107
3.5.3. RCEC viability 108
3.5.4. Morphogenesis on Matrigel 109

4 Discussion 113

References 121

Acknowledgements 133

Sommario

Uno dei principali impedimenti alla ricostruzione di tessuti ed organi nell'ingegneria tessutale è la mancanza di strategie che assicurino costante e stabile vascolarizzazione. L'acquisizione di nuove conoscenze sui meccanismi che intervengono nel processo angiogenico potrebbe permettere una efficace applicazione clinica nella ricostruzione di tessuti e organi da una parte e nella riduzione della eccessiva crescita vascolare in patologie angiogenesi-dipendente dall'altra.

L'angiogenesi è un processo complesso in cui numerosi cellule e mediatori cellulari interagiscono per stabilire uno microambiente specifico per la crescita di nuovi vasi sanguigni (Bouïs et al, 2006). Questo processo si verifica sia in condizioni fisiologiche (sviluppo embrionale, ciclo mestruale, gravidanza, guarigione di ferite) che patologiche (processi infiammatori, psoriasi, crescita di metastasi).

Durante il processo angiogenenico sono distinguibili diverse fasi:

- aumento della vasodilatazione e della vasopermeabilità (Milkiewicz et al., 2006)
- sintesi di enzimi proteolitici che degradano la matrice extracellulare
- aumento della proliferazione e della migrazione delle cellule endoteliali (D'Andrea et al., 2006)
- formazione e stabilizzazione del nuovo vaso con sintesi della membrana basale (Milkiewicz et al., 2006)

Negli ultimi tempi si sta affermando l'ipotesi che la demenza di Alzheimer (AD) non sia solamente una malattia neurodegenerativa caratterizzata da degenerazione neuronale e perdita delle connessioni sinaptiche ma anche una patologia vascolare. Numerose infatti sono le alterazioni riscontrabili a livello dei capillari cerebrali nei soggetti AD: vasocostrizione dei microvasi cerebrali, degenerazione delle cellule muscolari lisce vasali e alterazione della membrana basale. In particolare desta vasto interesse il possibile legame tra angiogenesi e AD derivante dall'osservazione di una aumentata densità vascolare in prossimità delle placche senili nei pazienti AD rispetto a soggetti anziani non dementi (Vagnucci and Li, 2003). Le placche senili, depositi extracellulari e vascolari di materiale proteico costituite in prevalenza dal peptide β-amiloide (Aβ), assieme ai grovigli neurofibrillari (NFT), costituiti dalla forma iperfosforilata della proteina τ, rappresentano le principali alterazioni neuro-patologiche riscontrabili nel cervello di soggetti AD (Robertson et al., 2003).

Numerosi studi *in vivo*, *ex-vivo* e *in vitro* riportano risultati contraddittori sulla capacità del peptide Aβ di stimolare il processo angiogenico (Paris et al., 2004; Cantara et al.,

2004). Scopo di questo lavoro di ricerca è il tentativo di comprendere alcuni meccanismi che favoriscono questo processo.

Inizialmente è stato valutato l'effetto di due isoforme del peptide Aβ, $A\beta_{1-40}$ e $A\beta_{1-42}$, *in vivo* ed *ex-vivo* rispettivamente su membrana corion-allantoidea di pollo (CAM) e su anello aortico di ratto e *in vitro* su cellule endoteliali cerebrali umane (HCEC) e di ratto (RCEC). Entrambi i peptidi Aβ manifestano effetto pro-angiogenico *in vivo* ed *ex-vivo* mentre *in vitro*, alla concentrazione 10^{-7}M, risultano essere pro-angiogenici su HCEC e anti-angiogenici su RCEC. Dati di letteratura riportano diverso effetto indotto dal peptide Aβ in relazione al modello cellulare utilizzato e in particolare l'effetto sembra dipendere dall'organo di provenienza delle cellule (Paris et al., 2004; Cantara et al., 2004). I risultati ottenuti negli studi da noi effettuati confermano che l'effetto del peptide Aβ è dipendente dal modello animale utilizzato dal distretto corporeo di provenienza delle cellule. Non essendo stato osservato diverso effetto delle due isoforme del peptide, per gli studi successivi è stato utilizzato solamente l'isoforma 1-42 del peptide Aβ alla concentrazione 10^{-7}M.

È stato valutato se il peptide $A\beta_{1-42}$ svolgesse il ruolo anti-angiogenico sulle RCEC influendo sulla via di rilascio e di espressione di una delle più potenti citochine pro-angiogeniche, il VEGF-A. Mediante un saggio immunoenzimatico (Quantikine® Rat VEGF Immunoassay, R&D Systems) è stato possibile osservare che dopo 3, 24 o 48 ore di trattamento con $A\beta_{1-42}$ il rilascio di VEGF-A nel terreno di coltura da parte delle RCEC risultava dell'ordine di quello delle cellule non trattate. Analogamente mediante Real Time RT-PCR non è stata evidenziata nessuna interferenza del peptide Aβ sulla via di trascrizione di mRNA per VEGF nelle RCEC.

Studi *in vivo* di letteratura riportano aumentata angiogenesi e aumento della sintesi e del rilascio di VEGF da parte degli astrociti dopo 7 giorni dall'iniezione di Aβ in ippocampo di ratto (Zand et al, 2005). Sono stati quindi valutati rilascio di VEGF-A ed espressione di mRNA per VEGF-A da parte degli astrociti di ippocampo di ratto (RHA) in coltura dopo trattamento per 3, 24 o 48 ore. Diversamente da quanto osservato *in vivo*, *in vitro* il Aβ non sembra influenzare l'espressione di VEGF-A da parte degli RHA.

Per cercare di spiegare il diverso effetto di Aβ *in vivo* ed *in vitro* si è ipotizzato che Aβ agisca come fattore pro-angiogenico indiretto inducendo il rilascio di fattori

angiogenici per le RCEC, diversi dal VEGF-A. Pertanto le RCEC sono state coltivate per 24 e 48 ore utilizzando terreno di coltura in cui erano stati precedentemente mantenuti gli RHA rispettivamente di controllo e trattati con Aβ per 24 e 48 ore. Successivamente le RCEC sono state sottoposte ai saggi di angiogenesi *in vitro*: proliferazione, migrazione, morfogenesi su Matrigel. I principali risultati evidenziano un aumento significativo della formazione di strutture capillaro-simili da parte delle RCEC coltivate su terreno di RHA sia di controllo sia trattati con Aβ per tutti i tempi considerati suggerendo che gli RHA rilascino alcune citochine pro-angiogeniche e che tale rilascio non sia influenzato da Aβ. Nel tentativo di identificare tali fattori, sono stati determinati mediante tecnica Multiplex i livelli di IL-1β, IL-6 e TNF-α nel terreno di coltura di RHA di controllo e trattati con Aβ prima e dopo la permanenza con le RCEC. Queste citochine possono essere prodotte sia da cellule endoteliali che da astrociti. Ad entrambi i tempi di incubazione si osserva aumento di IL-6 nei terreni di coltura rimasti a contatto con entrambi i tipi cellulari sebbene il terreno degli RHA trattati e messo a contatto con le RCEC presenti aumento minore rispetto al terreno degli RHA di controllo. Poiché IL-6 è stimolata da IL-1β sono stati valutati i livelli di IL-1β, IL-6 e TNF-α nei terreni di coltura dopo 6 e 12 ore. Sono stati riscontrati aumenti di tutte e tre le citochine considerate. In particolare è stato osservato che i livelli di TNF-α nel terreno degli RHAs trattati con $A\beta_{1-42}$ risultano maggiori rispetto al controllo mentre risultano diminuire negli altri terreni. È stato osservato che TNF-α aumenta l'espressione e il rilascio di fattori pro-angiogenici supportando l'importanza di TNF-α e il sistema Ang-1/Ang-2 e la loro regolazione autocrina nella neovascolarizzazione (Hangai et al., 2006). Inoltre la vitalità delle RCECs aumenta a 12 ore di trattamento con entrambi i terreni di coltura e diminuisce alle 48 ore. In letteratura è riportato che elevati livelli di citochine pro-infiammatorie inducono apoptosi, aumento dello stress ossidativo e sotto-regolazione di eNOS (Kofler et al., 2005). Probabilmente la sovra-regolazione di citochine pro-infiammatorie causa alterazione della vitalità cellulare. Altri studi sono però necessari al fine di chiarire quali meccanismi intervengano in tale processo.

In letteratura è riportato che $A\beta_{1-42}$ si co-localizza con VEGF a livello delle placche senili (Yang et al., 2004) e che l'isoforma 165 di VEGF umano ($hVEGF_{165}$) ma non la 121 è in grado di legare con elevata affinità il Aβ nella regione 26-35 preve-

nendone l'aggregazione e diminuendone l'effetto citotossico in cellule di feocromocitoma di ratto (Yang et al., 2005). È stato pertanto valutata la cinetica di aggregazione del peptide incubato in assenza e in presenza di $hVEGF_{165}$ nel tempo (0, 24, 96 e 168 ore) mediante saggio di Tioflavina T. Dai risultati si osserva che la presenza di $hVEGF_{165}$ sfavorisce la formazione di strutture β-sheet da parte del $A\beta_{1-42}$ e di conseguenza la capacità di aggregazione del peptide. Successivamente è stato valutato l'effetto del peptide appena solubilizzato e incubato per 24 ore a 37°C in assenza e in presenza di $hVEGF_{165}$ sulla vitalità delle RCEC. Era stata in precedenza valutata la concentrazione di $hVEGF_{165}$ che non indice variazione della vitalità e della proliferazione cellulare rispetto alla condizione basale. In accordo con i risultati di Yang e collaboratori (2004), il trattamento con $A\beta_{1-42}$ incubato per 24 ore in presenza di $hVEGF_{165}$ aumenta la vitalità delle RCEC rispetto al controllo, al trattamento con il peptide appena solubilizzato e al trattamento con $A\beta_{1-42}$ incubato in assenza di $hVEGF_{165}$. Pertanto l'inibizione della tossicità del Aβ potrebbe essere dovuta ad una riduzione della formazione di aggregati tossici ad opera del legame tra VEGF e Aβ. Inoltre il sequestramento del $A\beta_{1-42}$ da parte del $hVEGF_{165}$ inibisce anche l'effetto anti-angiogenico del peptide probabilmente in conseguenza della recuperata vitalità cellulare.

In conclusione è possibile affermare che il peptide Aβ è pro-angiogenico *in vivo*, *ex-vivo* e *in vitro* su cellule endoteliali cerebrali umane e anti-angiogenico su cellule endoteliali cerebrali di ratto, probabilmente come conseguenza dell'effetto citotossico effettuato dal peptide su queste ultime. Inoltre il $A\beta_{1-42}$ non interferisce sulla via di espressione e rilascio di VEGF da parte di cellule endoteliali cerebrali e di astrociti di ippocampo di ratto in coltura. Gli astrociti secernono sostanze che inducono angiogenesi e rilascio di IL-6 da parte delle cellule endoteliali cerebrali di ratto in coltura indipendentemente dal trattamento con $A\beta_{1-42}$. Infine la presenza di $hVEGF_{165}$ inibisce l'effetto tossico e anti-angiogenico del peptide probabilmente in seguito al sequestramento del $A\beta_{1-42}$ ad opera del legame $A\beta_{1-42}$-$hVEGF_{165}$.

Altri studi sono necessari al fine di comprendere i meccanismi di angiogenesi correlata con la AD sebbene sembri evidente che essa possa derivare dall'interazione di diversi tipi cellulari in risposta all'effetto del peptide Aβ su di esse. Sembra tutta-

via che l'alterazione dell'endotelio capillare e la conseguente ipossia contribuiscano all'attivazione di tale processo.

Summary

One of the main difficulties for the success of tissue and organ transplantation is the deficiency of techniques that ensure regular and stable vascularisation. The knowledge of mechanisms involved in the formation of new vessels could allow application of clinic strategies to facilitate tissue and organ transplantation on the one hand and the reduction of excessive vascular growth in many pathologies on the other.

Angiogenesis is a complex process, where several cell types and mediators interact to establish a specific microenvironment suitable for the formation of new vessels (Bouïs et al, 2006). It occurs in both physiological (embryo development, menstrual cycle, pregnancy, wound healing) and pathological conditions (inflammation, psoriasis, metastasis growth). Angiogenesis can be split up into different steps:

- increase of vasodilatation and vasopermeability (Milkiewicz et al., 2006)
- synthesis of proteolytic enzymes that degrade extracellular matrix
- increase of proliferation and migration of endothelial cells (D'Andrea et al., 2006)
- formation and stabilization of the new vessel and basal membrane synthesis (Milkiewicz et al., 2006)

In the last years an increasing amount of evidence suggests that Alzheimer's disease (AD) is not only a neurodegenerative disease characterized by neuronal degeneration and loss of synaptic connections but it is also a vascular pathology. In fact cerebral microvessel vasoconstriction, degeneration of vessel smooth muscle cells and alteration of the basal membrane have been observed in cerebral capillary AD brains. In particular the possible connection between angiogenesis and AD starts from the observations of increased vascular density close to senile plaques in AD patients in comparison to older non-demented people (Vagnucci and Li, 2003). Senile plaques (extracellular and vascular deposits of proteinaceous material where the major component is β-amyloid peptide, Aβ) together with neuro fibrillary tangles (NFT) (composed of iperphophorylated form of τ protein) represent the main neuropathological alterations founded in AD brains (Robertson et al., 2003).

A large amount of *in vivo*, *ex-vivo* and *in vitro* experiments show contradictory data on Aβ peptide angiogenic capability (Paris et al., 2004; Cantara et al., 2004). The aim of the present research is the attempt to understand some of the mechanisms that favour angiogenesis.

Firstly the effect of both Aβ isoforms, $A\beta_{1-40}$ and $A\beta_{1-42}$, have been evaluated in both *in vivo* and *ex-vivo* experiments on chicken Chorio-Allantoic Membrane (CAM) and rat aortic ring assays respectively and *in vitro* on Human Cerebral Endothelial Cells (HCECs) and Rat Cerebral Endothelial Cell (RCECs). Both Aβ peptides show a pro-angiogenic effect *in vivo*, *ex-vivo* and *in vitro* on HCECs while anti-angiogenic effect on RCECs. A large amount of data demonstrates that Aβ peptide effect is connected to the cellular model utilized and the effect seems to be linked to where the organ cells come from (Paris et al., 2004; Cantara et al., 2004). Our results corroborate those obtained in literature where the effect of Aβ peptides depends on the animal model used and on where body zone cells come from. No differences have been observed between the two Aβ isoforms and for the subsequent experiments only $A\beta_{1-42}$ concentration 10^{-7}M has been utilized.

It was then assessed whether the anti-angiogenic role of $A\beta_{1-42}$ on RCECs could be related to the alteration of the release and expression of one of the most powerful pro-angiogenic cytokines, VEGF-A. The quantitative determination of rat VEGF-A concentration in cell culture mediums has been evaluated using an immunoassay (Quantikine® Rat VEGF Immunoassay, R&D Systems). VEGF-A release in cell culture mediums after 3, 24 or 48 hours of treatment with $A\beta_{1-42}$ do not vary in comparison to non-treated cells. By Real Time RT-PCR no differences on RCEC mRNA transcription were observed with the same experimental conditions.

In vivo studies demonstrate angiogenesis and increased synthesis and release of VEGF from astrocytes 7 days after the injection of $A\beta_{1-42}$ in rat hippocampus (Zand et al., 2005). Starting from these data the effect on release of VEGF-A and expression of VEGF-A mRNA on 3, 24 or 48 hours $A\beta_{1-42}$ treated rat hippocampal astrocytes (RHAs) have been evaluated. Diversely to *in vivo* results, *in vitro* Aβ peptide does not affect expression and release of VEGF-A on RHAs.

In order to understand the different *in vivo* and *in vitro* effect of Aβ and assuming that Aβ could act as indirect pro-angiogenic factor inducing release of angiogenic factors different from VEGF, 24 and 48 hours control and Aβ treated RHA culture mediums have been tested for 24 and 48 hours on RCECs. Subsequently angiogenic assays have been performed on RCECs: proliferation, migration and capillary-like structures formation on Matrigel. The main results demonstrate increased formation of capillary-like structures on RCECs grown in both control and Aβ treated RHA mediums after all the times considered. Results suggest that RHAs release pro-angiogenic cytokines independently of Aβ treatment. In order to determine which factors cause that effect, levels of IL-1β, IL-6 and TNF-α on RHA culture mediums before and after the stay with RCECs have been determined by Multiplex technique.

Those cytokines are produced by both ECs and astrocytes. Cell culture mediums left on both cell types contain increased levels of IL-6 in comparison to RHA culture mediums although Aβ treated RHA mediums left on RCECs contain lower levels in comparison to control RHA mediums. IL-6 is stimulated by IL-1β thus levels of IL-1β, IL-6 and TNF-α on cell culture mediums after 6 and 12 hours were evaluated. Levels of all the cytokines increase in comparison to control. In particular levels of TNF-α increase on $A\beta_{1\text{-}42}$ treated RHA mediums in comparison to control while they decrease on other mediums. TNF-α increases expression and release of other pro-angiogenic factors supporting the importance of TNF-α and Ang-1/Ang-2 and their autocrine regulatory loops in neovascularisation (Hangai et al., 2006).

Moreover RCEC viability increases after 12 hours and decreases after 48 hours of treatment with both cell cultures. Literature data reports that high concentrations of pro-inflammatory cytokines increase apoptosis, oxidative stress and down-regulate eNOS bioactivity (Kofler et al., 2005). Other studies are necessary to clarify what mechanisms take part in this process.

$A\beta_{1\text{-}42}$ co-localize with VEGF in senile plaques (Yang et al., 2004) and the 165 isoform of human VEGF ($hVEGF_{165}$) but not the 121, it binds with high affinity Aβ peptide in the region 26-35 preventing aggregation and decreasing cytotoxic effect on rat pheochromocytoma cell cultures (Yang et al., 2005). Starting from these data firstly the aggregation kinetic of $A\beta_{1\text{-}42}$ in absence or presence of $hVEGF_{165}$ was performed following Thioflavin T (ThT) fluorescence at 0, 24, 96 and 168 hours: the presence of $hVEGF_{165}$ disfavours the formation of β-sheet structures in Aβ within 24 hours and thus the possibility to form aggregates. Subsequently the effect on RCEC viability of freshly solubilised $A\beta_{1\text{-}42}$ and 24h aged $A\beta_{1\text{-}42}$ in absence or in presence of $hVEGF_{165}$ had been observed. Previously the concentration of $hVEGF_{165}$ that did not vary cellular viability and proliferation in comparison to basal condition. In agreement with Yang and co-workers' results the presence of $hVEGF_{165}$ incubated with $A\beta_{1\text{-}42}$ decreases the cytotoxicity of 24 hours aged $A\beta_{1\text{-}42}$ incubated without the cytokine. Cytotoxic inhibition of Aβ could be the result of decreased formation of toxic aggregates through the binding of $hVEGF_{165}$. Moreover the binding inhibits anti-angiogenic effect of $A\beta_{1\text{-}42}$ probably as consequence of the reduced cytotoxic effect.

In summary Aβ peptides are pro-angiogenic *in vivo*, *ex-vivo* and *in vitro* on human cerebral endothelial cells while they are anti-angiogenic on rat cerebral endothelial cells, probably as consequence of their cytotoxic effect on these cells. Moreover $A\beta_{1\text{-}42}$ peptide does not affect the release of VEGF-A and the expression of mRNA of VEGF-A on rat cerebral endothelial cells and rat hippocampal astrocytes cultures. Astrocytes release factors that induce angiogenesis and release of IL-6 on

rat cerebral endothelial cells independently of the presence of $A\beta_{1\text{-}42}$ peptide. Finally the presence of $hVEGF_{165}$ inhibits toxic and anti-angiogenic effects of the peptide probably taking away $A\beta_{1\text{-}42}$ through the binding $A\beta$-$hVEGF_{165}$.

Other experiments are necessary to understand mechanisms connected to AD although it seems that the result could depend on numerous different cell types in response of Aβ effects. Nevertheless capillary alteration and the hypoxia seem to contribute to the process.

Abbreviations

Aβ	β-Amyloid
AD	Alzheimer's Disease
ADDLs	Aβ-Derived Diffusible Ligands
aFGF (FGF-1)	acidic Fibroblast Growth Factor
AJ	Adherens Junctions
Ang	Angiopoietin
APLP	APP-Like Protein
APP	Amyloid precursor protein
BBB	Blood-Brain Barrier
bFGF (FGF-2)	basic Fibroblast Growth Factor
BLB	Blood Labyrinth Barrier
BM	Basement Membrane
BME	Basal Medium Eagle
BNB	Blood-Neural Barrier
BNB	Blood. Nerve Factor
BRB	Blood Retinal Barrier
BrdU	BromodeoxyUridine
BSA	Bovine Serum Albumin
BSCB	Blood-Spinal Cord Barrier
CAM	Corio-Allantoic Membrane
CEC	Cerebral Endothelial Cell
CNS	Central Nervous System
COX-2	CycloOXygenase-1
CSF	CerebroSpinal Fluid
DAPI	DiAmidino-2-Phenyl-Indole
ECM	ExtraCellular Matrix
EC	Endothelial Cell
EGF	Epidermal Growth Factor
EGFR	Epidermal Growth Factor Receptor
eNOS	endothelial Nitric Oxide
EPCs	Endothelial Progenitor Cells
FBS	Foetal Bovine Serum
GFAP	Glial Fibrillary Acidic Protein
HBD	Heparin Binding Domain
HCEC	Human Cerebral Endothelial Cell
HGF	Hapatocyte Growth Factor
HSPG	Heparin Sulphate ProteoGlycans
HUVECs	Human Umbelical Vein Endothelial Cells
$hVEGF_{165}$	human Vascular Endothelial Growth Factor 165
ICAM-1	InterCellular Adhesion Molecule-1
IFN	Interferon
IL	Interleukin
iNOS	inducible Nitric Oxide

JAM	Junctional Adhesion Molecules
MHC	Major Histocompatibility Complex
MMPs	MatrixMetallo Proteases
MTT	3-(4,5-dimethylthiazol-2-yl)-2,5-diphenyltetrazoliumbromide
MV	Endothelial Cell Growth Medium
MV2	Endothelial Cell Growth Medium
NFTs	NeuroFibrillary Tangles
NO	Nitric Oxide
PAI-1	Plasminogen Activator Inhibitor
PBS	Phosphate Buffer Solution
PDGF	Platelet-Derived Growth Factor
PI3K	Phosphatidyl-Inositol 3 Kinase
PlGF	Platelet Growth Factor
PS	Presenilin
RAGE	Receptor for Advanced Glycation End Products
RCEC	Ret Cerebral Endothelial Cell
RHA	Rat Hippocampal Astrocyte
ROS	Reactive Oxide Species
SP	Senile Plaques
TGF-α	Transforming Growth Factor-α
TGF-β	Transforming Growth Factor-β
ThT	Tioflavin T
TJ	Tight Junction
TNFR	Tumor Necrosis Factor Receptor
TNF-α	Tumor Necrosis Factor-α
VCAM-1	Vascular Cell Adhesion Molecule-1
VE-cadherins	Vascular Endothelial-cadherins
VEGF	Vascular Endothelial Growth Factor
VEGFR	Vascular Endothelial Growth Factor Receptor
vWf	von Willebrand factor
ZO	Zonula Occludens protein

1 Introduction

Regenerative medicine holds significant promise to provide an alternative or complementary treatment for the millions of people affected annually by tissue and organ loss from accident, birth defects and diseases. Tissue engineering, the combination of cells within biomaterials, is primarily concerned with the *ex-vivo* creation of long-lasting, viable tissues and cells in large yield (Nolan et al, 2008). It applies the principles of engineering and life sciences toward the development of biological substitutes that restore, maintain or improve tissue function or a whole organ. In the last few years the success is limited to avascular or thin tissues with slow metabolism which rely on either diffusion or quick angiogenesis due to an inflammatory wound-healing response. Engineering more complex tissues necessitate growing a vasculature that promotes cell survival, tissue organization and rapid vascularisation following implantation (Rivron et al., 2008). Recent studies have investigated the use of scaffolds that must mimic or recapitulate the natural cell-to-cell and cell-to-matrix interactions that can be critical in maintaining cellular phenotype and viability (Nolan et al., 2008).

Tissues need newly formed blood vessels or capillaries to pass through them for the delivery of nutrients and oxygen. After implantation, blood vessels from the host will invade the implant but it takes days to develop the new vasculature network in the graft. During this reconstructive period, the cells far from the host capillaries experience nutrient limitations, which can result in cell death. When the graft has been vascularised the cells that survived can proliferate and expand again.

Another limiting factor in the survival of an implant is oxygen. In particular hypoxia plays a central role in angiogenesis as it stimulates the production of angiogenic/vasculogenic factors, like Vascular Endothelial Growth Factor (VEGF) (Rivron et al., 2008). Hung e co-workers (2007) demonstrated that a short-time hypoxia (1%CO_2) treatment on human multipotent stromal cells enhanced their engraftment *in vivo* suggesting that short-term exposure to hypoxia before transplantation might be a simple way to improve transplant survival. The vascularisation of *in vitro*-generated implants should follow a hierarchical network and include consequently a vessel allowing microsurgical connection to the host vasculature linked to smaller branches

mimicking arterioles or venules and leading to a capillary tree embedded in the tissue. Two strategies are developed to grow capillaries in an implant: by promoting invasion of vessels from host or by forming *de novo* a vascular network in the construct before implantation (Rivron et al., 2008).

The field of tissue engineering and biomaterials is advancing as the consequence of the highly dynamic nature of tissue engineered substitutes. The close collaboration between cell and molecular biologists, material science and biochemical engineers and clinicians accelerate further development in tissue engineering (Nolan et al., 2008).

1.1. Angiogenesis

The blood and the lymphatic vascular system penetrate every organ and tissue to supply cells with nutrients and oxygen, providing for the circulation of fluids and various signalling molecules. The formation of new vessels is a process divided in two different manners: **vasculogenesis** and **angiogenesi**s.

Vasculogenesis, the development of the blood vascular system, is one of the first events in embryogenesis. During early embryonic development, mesodermal cells differentiate into hemangioblasts, progenitors of both hematopoietic and Endothelial Cells (ECs) giving rise to blood vessels. During differentiation, hemangioblasts produce angioblasts and their aggregation results in the formation of blood islands. The fusion of blood islands results in the appearance of the primary blood vascular plexus consisting of fine capillaries formed by ECs. At this stage capillaries acquire an arterial or venous character. The stage of vasculogenesis is completed together with the formation of the primary vascular plexus and all further transformations of the vascular net proceed during angiogenesis (Karamysheva, 2008).

Angiogenesis is the outgrowth of new vessels from pre-existing vasculature. It is an essential process during embryogenesis, wound healing and the ovarian cycle but it also plays a major role in several pathologic processes such as tumor vascularisation, diabetic retinopathy, psoriasis and rheumatoid arthritis (Bouïs et al., 2006). In adults, formation and growth of new vessels are under strict control. These processes are activated only under strictly defined conditions like wound healing. Strict regula-

tion of this system and balanced functioning is very important for the organism because both excessive formation of blood vessels and their insufficient development lead to serious diseases (Karamysheva, 2008). The process of capillary growth has been studied by scientists since 1939 when Clark and Clark (1953) observed the process in real time using intravital microscopy of the microvascular network within rabbit ear chamber. In the early 1970s Gimbrone and colleagues (1973) first achieved the establishment of long-term EC cultures. Subsequently the development of in vitro models of capillary network formation contributed to the understanding the angiogenic process (Folkman and Haudenschild, 1980).

1.1.1. Angiogenic phases

Stimuli known to initiate angiogenesis include hypoxia, inflammation and mechanical factors such as stress and stretch. These stimuli either directly or indirectly activate ECs by initiating the autocrine or paracrine production and release of growth factors or cytokines. Angiogenic sprouting of blood vessels occurs in a series of events, which can roughly be divided into a destabilisation phase, a proliferation and migration phase and a maturation phase (Fig. 1.1). All these steps offer potential points for pro- or anti-angiogenic clinical intervention (Milkiewicz et al., 2006).

Destabilization

Endothelial permeability is regulated by adherens junction, which are formed primarily through extracellular homophilic interaction between Vascular Endothelial (VE)-cadherins, with intracellular stabilization to the actin cytoskeleton via interactions with β-catenin and α-catenin. An increase in permeability may be triggered by tyrosine phosphorylation of components of the junctional complex, which causes dissociation of the complex and the loosening of cell-cell contacts (Milkiewicz et al., 2006).

Angiogenic stimulus activates ECs that attract and bind leukocytes and blood platelets and the consequent release of a multitude of pro- and anti-angiogenic factors. ECs lose their contacts with each other, the Basement Membrane (BM) and their supporting cells, pericytes and smooth muscle cells. The consequence is increased vascular permeability and deposition of fibrin into the extra-vascular space, vessel wall disassembly and BM degradation (Bouïs et al., 2006). ECs express integrins, in particular $\alpha_v\beta_3$, thus facilitating the EC adhesion to the Extra Cellular Matrix (ECM)

components and their migration. Moreover, ECs secrete and activate proteolytic factors, such as Matrix MetalloProteases (MMPs), which degrade the ECM facilitating the migration of ECs (D'Andrea et al., 2006).

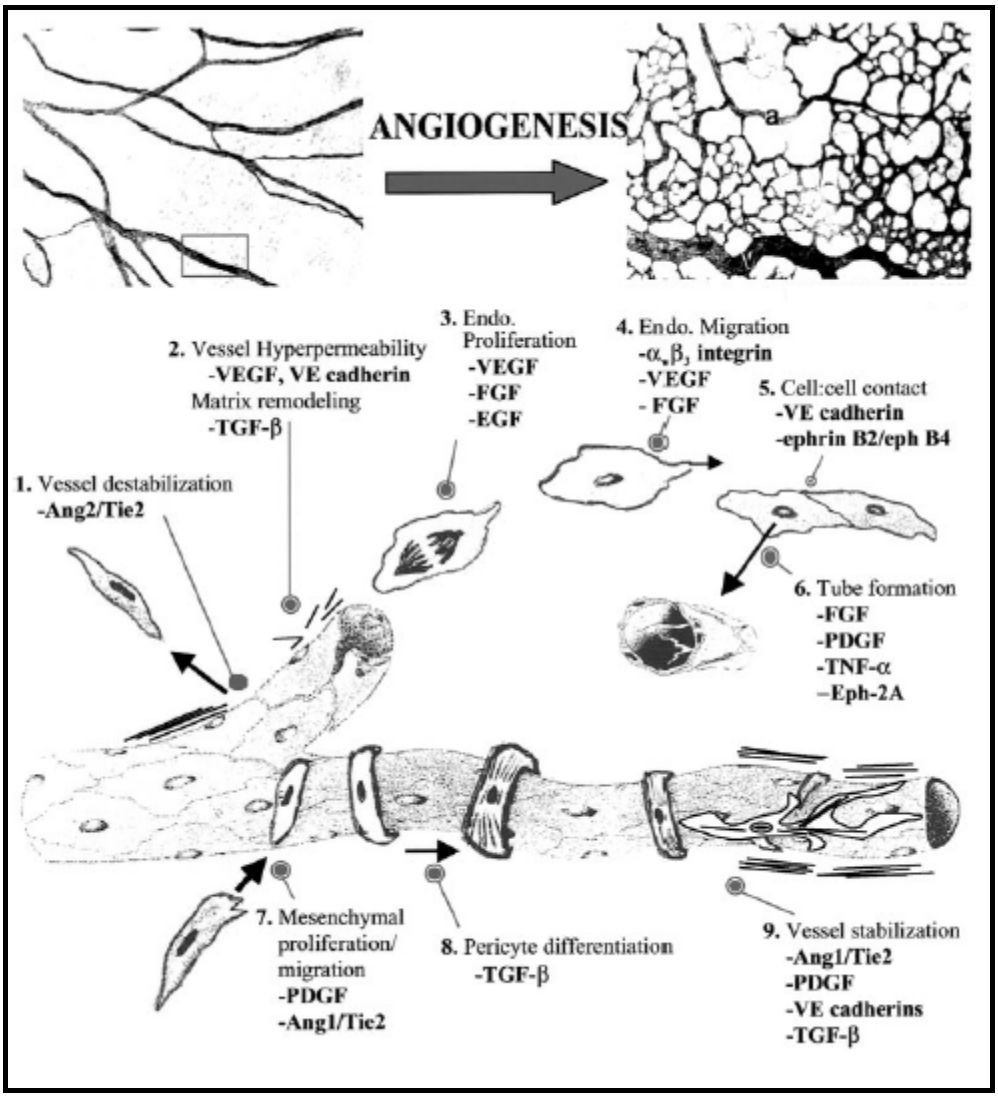

Fig. 1.1: mechanisms of physiological angiogenesis. Normal angiogenesis depends on the coordination of several independent processes. Removal of pericytes from the endothelium and destabilization of the vessels (1) by Angiopoieitn-2 (Ang-2) shift endothelial cells from a stable, growth-arrested state to a plastic, proliferative phenotype. VEGF-induced hyperpermeability (2) allows for local extravasation of proteases and matrix components from the bloodstream. Endothelial cells proliferate (3) and migrate (4) through the remodelled matrix (5), and then they form tubes through which blood can flow (6). Mesenchymal cells proliferate and migrate along the new vessel (7) and differentiate into mature pericytes (8). Establishment of EC quiescence, strengthening of cell-cell contacts and elaboration of the new matrix stabilize the new vessels (9). TGF-β, Transforming Growth Factor-β; EGF, Epidermal Growth Factor; PDGF, Plate-Derived Growth Factor; TNF-α, Tumor Necrosis Factor-α; a, arteriole; v, venule (Papetti and Herman, 2002).

Proliferation and migration

During angiogenesis the increase in proliferation is one of the many events that is required for the formation of a new capillary blood vessels. Vascular EC proliferation is associated with the degradation of the BM, which leads to sprouting of pre-existing microvessels (Kalluri, 2003). Proteolysis of BM matricellular components is necessary to promote EC invasion into the surrounding interstitial matrix (Milkiewicz et al., 2006). The activated EC migrate on and into the fibrin scaffold and invade the underlying ECM towards the angiogenic stimulus (Bouïs et al., 2006). Cellular attachments to matrix molecules and the intracellular modulation of cytoskeletal components both determine the migratory proprieties of ECs. Integrins play a prominent role in cell-matrix adhesion. It has been observed that the expression of integrins $\alpha_v\beta_3$ and $\alpha_v\beta_5$ is increased in proliferating ECs. Moreover the actin cytoskeleton is regulated dynamically by Rho family activity. Both RhoA and Rac1 GTPases are active in the early stages of endothelial cell network formation and these enzymes contribute significantly to the success of network formation and cell alignment. RhoA plays a major role in stress fiber formation and cell contraction/reaction whereas Rac1 is localized to the leading edge of migrating cells and regulates actin polymerization and sprout protrusion (Milkiewicz et al., 2006).

Lumen formation and stabilization

Capillary sprouts may form a lumen by intracellular canalization, which occurs through fusion of cytoplasmatic vesicles or by alternative process of intercellular canalization, in which a lumen is created by the membrane apposition of two different cells. Stabilization on the nascent capillaries is a significant step in completion of the angiogenic process. This in part is accomplished through the production of factors that promote a differentiated and stable capillary morphology (Milkiewicz et al., 2006).

Once a new vessel has been formed, EC proliferation and migration are inhibited and a new BM is secreted. The junctional complexes between the ECs as well as with the BM mature and peri-endothelial cells are recruited and differentiate (Bouïs et al., 2006). To obtain a functional vascular network, the newly formed vessel must be remodelled to form a mature vessel. The release of Platelet-Derived Growth Factor (PDGF) is fundamental for this maturation as it stimulates the recruitment of peri-

cytes and smooth muscle cells which stabilize the morphology of the vessel and prevent the regression of ECs (D'Andrea et al., 2006).

Angiogenesis takes place when quiescent ECs switch to an activated form. This change is regulated by a balance between positive and negative regulators, rather than by a single factor alone. The balance in favour of pro-angiogenic factors (increasing production of pro-angiogenic factors or decreasing secretion of anti-angiogenic factors) brings about the activation of the angiogenic process (Mandriota and Pepper, 1997).

1.1.2. Cell types involved in angiogenesis

Many cell types are involved in angiogenesis:

- ECs;
- Endothelial Progenitor Cells (EPCs);
- Pericytes and smooth muscle cells;
- Inflammatory cells.

ECs

ECs are the most quiescent and genetically stable cells of the body. Their turnover time is usually hundreds of days in contrast to bone-marrow cells which maintain an average turnover time of 5 days. ECs are bound to capillary BM which is composed of type IV collagen, laminin, heparin-sulphate proteoglycans, perlecans, nidogen/entactin, SPARC/BM-40/osteopontin, type XV collagen, type XVIII collagen and other molecules. This indicates that the primary signals originating from capillary BM inhibit proliferation and promote an environment that facilitates appropriate cell-cell adhesion (Kalluri, 2003).

During angiogenesis to prevent the disintegration of the vascular network under angiogenic stimulus and the blood supply to tissue in this region, just some ECs inside the capillary initiate angiogenesis. These cells are called "tip-cells" and occupy the leading position while new vessels grow: they react to the VEGF-A gradient that specifies the direction of their migration and which induces the capillary to grow towards the gradient (Karamysheva, 2008) sprouting phyllopodii towards the VEGF-A gradient (Gerhardt et al., 2003). This effect is caused by the interaction of VEGF-A with the VEGF receptor (VEGFR2), the concentration of which is high in tip-cells. Once tip-

cells are selected to move forward, formation of new capillaries should begin because of the proliferation and migration of other ECs (Karamysheva, 2008).

EPCs

The first EPCs were described as CD34-enriched mononuclear cells that acquired endothelial surface marker expression in culture (Asahara et al., 1997). Subsequent studies showed that a subpopulation of circulating $CD34^+$ cells expressing $CD34^+$ $CD133^+$ $VEGFR2^+$ could form endothelial colonies *in vitro* (Peichev et al., 2000; Gill et al., 2001). Other studies have shown that $CD11b^+$ or $CD14^+$ mononuclear cells give rise to endothelial cell-like colonies both *in vitro* and *in vivo*. Thus it appears that endothelial-like cells can arise from within bone marrow-derived haematopoietic progenitor cell populations or monocyte populations (Garmy-Susini and Varner, 2005).

EPCs cultivated from different sources showed a marked expression of growth factors such as VEGF and Hepatocyte Growth Factor (HGF). The release of growth factors in turn may influence the classical process of angiogenesis, the proliferation and migration as well as survival of the mature cell (Fig. 1.2). The capacity of EPCs to physically contribute to vessel-like structures may contribute to their potent capacity to improve neovascularisation (Urbich and Dimmeler, 2004).

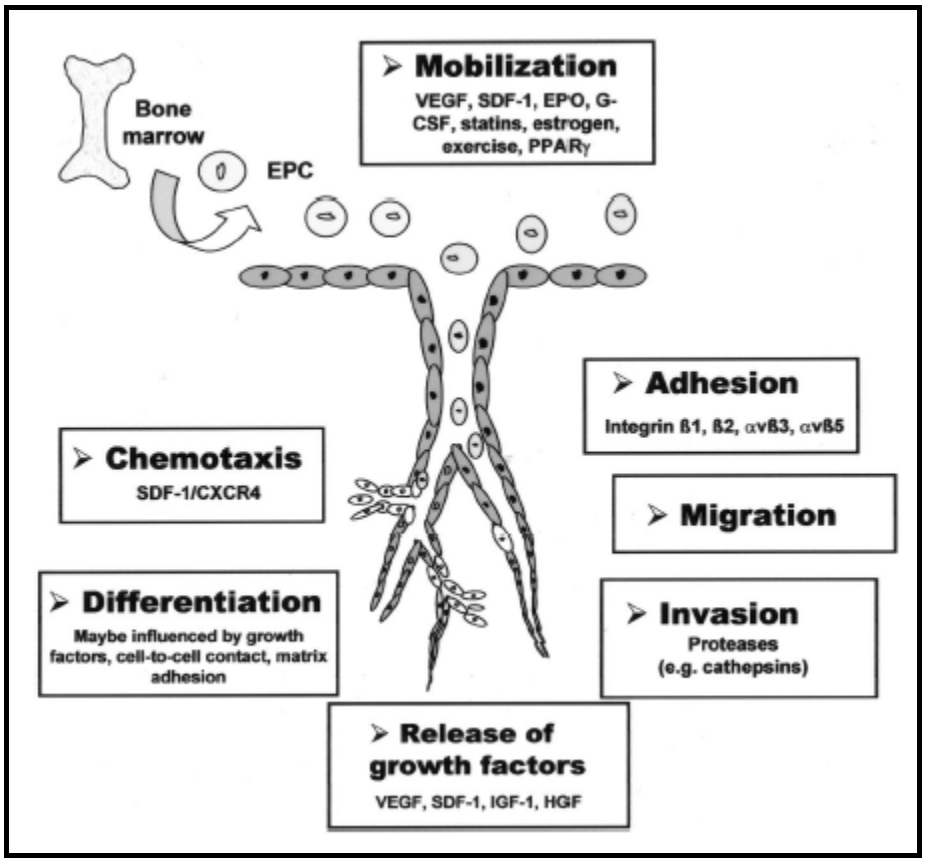

Fig. 1.2: mechanism of EPCs homing and differentiation. Recruitment and incorporation of EPCs into ischemic tissue requires a coordinated multistep process including mobilization, chemoattraction, adhesion, transmigration, migration, tissue invasion and in situ differentiation **(Urbich and Dimmeler, 2004)**

Pericytes and smooth muscle cells

The maturation of primordial vascular tubes is accompanied by the emergence of peri-endothelial cells that participate in matrix formation and that eventually become pericytes (cells locate in the same BM as the ECs) or vascular smooth muscle cells (cells locate outside the vascular BM and equipped with specific actin-myosin contractile filaments). Recently the transmembrane molecule endoglin has been identified as an essential regulator of pericytes and vascular smooth muscle cells differentiation that modulate the interaction of Transforming Growth Factor β (TGFβ) superfamily members and their receptors and even is expressed in vascular smooth muscle cells (Kurz, 2000).

Inflammatory cells

Most components of the immune system are involved in angiogenic processes (Fig. 1.3). A disruption of the microenvironment homeostasis leads to activation of

resident cells as mast cells, resident macrophages and dendritic cells (Albini and Sporn, 2007). In particular macrophages are known to produce a series of angiogenic factors including VEGF. Exposure of macrophages to hypoxia enhances expression of molecules related to angiogenesis, as MMP9, MMP12, Tumor Necrosis Factor-α (TNF-α) and Interleukin-10 (IL-10). In addition to being a source of VEGF macrophages are also influenced by this angiogenic factor, modulating their biological activity in response to VEGFR1 ligands.

In the last few years it has become apparent that neutrophils, like macrophages, are sensitive to the microenvironmental clues and adjust their behaviour in response to the local and distant signals (Noonan et al., 2008). They have been shown to play an important role in physiological and pathological angiogenesis (Heryanto et al., 2004). Neutrophil dependent angiogenesis *in vivo* has been shown to require VEGF-A release by neutrophils upon recruitment and stimulation. In response to stimulation they degranulate and release proteases, activate phagocytosis and oxidate burst generation before dying. In addition to VEGF-A neutrophils have been shown to make a wide range of angiogenesis molecules and an equally wide range of anti-tumor and anti-angiogenic molecules (Benelli et al., 2003). The key appears to lie within the response of these cells to the signal from the microenvironment (Noonan et al., 2008).

The high levels of VEGF may recruit leukocytes and natural killer cells. ECs exposed to VEGF up-regulate InterCellular Adhesion Molecule-1 (ICAM-1) expression which play a key role for CD18 mediated neutrophil adhesion and recruitment. VEGF also induce Vascular Cell Adhesion Molcecule-1 (VCAM-1) expression on ECs which together with ICAM-1 recruit activated natural killer cells. Natural killer cells are known as negative regulators of angiogenesis but they can also induce angiogenesis by secretion of pro-angiogenic cytokines like VEGF, Platelet Growth Factor (PlGF) and Interleukin-8 (IL-8) (Hanna et al., 2006).

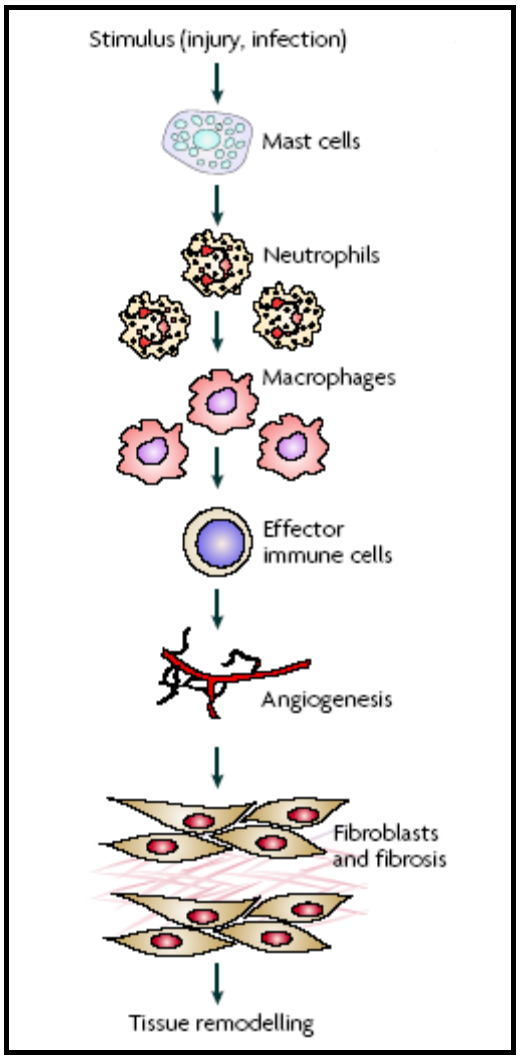

Fig. 1.3: the sequence of events in acute inflammation and tissue repair. The process of inflammation initiates a series of catabolic and anabolic processes that occur in a defined order. Firstly the activation of resident cells (mast cells, resident macrophages and dendritic cells) and rapid entry of granulocytes in response to injury. Further recruitment of macrophages and infiltration of effector immune cells (lymphocytes) to enable ECs and fibroblast to form new blood vessels and a collagenous matrix. The last step is tissue remodelling (Albini and Sporn, 2007)•

1.1.3. Pro-angiogenic factors

Pro-angiogenic factors can be divided into two categories:

- **direct factors**, when they stimulate EC proliferation or migration directly
- **indirect factors**, when EC proliferation and/or migration which is observed *in vitro* must have been induced by some other factors or cells, perhaps indirectly mobilized by the original angiogenic molecule (Folkman and Shing, 1992)

Numerous molecules perform critical functions within the complex angiogenic cascade. Production and activation of these growth factors, EC growth factor receptors and intracellular signalling mediators and transcription factors trigger the phases that comprise the abluminal sprouting form of angiogenesis (Milkiewicz et al., 2006). Some of the soluble growth factors, membrane-bound molecules and mechanical forces that mediate angiogenic process are summarized in Table 1.1.

Factors	**Biological actions**
Soluble mediators	
VEGF	increases EC permeability stimulates EC uPA/PAI-1 production stimulate EC proliferation inhibits EC apoptosis enhances EC migration stimulation *in vivo* angiogenesis
Ang-1	stimulates *in vitro* EC sprout formation increases girth and stability of endothelium
Ang-2	antagonizes Ang1 signalling/destabilizes endothelium
aFGF bFGF	stimulates EC proliferation enhances EC migration stimulates EC PA/collagenase production stimulates EC tube formation stimulates *in vivo* angiogenesis
PDGF	stimulates DNA synthesis in ECs stimulates ECs to form chord *in vitro* stimulates proliferation of smooth muscle cells and pericytes induces vWF, VEGF and VEGFR2 expression in cardiac ECs increases capillary wall stability
TGF-β	supports anchorage-independent growth of fibroblast inhibits proliferation and migration of ECs stimulates/inhibits formation of EC tubes *in vitro* produces net antiproteolytic activity via modulation of uPA/PAI-1 expression levels inhibits production of other proteases/stimulates production of protease inhibitors stimulates VSMA production by pericytes chemotactic for monocytes and fibroblasts stimulates *in vivo* angiogenesis in presence of inflammatory response increases vessel wall stability
TNF-α	stimulates angiogenesis *in vivo* stimulates formation of EC tubes *in vitro* inhibits EC proliferation
EGF, TGF-α	stimulate EC proliferation stimulate angiogenesis *in vivo*
G-CSF, GM-CSF	stimulate EC proliferation and migration
Angiogenin	stimulates angiogenesis *in vivo* supports EC binding and spreading
Angiotropin	stimulates random capillary EC migration stimulates EC tube formation stimulates *in vivo* angiogenesis
Tissue factor	contributes to development of yolk sac vasculature
Factor V	contributes to development of yolk sac vasculature
Prostaglandin	stimulates *in vivo* angiogenesis

Nicotinamide	stimulates *in vivo* angiogenesis
Monobutyrin	stimulates *in vivo* angiogenesis stimulates EC migration *in vitro*
Membrane bound-proteins	
$\alpha_v\beta_3$-integrin	highly expressed on activated ECs mediated EC attachment, spreading and migration present on angiogenic capillary spouts required for bFGF-stimulated angiogenesis *in vivo* localizes MMP-2 to capillary sprouts suppresses EC apoptosis
$\alpha_v\beta_5$-integrin	required for VEGF-stimulated angiogenesis *in vivo*
$\alpha_5\beta_1$-integrin	required for non-VEGF growth factor-stimulated angiogenesis *in vivo*
VE-cadherin	may mediate permeability of endothelium required for *in vivo* angiogenesis prevents EC apoptosis
Eph-4B/Ephrin-B2	colocalize at venous/arterial interfaces of developing embryo required for angiogenesis of head and yolk sac and for myocardial trabeculation
Ephrin-A1	required for *in vivo* angiogenesis induced by TNF-α chemotactic for ECs in vitro
Eph-2A	required for EC tube formation *in vitro*
Biochemical forces	
Blood flow/shear stress	Increases endothelial stress fiber formation (if laminar) promotes EC division (if turbulent) stimulates transcription of bFGF and TGF-β genes

Table 1.1: factors that regulate normal angiogenesis. VEGF; uPA, urokinase Plasminogen Activator; PAI-1, Plasminogen Activator Inhibitor-1; Ang-1, Angiopoietin-1; Ang-2, Angiopoietin-2; vWf, von Willebrand factor; aFGF, Fibroblast Growth Factor a; bFGF, Fibroblast Growth Factor b; PDGF, Platelet Derived Growth Factor; VEGFR2, Vascular Endothelial Growth Factor Receptor type 2; TGF-β, Transforming Growth Factor β; VSMA, Vascular Smooth Muscle Actin; TNF-α, Tumor Necrosis Factor-α; EGF, Epidermal Growth Factor; TGF-α, Transforming Growth Factor-α; G-CSF, Granulocyte-Colony Stimulating Factor; GM-CSF, Granulocyte/Macrophage-Colony Stimulating Factor (Papetti and Herman, 2002).

VEGF family

The VEGF family and its receptors have been known for long to play a central and specific role in angiogenesis as they mediate vascular permeability, EC proliferation, migration and survival (Bouïs et al., 2006). VEGF was originally described as a homodimeric 34-42kDa protein that increased vascular permeability in the skin. It was identified by a partial purification from the ascites fluid and cell culture supernatants of a guinea-pig hepatocarcinoma cell line and termed Vascular Permeability Factor (VPF). In 1989 Ferrara and Henzel identified a growth factor for ECs in conditioned medium from bovine follicular pituitary cells and called it VEGF. This was subsequently sequenced and found to be identical to VPF (Leung et al., 1989; Keck et al., 1989).

The VEGF gene family consists of **VEGF-A**, **VEGF-B**, **VEGF-C**, **VEGF-D**, **VEGF-E** and **PlGF**. These glycoproteins belong to a structural superfamily of

growth factors which includes PDGF. VEGF-A is mainly involved in angiogenesis while VEGF-C and VEGF-D are involved in lymphangiogenesis (Byrne et al., 2005).

Growth factors of VEGF family exert their biological effect via interaction with receptors located on EC membranes. Three receptors have been identified: Flt-1 (VEGFR1), KDR/Flk-1 (VEGFR2) and Flt-4 (VEGFR3) (Papetti and Herman, 2002). The VEGF receptors are transmembrane proteins with a single transmembrane domain (Fig. 1.4). The extracellular region of VEGF receptors is formed by seven immunoglobulin-like domains (IG I-VII), whereas the intracellular part exhibits tyrosine kinase activity and the tyrosine kinase domain in these receptors is separated into two fragments (TK-1 and TK-2) by an inter-kinase insert. All VEGF receptors are highly homologous (Karamysheva, 2008).

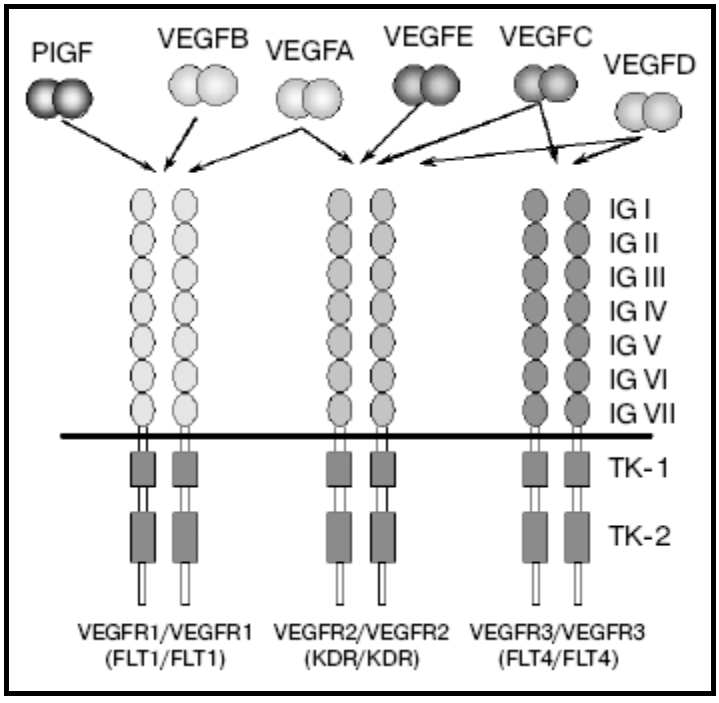

Fig. 1.4: interaction of growth factors to the VEGF family with their own VEGFR receptors (Karamysheva, 2008).

VEGF-A is a secreted glycoprotein that assembles into a disulphide-linked homodimer. There are at least eight known human isoforms that are the result of alternative RNA splicing and termed $VEGF_{121}$, $VEGF_{145}$, $VEGF_{162}$, $VEGF_{165}$, $VEGF_{165B}$, $VEGF_{183}$, $VEGF_{189}$ and $VEGF_{206}$ according to their length in amino acid (Fig. 1.5) (Bouïs et al., 2006). $VEGF_{121}$ and $VEGF_{165}$ are secreted into the extracellular environment whereas $VEGF_{189}$, $VEGF_{206}$ and to some extend $VEGF_{165}$ remain cell- or

matrix-associated via their affinity for heparin sulfates. Functional VEGF receptors were originally characterized as EC specific but they have recently been found on other normal cell types including vascular smooth muscle cells and monocytes/macrophages (Papetti and Herman, 2002). $VEGF_{121}$ is soluble whereas the larger isoforms bind to the cell surface or to the ECM through heparin- or proteoglycane-binding domains (Bouïs et al., 2006). $VEGF_{165}$ is the most abundant and potently mitogenic of the numerous splice isoforms of VEGF-A and binds to VEGFR1, VEGFR2 (Milkiewicz et al., 2006), Neuropilin-1 (NRP-1) and Neuropilin-2 (NRP-2) (Bouïs et al., 2006).

In rats there are five main splice variants of VEGF-A denoted $VEGF_{120}$, $VEGF_{144}$, $VEGF_{164}$, $VEGF_{188}$, $VEGF_{205}$ (corresponding to the number of amino acids) and the 120 and 164 isoforms are the most prevalent (Mac Gabhann et al., 2006). $VEGF_{120}$ is a homodimeric glycoprotein (36kDa) missing the exon-7 encoded domain. Because of this domain only $VEGF_{164}$ can bind to the Heparin Sulphate Proteoglycans (HSPG) present in high concentration in the ECM and BM spaces and the two splice variants are responsible for different signalling in both physiological and cancer angiogenesis (Mac Gabhann et al., 2006).

VEGF-A transcription is stimulated by hypoxia as a result of Hypoxia Inducible Factor (HIF-1) binding to a Hypoxia Response Element (HRE) within the VEGF-A promoter. VEGF-A production also is increased by inflammatory mediators (IL-1α and IL-1β, TGF-β, prostaglandin E2) or activation of CycloOXygenase-2 (COX-2) as well as by mechanical forces of shear stress and cell stretch. VEGF promotes EC survival through activation of the Phosphatidyl-Inositol 3 Kinase (PI3K)/Akt pathway and through association with $\alpha_v\beta_3$ integrin and activation of focal adhesion kinase (Milkiewicz et al., 2006). It may increase EC permeability by enhancing the activity of vescicular-vacuolar organelles, clustered vesicles in EC lining small vessels that facilitate transport of metabolites between luminal and abluminal plasma membranes. Alternatively VEGF may enhance permeability by loosening adherens junctions between ECs in a monolayer via rearrangement of cadherin/catenin complexes. Increased vascular permeability may allow for the extravasation of plasma proteins and formation of ECM favourable to ECs and stromal cell migration. Moreover VEGF stimulates EC production of Plasminogen Activator Inhibitor-1 (PAI-1) and interstitial collagenase. Therefore VEGF induces a balanced system of proteoly-

sis that can remodel ECM components necessary for angiogenesis (Papetti and Herman, 2002).

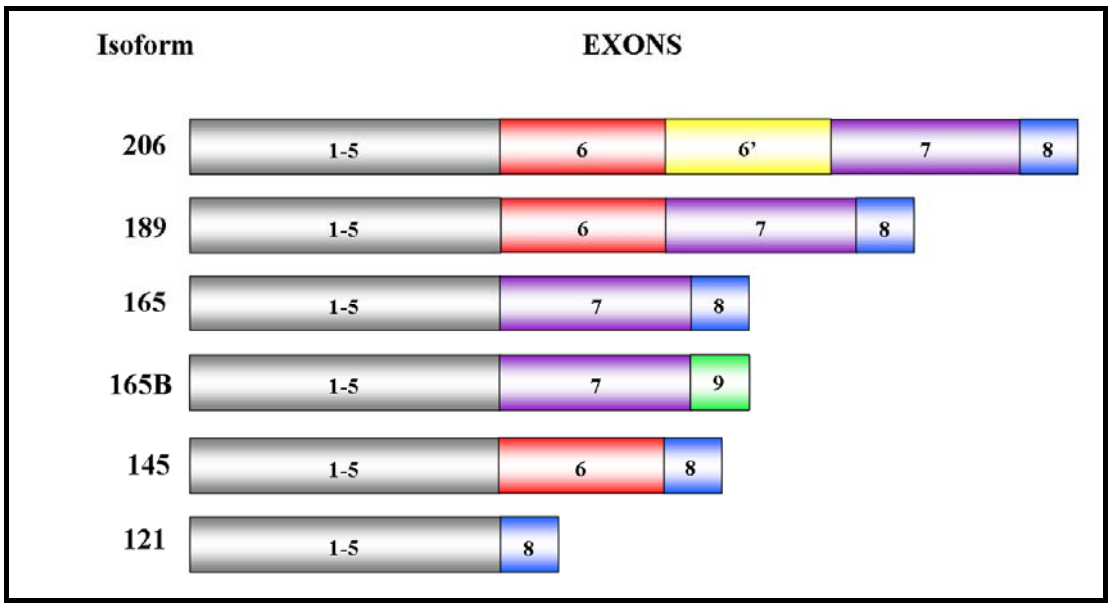

Fig. 1.5: human VEGF-A isoforms. There are at least 6 different isoforms of VEGF-A, which arise by alternative exon splicing. $VEGF_{165}$ is the most potent in terms of inducing angiogenesis whereas $VEGF_{165B}$ inhibits angiogenesis. All isoforms contain exons 1-5 (Byrne et al., 2005, modified).

VEGF-B is a growth factor that shares approximately 44% amino acid sequence identity with $VEGF_{165}$ (Bouïs et al., 2006) and 30% identity with PlGF (Papetti and Herman, 2002). It exists in the two isoforms VEGF-B_{167} and VEGF-B_{186} and can form heterodimers with VEGF (Bouïs et al., 2006). VEGF-B binds and activates VEGFR1 as well as NRP-1 (Papetti and Herman, 2002) inducing expression and increased activity of PAI-1 suggesting a role in ECM degradation and EC migration (Bouïs et al., 2006). VEGF-B is mitogenic for ECs and similarly to PlGF may cooperate with VEGF through its ability to form heterodimers with VEGF (Papetti and Herman, 2002) but it does not appear necessary for angiogenesis as demonstrated in mice deficient in VEGF-B that exhibit only minor cardiac defects (Aase et al., 2001).

VEGF-C and **VEGF-D** (also known as c-Fos Induced Growth Factor, FIGF) form a subgroup within the VEGF family as they consist of a central VEGF homology domain with N- and C-terminal extensions that are cleaved during protein maturation and are not seen in the other VEGFs or PlGF (Bouïs et al., 2006). VEGF-C and VEGF-D respectively share 32 and 31% identity with $VEGF_{121}$ and $VEGF_{165}$ (Papetti and Herman, 2002). Both consist of non-covalent dimmers and bind to VEGFR2 and

VEGFR3. VEGF-C seems to play a predominant role in lymphangiogenesis and is mainly expressed during embryogenesis whereas VEGF-D is also expressed in adult heart, lung and skeletal muscle (Bouïs et al., 2006). They posses mitogenic activity for ECs *in vitro* even though it is significantly less potent (5- to 100-fod) than that induced by VEGF-A. Both VEGF-C and VEGF-D stimulate angiogenesis *in vitro* and *in vivo* but their physiological roles are still undefined (Papetti and Herman, 2002).

VEGF-E refers to a group of VEGF-related proteins encoded by the *orf* virus, a parapoxvirus that infects sheep, goats and occasionally humans that share between 16 and 27% amino acid identity to mammalian VEGF-A. These viral proteins have retained VEGF function because they signal through VEGFR-2 ad stimulate angiogenesis *in vitro* and *in vivo* (Papetti and Hermann, 2002; Byrne et al., 2005). A novel isoform of VEGF-E is the VEGF-E_{NZ-7} which binds at high affinity and activates VEGFR-2 resulting in receptor autophosphorylation and rise in free intracellular Ca^{2+} concentration (Otrock et al., 2007).

Angiopoietins (Ang)

Four Ang have been identified and form a family of secreted proteins, Ang-1, Ang-2, Ang-3 and Ang-4 (Fielder and Augustin, 2006), that all bind to endothelium-specific receptor tyrosine kinases, the Tyrosine kinase with immunoglobulin and epidermal growth factor homology domains 1 and 2 receptor (Tie1 and Tie2) (Bach et al., 2007). The Tie receptors are almost exclusively expressed by ECs and hematopoietic stem cells. Tie1 and Tie2 share a similar overall structure consisting of an extracellular domain with 33% similarity and an intracellular tyrosine kinase domain with 76% similatity (Fielder and Augustin, 2006). Ang and Tie receptors play a key role in angiogenesis (Otrock et al., 2007).

The best characterized are Ang-1 and Ang-2 which are both approximately 70kDa secreted ligands for the receptor Tie2. They are 60% identical and both contain an NH_2-terminal coiled-coil domain and a COOH-terminal fibrinogen-like domain.

Ang-1 binds specifically to Tie2 thus activating it by inducing phosphorilation. This interaction does not promote the growth of cultured ECs however it induces migration, tube formation, spouting and survival (Bach et al., 2007). Ang-1 is constitutively expressed by many different cell types: pericytes, smooth muscle cells, fibroblast and

some tumor cells (Fielder and Augustin, 2006). Its mRNA is detectable at embryonic days 9-11 in the myocardium and later in the mesenchyme surrounding blood vessels (Otrock et al., 2007). In adults the Ang-1/Tie2 signalling system is essential for the maturation of vessels by maximizing the interaction between ECs and their surrounding support cells and matrix and stabilizing vessels (Post et al., 2008). Moreover constitutive Ang-1 expression and low-level Tie2 phosphorylation in the adult vasculature suggest that Ang-1-mediated signalling functions as the default pathway to control vascular quiescence. Ang-1 is anti-inflammatory, protects against cardiac allograft arteriosclerosis and radiation-induced EC damage, promotes wound healing, inhibits VEGF-induced blood vessel formation and adhesion molecule expression. On the contrary its overexpression induces blood vessel and lymphatic angiogenesis (Fiedler and Augustin, 2006).

Ang-2 is the natural antagonist of Ang-1 by the inhibition of Tie2 signalling (Post et al., 2008). It is mainly produced by ECs and pericytes (Bach et al., 2007) and is also detectable in Kaposi's sarcoma cells and in Müller cells in the retina. Ang-2 mRNA is almost undetectable in the quiescent vasculature (Fielder and Augustin, 2006) but it is induced dramatically at the site of vascular remodelling, promoting vessel destabilization (Bach et al., 2007), loosening of cell-matrix and cell-cell interaction. This antagonistic effect is thought to be a requirement for the sensitivity of ECs to other angiogenic factors such as VEGF (Post et al., 2008). Ang-2 up-regulation in the absence of other exogenous stimuli might result in vascular destabilization and subsequent vessels regression. Diversely to when present for a prolonged period or at high concentration, Ang-2 alone induces Tie2 phosphorylation in ECs and enhances their angiogenicity (Fig. 1.6). Ang-2 expression is induced by various cytokines, including VEGF and bFGF and by microenvironmental factors (Fielder and Augustin, 2006). In ECs it is controlled by the Akt/FOXO1 pathway. Expression of an activated version of FOXO1 results in up-regulation of Ang-2 levels, whereas an activated version of Akt represses Ang-2 expression by phosphorylating and inhibiting FOXO1 (Daly et al., 2006). The temporal-spatial imbalance between the angiopoietins is crucial to the angiogenic switch. The presence of a higher level of Ang-2 compared to Ang-1 leads to increased angiogenesis and a more aggressive, larger, heavier tumour with a higher rate of prolifera-

tion which can be highly metastatic. A lower ratio of Ang-2:Ang-1 gives a slower rate of angiogenesis (Bach et al., 2007).

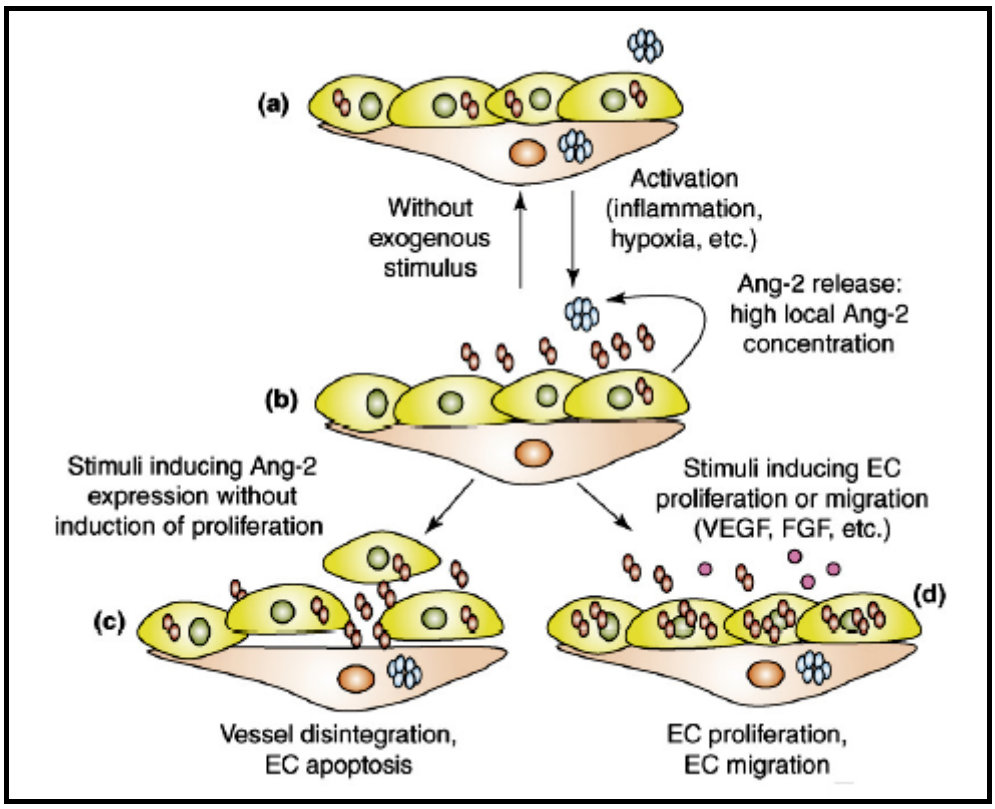

Fig. 1.6: proposed model of Ang-Tie2 interaction in regulating (a) vascular quiescence, (b) vascular responsiveness, (c) vascular regression and (d) angiogenesis. (a) The quiescent phenotype of the endothelium is maintained by constitutive Tie2 activation mediated by the binding of oligomeric Ang-1 (blue), secreted by smooth muscle cells and pericytes (orange). Quiescent ECs (green) store dimeric Ang-2 (red). (b) The activation of ECs results in Ang-2 liberation which interfere with Ang-1-Tie2 signalling and yields ECs responsive to the activities of other cytokines. (c) The continue exposure of ECs to Ang-2 in absence of other cytokines (pink) results in EC apoptosis and subsequent vessel regression. (d) The continue induction of Ang-2 protein expression primes ECs towards angiogenic stimuli. Transcriptional up-regulation of Ang-2 in ECs is an early event of the angiogenic cascade (Fielder and Augustin, 2006).

Ang-3 and **Ang-4** were described as ligands for Tie2 receptor in 1999 by homology cloning. Ang3 appears to be the mouse equivalent of the human protein Ang4. Ang4 has been shown to increase Tie2 phosphorylation and induce survival and migration unlike Ang3 which does not produce significant changes (Bach et al., 2006).

Fibroblast Growth Factor family (FGFs)

FGFs are major growth and differentiation factors in embryonic development as well as in the adult playing a role in neuronal signalling, inflammatory processes, hematopoiesis, angiogenesis, tumor growth and invasion. The FGFs are comprised of

23 members of small polypeptides of 155-268 amino acids, most of them constitutively secreted, with a few family members remaining intracellular and a few FGFs lacking a signal sequence, still leaving the cell through an unknown mechanism, possibly involving a carrier protein. FGFs strongly bind to components of the ECM as HSPG from which they can be released by heparin or during ECM breakdown.

The FGFs binds to surface receptors (FGFR) consisting of three extracellular immunoglobulin-like domains, a single transmembrane domain and an intracellular tyrosine kinase domain which dimerizes upon ligand binding and initiates the intracellular signal transduction. There are four major FGFR genes that lead to a variety of receptors of different specificities by alternative splicing (Bouïs et al., 2006). In particular FGFR1 signalling stimulates migration and differentiation whereas FGFR2 regulates only migration (Milkiewicz et al., 2006). Two members of the FGFR gene family have been recently described, FGFR5 lacking an RTK-domain and FGFR6 belonging to the Major Histocompatibility Complex (MHC) family (Zangari et al., 2004). FGFs stimulate EC proliferation and migration as well as EC production of plasminogen activator and collagenase. They stimulate also the proliferation of pericytes, fibroblasts, myoblasts, chondrocytes and osteoblasts.

The two most extensively studied members of FGFs, acidic FGF (aFGF or FGF1) and basic FGF (bFGF or FGF2), are ubiquitously expressed 18 to 25kDa polypeptides. Both aFGF and bFGF induce processes in ECs in vitro that are critical to angiogenesis (Papetti and Herman, 2002). bFGF has four known alternative splice forms all inducing proliferation, chemotaxis and urokinase type plasminogen activator activity, VEGF and VEGFR2 up-regulation in ECs, whereas only one isoform is known for aFGF (Bouïs et al., 2006). bFGF binds to one of four receptor tyrosine kinases on the cell surface. The binding is enhanced by interactions with cell surface HSPG (syndecans, glypicans) but may compete for sequestration of bFGF by other HSPG such as perlecan and agrin within the interstitial matrix. Binding of bFGF to its receptors initiates Protein Kinase C (PKC) dependent signalling and/or Grb2-SOS mediated activation of Mitogen Activated Protein Kinases (MAPK) pathway (Milkiewicz et al., 2006).

Platelet-derived growth factor family (PDGF)

Besides VEGF and FGFs, **PDGF** has been shown to be one of the most potent angiogenesis inducers. It can be secreted by different cell types: platelets, macro-

phages, ECs, fibroblasts, keratinocytes (Bouïs et al., 2006), myoblasts, astrocytes and epithelial cells (Papetti and Herman, 2002). The PDGF family consists of four different PDGF strands (A-D) establishing functional homodimers (PDGF-AA, PDGF-BB, PDGF-CC, PDGF-DD) or a heterodimer PDGF-AB (Karamysheva, 2008) composed of PDGF chains A and B. Most cells express both PDGF-A and B although a few express only one isoform. PDGF receptors (PDGFR) are made up of complexes between α- and β-subtypes: PDGFRα can bind both PDGF A and B chains whereas PDGFRβ only PDGF B. Therefore, of the three types of receptors (αα, ββ and αβ) only one (αα) can bind all three PDGF isoforms (Papetti and Herman, 2002). PDGFR are transmembrane proteins whose intracellular region contains the tyrosine kinase domain separated into two fragments by an interkinase insert but the extracellular region of PDGFR is formed by five immunoglobulin-like domains (Karamysheva, 2008).

The effects of PDGF on vascular cells *in vitro* and *in vivo* suggest a role for this growth factor angiogenesis. Capillary ECs express PDGFRβ and are stimulated by PDGF-BB not only to increase DNA synthesis but also to form angiogenic chords and sprouts *in vitro*. PDGF also stimulates the proliferation and recruitment of cultured smooth muscle cells and pericytes both of which have been shown to express PDGFRβ (Papetti and Herman, 2002). Less abundant forms PDGF-CC and PDGF-DD bind, respectively, homodimers PDGFRα and PDGFRβ as well as heterodimers PDGFRαβ. These two forms exhibit higher structural similarity with VEGF compared to other PDGF variants (Karamysheva, 2008).

Transforming Growth Factor-β family (TGF-β)

TGF-β superfamily consists of close to 30 members including TGF-βs (TGF-β1, TGF-β2 and TGF-β3), bone morphogenetic proteins, activins and inhibins (Holderfield and Huges, 2008). The TGF-βs represent a family of highly conserved 25kDa disulphide-linked homodimeric cytokines typified by TGF-β1. Before the secretion from the cell, cleavage by a furin peptidase generates a COOH-terminal 112-amino acid peptide that noncovalently associates with the NH_2-terminal proregion and dimerizes to form mature TGF-β. Secreted TGF-β can not bind TGF-β receptors and is biologically inactive. The latent complex is activated by proteases such as plasmin and cathepsin S, low pH, chaotropic agents such as urea and heat (Papetti and Herman, 2002).

The receptors fall into 2 major classes, both of which are serine-threonine kinases. Type II receptors, of which there are 5 in humans including TGF-βRII and BMP receptor (BMPR)II, undergo a conformational change on binding to their ligand allowing them to phosphorylate and activate type I receptor. There are 7 known type I receptors, which once activated, phosphorylate various smads, which convey the transcription of target genes (Holderfield and Huges, 2008).

TGF-β is expressed by a wide variety of normal and transformed cells. It is found in ECM of many tissues. In the microvasculature both ECs and pericytes produce TGF-β and possess TGF-β receptors. It can stimulate or inhibit cell proliferation, control cell adhesion by regulating production of ECM, protease inhibitors and integrins and it can induce cellular differentiation. Moreover it regulates expression of a number of genes in ECs, particularly those involved in the establishment of, and interaction with, the BM. TGF-β also induces PDGF-B and the subsequent recruitment of pericytes. It has been demonstrated that TGF-β is also involved in angiogenesis because of its chemotaxis towards a wide range of cells, including monocytes and fibroblast that secrete angiogenic factors (Papetti and Herman, 2002).

Tumor Necrosis Factor-α (TNF-α)

TNF is secreted by activated macrophages and activate T lymphocytes and it has pleiotropic proprieties among which is the ability to cause apoptosis of tumor-associated ECs that can result in the complete destruction of the tumor vasculature.

TNF is a transmembrane protein, which upon cleavage by the metalloproteinase TACE produces a soluble trimer of 157 amino acid. Both isoforms of TNF (membrane and soluble) bind two distinct receptors that are ubiquitous, p55 or TNF-R1 and p75 or TNF-R2 (Lejeune et al., 2006).

Although TNF-α is primarily involved in inflammation and immunity, it shares many proprieties with TGF-β, stimulating angiogenesis *in vivo* and inhibiting EC growth (Papetti and Herman, 2002).

Epidermal Growth Factor (EGF)

EGF is secreted by platelets, macrophages and monocytes and in salivary, lacrimal and duodenal glands as well as in the kidney (Bouïs et al., 2006). EGF binds to the EGF receptor (EGFR) (also known as Human Epidermal growth factor Receptor, HER1) or other members of the HER family, HER2-4. These receptors are tyrosine

kinases and ligand binding induces receptor dimerization followed by signalling through Ras/MAPK PI3K pathways. HER2 signalling induces VEGF production via increases in HIFα protein synthesis (Milkiewicz et al., 2006). It has no direct effects on vascular endothelium but it is nevertheless involved in tumor proliferation, metastasis, apoptosis, angiogenesis and wound healing (Bouïs et al., 2006).

Others soluble growth factors

Many other soluble factors have been implicated in playing an important role in angiogenesis, but their effects on the vasculature are not as widespread as the previously discussed factors (Otrock et al., 2007).

Transforming growth factor-α (**TGF-α**) binds EGFR. It is a 5 to 6kDa protein that is mitogenic for ECs *in vitro* and induces angiogenesis *in vivo*.

Granulocyte Colony Stimulating Factor (**G-CSF**) and granulocyte/macrophage colony-stimulating factor (GM-CSF), proteins required for growth and differentiation of hematopoietic precursors, induce migration and proliferation of ECs to a limited extend (Papetti and Herman, 2002).

Several others soluble substances have been shown to affect angiogenesis. **Angiogenin** induces angiogenesis in the chorioallantoic membrane and rabbit cornea assays (Otrock et al., 2007). It is a 14.1kDa polypeptide isolated from a human adenocarcinoma cell line. It is not mitogenic or chemotactic for ECs *in vitro*. Angiogenin also binds to extracellular components and can support the adhesion and spreading of ECs *in vitro*. It is synthesized in small amount in the developing fetus and in large amount in the adult (Papetti and Herman, 2002).

Angiotropin is a 4.5kDa polyribonucleopeptide that induces capillary EC migration. It is important in triggering the proliferative reactions in wound healing by activating microvascular ECs (Otrock et al., 2007).

Two proteins involved in the coagulation cascade, **tissue factor** and **tissue factor V**, as well as certain nonpeptide low-molecular-weight molecules such as **prostaglandins**, **nicotinamide** and **monobutyrin** appear to contribute to angiogenesis but their roles are still controversial and their mechanisms of action unknown (Papetti and Herman, 2002).

Integrins

Integrins are a family of glycosylated, heterodimeric transmembrane adhesion receptors involved in cell-cell and cell-ECM interactions (D'Andrea et al., 2006). The attachment of ECs to the BM, ECM and each other usually occurs in specialised focal contacts where the cytoskeletal actin filaments are linked to **integrin** bound to the ECM through specialised cytoplasmatic proteins (Bouïs et al., 2006). They consist of non-covalently associated α- and β-subunits. There are 18 α- and 8 β-subunits known that can combine in more that 20 different heterodimeric receptors, most of which interact with specific ECM ligands through recognition of specific amino acid sequences, the most relevant and investigated sequence is the Arg-Gly-Asp (RGD) sequence (D'Andrea et al., 2006).

The role of $\alpha_v\beta_3$ integrin in mediating angiogenesis is evident in the binding of ECM components and matrix MMP-2 (Otrock et al., 2007). It is important for EC functions in neovascularization and is abundantly expressed on angiogenic blood vessels, in granulation tissue but not on vessels from normal skin. $\alpha_v\beta_3$ integrin mediates EC functions *in vitro* and plays an important role in angiogenesis *in vivo*. Its ligation also induces mitogen-activated protein kinase activation and suppresses apoptosis in ECs, mediating EC survival by promoting proliferation and activation (Papetti and Herman, 2002). Other integrins, β_1 integrins as $\alpha_1\beta1$, $\alpha2\beta1$ and $\alpha5\beta_1$ were shown to be essential for angiogenesis but more research is needed to clarify the pro- and anti-angiogenic mechanisms of these integrins (Bouïs et al., 2006).

Cadherins

Cadherins comprise a large family of Ca^{2+}-binding transmembrane molecules that promote homotypic cell-cell interactions. The intracellular domain of cadherins mediates a linkage to the cytoskeleton by binding to β-catenin and plakoglobulin, two proteins anchored to cortical actin by α-catenin.

ECs possess two cadherins: VE-cadherin, which is localized to Adherens Junctions (AJ) exclusively in ECs and N-cadherin, which is not found at cell-cell contacts (Papetti and Herman, 2002). Numerous studies highlighted the importance of VE-cadherin in neovascularization. VE-cadherin plays a role in regulating the passage of molecules across endothelium (Otrock et al., 2007). Cadherins not only establish EC junctional stability in the vessel wall but also enhance EC survival by promoting transmission of

VEGF antiapoptotic signal to the nucleus, a crucial result necessary for remodelling and maturation of vessels in angiogenesis (Papetti and Herman, 2002).

Eph-B4/Ephrin-B2

A group of RTKs and their ligands, playing a major role in angiogenesis are the ephrin (Eph) receptors and their ligands the **ephrins**. Ephrin ligands are membrane-tethered and Eph-receptor-ephrin-binding leads to signal transduction in both cells.

Eph receptors belong to the largest known family of receptor tyrosine kinases consisting of at least 14 membrane-bound proteins (Papetti and Herman, 2002): A receptors (EphA1-A8) and B receptors (EphB1-B6) (Bouïs et al., 2006) with 8 transmembrane ligands (ephrins) already identified (Papetti and Herman, 2002): Ephrin-A (ephrin A1-A5) are attached to the outer leaflet of the plasma membrane via a glycosilylphosphotidylinositol (GPI) anchor, whereas Ephrin-B (ephrin-B1-B3) contains transmembrane and cytoplasmatic domain. The cytoplasmatic and transmembrane domains of class B ephrin are similar to cell surface receptor molecules. The binding between ephrin and the receptor leads to Eph receptor dimerisation and phosphorylation of the cytoplasmic domains.

Expression of ephrins can be induced by TNF-α and VEGF. They promote migration, repulsion, adhesion and attachment to the ECM via integrins (Bouïs et al., 2006). Moreover in the nervous system they appear to assist axon guidance through repulsive signals and establish borders between neuronal compartments (Papetti and Herman, 2002).

Biomechanical forces

The mechanical forces mediated by blood flow have profound effects on vessel growth (Papetti and Herman, 2002). A flowing fluid through a tube exerts a force tangential to the tube, called **shear stress** and another that is perpendicular to the tube wall and is caused by the pressure in the vessel, called **circumferential stretch**. Mature vessels can react to both these forces. Shear stress from blood flow has been shown to cause changes in morphology, cytoskeleton organization, ion channel activation and gene expression within ECs *in vitro*. In these mature systems chronic elevations in shear stress lead to increased vessel diameter , whereas chronic increases in pressure lead

to decreased vessel diameters. This observation has lead to a pressure-shear hypothesis, whereby vessels adapt to shear stress as a function of local pressure.

The presence of **laminar flow**, which is a type of fluid flow where the streamlines of the fluid motion are parallel, has been found to have atheroprotective effects on mature blood vessels. **Laminar shear stress** reduces apoptosis and induces antiapoptotic genes, such as Bcl-X_L. Moreover it keeps cells from proliferating by inhibiting DNA synthesis. The signals that are created by flow are sensed through integrins and the cytoskeleton (Jones et al., 2006).

Thus microvascular blood vessels are remodelled in angiogenesis through several diverse mechanisms. Growth factors secreted from distant cells, transmembrane proteins binding to ECM components or to receptors on other cells and hemodynamic forces all act in concert to regulate normal angiogenesis. In a physiological setting, these factors exert both positive and negative influences on blood vessel growth to ensure that angiogenesis is confined to metabolic demands of growing and healing tissues (Papetti and Herman, 2002).

1.1.4. Endogenous inhibitors of angiogenesis

Much of the intracellular signalling associated with the angiogenic cascade appears to provide positive feedback for the continued activation of angiogenesis through their receptors (Bouïs et al., 2006). Some of the endogenous inhibitors are reported in Table 1.2.

Angiostatin	
Anti-angiogenic anti-thrombin III	
Canstain	
Endostatin (collagen XIII fragment)	
Fibronectin fragment	
Heparinases	Interferon-α (IFN-α)
	Interferon–β (IFN-β)
	Interferon–χ (IFN-χ)
Interleukin-4 (IL-4)	
Interlukin-12 (IL-12)	
Interleukin-18 (IL-18)	
Plasminogen activator inhibitor	
Pigment epithelium derived factor (PEDF)	
Prolactin 16KDa fragment	
Thrombospondin-1 (TSP-1)	
Retinoids	

Table 1.2: some inhibitory regulators of angiogenesis (Pandya et al., 2006, modified).

Angiostatin

Angiostatin is a 38kDa fragment of plasminogen and was first determined to have anti-angiogenic proprieties because it inhibited neovascularization in a mouse tumor model. Angiostatin also inhibit EC proliferation, resulting in tumor dormancy through decreased cell replication and increases in apoptosis (Milkiewicz et al., 2006). It has been shown to bind to ATP-synthase on the surface of ECs and it also binds to and inhibits tPA. Several MMPs as well as tumor-cell-derived plasmin thiolreductase have been shown to cleave plasmin to angiostatin (Bouïs et al., 2006).

Endostatin

Endostatin is a 20kDa carboxy-terminal fragment of collagen XVIII that was shown to specifically inhibit EC proliferation and tumor growth. Endostatin inhibits VEGF-induced migration in Human Umbilical Vein ECs (HUVECs). Endostatin interferes with VEGF-stimulated VEGFR2 signalling, which may occur through direct interaction of endostatin with VEGFR2 (Milkiewicz et al., 2006). Angiostatin and endostatin has been shown to act synergistically to inhibit tumor angiogenesis (Bouïs et al., 2006). Endostatin also inhibits the activation of pro-MMP-2 and inhibits the catalytic activity of both MMP-2 and MT1-MMP, which may explain the decrease in invasion in ECs treated with endostatin. Moreover it promotes EC apoptosis by the downregulation of Bcl-2 and Bcl-XL (Milkiewicz et al., 2006).

Other anti-angiogenic factors

Anti-thrombin, a plasma proteinase inhibitor of the serpin superfamily, is a heparin-binding protein and the major plasma inhibitor of coagulating proteases, primarily thrombin and factor Xa. In addition anti-thrombin is also recognized as a proteinase inhibitor of plasma kallikrein, plasmin and trypsin. The molecular mass of anti-thrombin is 58kDa and it contains 432 amino acids. Anti-angiogenic and anti-tumor growth proprieties have been attributes to both the cleaved and the uncleaved latent forms of human plasma-derived anti-thrombin (Cao et al., 2002).

Interferons (IFNs) have shown a significant anti-tumor activity in pre-clinical models and are the most commonly used cytokines in patients. IFN-α expression precedes the majority of the innate response cytokines and it has been proposed to be the first cytokine secreted by antigen-presenting cells after antigen stimulation (Minuzzo et al., 2007).

Tumstain, an anti-angiogenic and pro-apoptotic mediator, is a 232 amino acid peptide released from the α3 chain of collagen IV through cleavage by MMP-9. It can bind to $\alpha_v\beta_3$ integrin arresting EC DNA synthesis by the inactivation of the focal adhesion kinase/PI3K/Akt/mTOR pathway.

Vasohibin was described as a gene induced in VEGF-stimulated ECs. The gene encodes for a secreted protein that is an inhibitor of tumor angiogenesis. The precise mechanism by which vasohibin blocks angiogenesis is not yet known, although direct antagonism of growth factor receptors has been excluded probably as a negative feedback regulator of angiogenesis (Milkiewicz et al., 2006).

Arrestin, **canstatin**, **restin** as well as **fragments of prolactin** and other small fragments could inhibit angiogenesis (Bouïs et al., 2006).

1.1.5. Methods for assessing angiogenesis

A large number of *in vitro*, *ex-vivo* and *in vitro* assays have been performed in the last few years and the combination of some assays can help in the understanding of cellular and molecular events during angiogenesis. Although the ECs whose migration, proliferation, differentiation and structural rearrangement is central to the angiogenic process, it is not the only cell type involved in angiogenesis. The supporting cells, the ECM produced by ECs and their apposed mesenchymal cells and the circulating blood with its cellular and humoral components are also involved (Staton et al., 2004). The main angiogenic assays are reported in Table 1.3.

Type of assay	***Specific assays***	***Advantages***	***Disadvantages***
Organ culture	All	Mimic the *in vivo* situation Include surrounding cells and matrix ECs are not proliferating at start of assay	Difficult to quantify Growth requirements differ between explant and cell out growth Time consuming
In vivo	Sponge implant	Inexpensive Technically simple	Nonspecific immune responses may lead to an angiogenic response Sponge composition varies, making inter experimental comparisons difficult
	Matrigel plug	Nonartificial, providing a more natural environment for angiogenesis	Expensive Analysis is time consuming
	CAM assay	Technically simple Inexspensive Suitable for large-scale screening	Very sensitive to oxygen tension Due to the pre-existing vascular network, visualization of new capillaries can be difficult Immune response can mask new

			vasculature
	Corneal Angiogenesis	Reliable	Expensive Technically difficult Ethically questionable
	Dorsal air sac model	Technically simple Natural environment in which to study blood vessels	Invasive Visualization of new capillaries can be difficult due to pre-existing ones
	Chamber Assay	Can follow 3D vessels growth over a relatively long period Minimizes number of mice used	Invasive Technically difficult Expensive (in rabbits) Can get surgery associated angiogenesis
	Tumour models	Can follow pharmacokinetics of drug as well as anti-angiogenic effects Long term studies possible	Tumor environment depends on tumor growth site Real-time studies not possible
	Angiomouse®	Visualization is noninvasive Allows for real-time imaging of angiogenesis	Sensitivity can be limited by quenching due to surrounding tissue, especially skin Hypoxia can decrease GFP gene expression and hence, the degree of fluorescence
	Zebrafish	Relatively fast assay (6-12h) Fully quantitative Disruption to vasculature does not damage embryo	Does not indicate exact point in angiogenic cascade specifically disrupted Expensive to maintain in breeding condition Does not distinguish between cytotoxic effects and genuine inhibition
Proliferation	MTT	Measures cell number	Cells not necessarily proliferating Does not measure toxicity of drug
	Tritiated thymidine	Measures DNA replication	Uses radiation Does not measure toxicity of drug
	BrdU	Measures DNA replication No radiation	Does not measure toxicity of drug
	Cell-cycle analysis	Measures apoptosis and therefore toxicity of drug Measures DNA replication Measures percentage of cells proliferating	Cells have to be in suspension for analysis
Migration	Boyden Chamber	Measures migration in response to a gradient Extremely sensitive to small changes in concentration	Technically difficult to set up Problems in maintaining *trans* filter gradients Difficult to obtain accurate cell count Time consuming to analyze
	Phagokinetic track	Measures total cell movement Measures directional effects of drug	Only a small number of cells studied Unnatural substrate to migrate on
	Wound healing	Measures rate of EC migration	Quantification is somewhat arbitrary Technical problems in achiev-

			ing identical conditions of confluence
Differentiation	Matrix assays	ECs pushed down differentiation pathway Formation of tube-like structures Quick	Lumen formation is under debate Nonendothelial cells also form tubes Homogenous pattern of tubule lengths
	3D gel	More closely mimics the *in vivo* situation Tubules form in all three dimension	Long time period Problems of quantifying a 3D strucures
	Co-culture	Tubules from lumen More heterogenous pattern of tubule lengths Closer to *in vivo*situation	Long time period Undefined interactions between ECs and others cells

Table 1.3: popular *in vivo* and *in vitro* "angiogenesis" assays: strengths and weaknesses (Staton et al., 2004, modified)•

In vivo assays

The subcutaneous implantation of a polymer matrix (in the form of sponge or a Matrigel gel/plug) containing cells and/or an angiogenic factor has been used to study *in vivo* angiogenesis. Neovascularization can be assessed by a variety of methods including immunohistological staining, the blood/haemoglobin content of the sponge or by the levels of a radioactive tracer in blood. Differences in sponge size, shape and composition make comparisons between different studies difficult. Furthermore implantation can cause nonspecific immune responses that may themselves lead to an angiogenic response. Moreover **Matrigel**, that is liquid at 4°C and becomes a solid gel at 37°C, can be injected subcutaneously where it forms a solid plug allowing the slow release of the substance. The angiogenic response can then be quantified by the extent of CD31-positive vessel growth into the plug or by measuring the haemoglobin content of the plug (Staton et al., 2004).

Grafting of tissue onto the **CAM** of the chicken embryo is another common approach in angiogenesis research. Inside the chicken egg, the CAM serves as a transient gas exchange surface similar to the lung. This membrane first appears at day 3 of incubation and rapidly grows until day 10, where the adjacent mesodermal layers of the chorion and the allantois fuse to form the CAM, which is characterized by a dense microvascular network (Ribatti et al., 2001). Xenograft from mammalian species can be implanted into the CAM without rejection, because the early chicken embryo lacks a complete immune system (Laschke and Menger, 2007). In the CAM assay the eggshell is cracked and peeled away from the region over the air space that exists between the

shell and the inner shell membrane (ISM) at one pole of the egg. This space can be visualized before the egg is cracked by holding the egg under intense light. Once the opaque CAM-ISM dual layer is exposed, irrigation of the CAM-ISM with saline will cause the dual layer to become translucent, allowing for visualization of the CAM vasculature. Introducing fresh saline into the air space will wash away the blood, providing a clean membrane for experimentation. Sponges that contain test solution are implanted into the egg and at day 12 the effect is observed (Leng et al., 2004).

In the **corneal angiogenesis assay** an angiogenic response can be initiated by implantation of a slow-release pellet or polymer containing the angiogenic substance. If the animal is administered with a test compound the vascular response can be quantified by computer image analysis following perfusion of the cornea with India ink.

The **rabbit ear chamber**, **dorsal skinfold chamber** and **cranial window chamber** are other *in vivo* types of transparent chamber to observe chronic angiogenesis (Staton et al., 2004).

Ex-vivo assays: organ cultures

As angiogenesis does not involve ECs alone, studies have attempted to assess angiogenesis in whole or partial organ culture, including assays such as the **rat aortic ring**, the **chick aortic arch**, **porcine carotid assays**. In these assays disk or sections of the relevant material are cultured *in vivo*, often in a matrix such as fibrin and over a period of 10-14 days the outgrowth of ECs or other cells is monitored. The model is not truly representative of the microvascular environment. These explants assays are considered to come closets to mimicking the *in vivo* situation because they include the surrounding nonendothelial cells and a supporting matrix (Staton et al., 2004). Nicosia and Ottinetti demonstrated that rat aortic rings reproducibility generate microvessel outgrowths in fibrin or collagen gels and provide a sensitive assay for the study of angiogenic agonists and antagonists in a chemically defined environment (1990).

In vitro assays

In vitro models of angiogenesis have focused to date predominantly on proliferation, migration and tubule formation by ECs in response to exogenous inhibitory or stimulatory agents (Staton et al., 2004). These assays have the advantages of low costs

and the ease of examining the effects of regulating factors on individual cells involved in angiogenesis (Laschke and Menger, 2007).

ECs *in vitro* are not alike, demonstrating phenotypic differences. Differences have been identified between HUVECs and ECs of microvascular origin such as by structural differences as by organ-associated differences. Moreover *in vitro* ECs may behave differently under a flowing culture condition and with attachment to different matrices. Although these assays are rapid they do not permit study of the complex physiological interactions that occur *in vivo*. The assessment of the indirect effects of a compound are difficult to reproduce. Wherever possible, *in vitro* assays should be carried out using ECs from more than one source, or more importantly, be followed up with one or more *in vivo* assay of angiogenesis (Staton et al., 2004).

Cell proliferation assays are easy to perform and highly reproducible, lending themselves to precise quantification (Auerbach et al., 2003). A number of markers of cell division can be used to assess their proliferation in culture. There are two major classes of proliferation assays: those that determine net cell number and those that evaluate cell-cycle kinetics. Net cell number can be established by use of a haemocytometer or by use of an electron counter. Another method is 3-(4,5-dimethylthiazol-2-yl)-2,5-diphenyltetrazolium bromide (MTT), a tetrazolium salt, which is cleaved by active mitochondria to form a dark blue formazan product. This has been used as a measure of proliferation as living cells produce the formazan product and correlation has been shown with cell number. Alternatively DNA synthesis, a measure of proliferation can be assayed by thymidine incorporation or by staining the cells with a DNA-binding dye and then assessing the amount of bound dye using a colourimeter or enzyme-linked immunosorbent reader.

ECs move, via a process called chemotaxis, along a gradient of angiogenesis-inducing factor such as VEGF. Modified Boyden chamber assay has been used to assess EC **migration**. In these assays ECs are plated on top of a filter and migrate across this in response to a test angiogenic factor placed in the lower chamber. This assay is highly sensitive to small differences in concentration gradient. Different methods are employed to count cells per field of view such as with computerized systems using software that recognizes heamatoxylin and eosin-stained cells or 4,6-

DiAmidino-2-PhenylIndole (DAPI) nucleus-stained cells or counting by eye (Staton et al., 2004).

To assess the **tubule formation** different assays have been developed in the last few years. In these ECs are usually cultured on matrices consisting of fibrin, collagen or Matrigel, which stimulate the attachment, migration and differentiation of ECs into tubules in a manner that mirrors the *in vivo* situation (Kanzawa et al., 1993). Matrigel is a mixture of extracellular and basement membrane proteins derived from the mouse Engelbreth-Holm-Swarm sarcoma on which ECs attach and rapidly form tubules. A computational system evaluates the total number of nodes, connected and unconnected tubes as well as their lengths and the area occupied by cells per field. In this way it is possible to quantified and compare different conditions and experiments (Staton et al., 2004). Matrigel and fibrin clots can also be used to represent a 3D angiogenesis system. Initially ECs form tubes in the horizontal plane and over 12 or more days the endothelial tubes begin to branch upwards and penetrate the gel to form a 3D network of tubules (Gagnon et al., 2002). The analysis involves taking pictures at different heights in the gel from the bottom to the top. The length and the largest diameter of each vessel are measured.

Numerous other assays can be used to evaluate *in vitro* angiogenesis and the creation of innovative methods is under continuous study (Staton et al., 2004).

1.2. The Blood Brain Barrier

The Central Nervous System (CNS) is the most sensitive and critical system in the mammalian body (Kim et al., 2006). Proper neuronal function necessitates a highly regulated extracellular environment, wherein the concentrations of ions such as Na^+, K^+ and Ca^{2+} must be maintained within very narrow ranges. The metabolic demands of nervous tissue are considerable, with the CNS accounting for approximately 20% of oxygen consumption in humans. The CNS is also extremely sensitive to a wide range of chemicals introduced by diet and the metabolites produced and excreted without harm to peripheral organ systems (Hawkins and Davis, 2005). To ensure the protection of this compartment a highly selective barrier has been developed: the Blood-Neural Barrier (BNB), based on the cerebral microvessels barrier characteristic en-

suring the exclusion of many toxic substances. Microvascular ECs in the brain closely interact with other components such as astrocytes, pericytes, perivascular microglia and neurons to form a "neurovascular unit". BNB can be divided into different barriers: Blood-Brain Barrier (BBB), blood-CerebroSpinal Fluid barrier (blood-CSF barrier), Blood-Retinal Barrier (BRB), the Blood-Spinal Cord Barrier (BSCB), the Blood-Labyrinth Barrier (BLB) and the Blood-Nerve Barrier (BNB) (Choi and Kim, 2008) (Fig. 1.7).

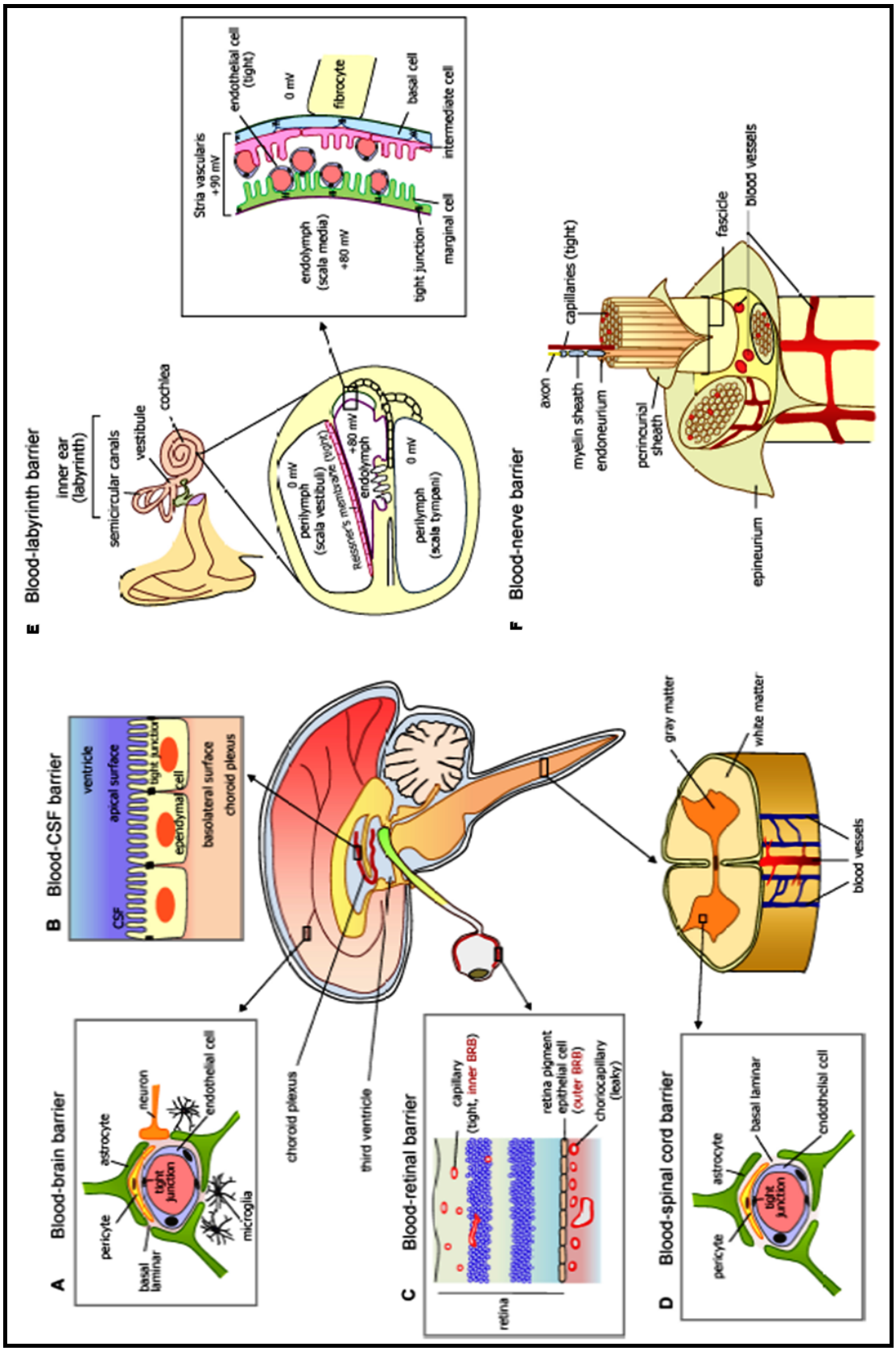

Fig. 1.7: the BBB (A), blood-CSF barrier(B), BRB (C), the BSCB (D), the BLB (E) and the BNB (F) are present at different sites (Choi and Kim, 2008, modified)•

In particular the BBB is the interface between blood and brain and is localized in the capillary ECs in the brain. The special proprieties of these cells are mainly induced by brain cells as astrocytes. In this context the BBB can be considered as an organ that protects and maintains the homeostasis of the brain (de Boer and Gaillard, 2005).

The first experimental evidence of the BBB was described by Paul Ehrlich in 1885, who noted that water-soluble dyes injected into the circulatory system stained all organs except the brain and the spinal cord. He attributed this observation to a low affinity of nervous tissue to the dye. Subsequent experiments by Edwin Goldmann showed that the injection of trypan blue into the CSF stained all cell types in the brain but failed to penetrate into the periphery. This suggested the existence of a barrier to the dye between the CNS and the peripheral circulation (Hawkins and Davis, 2005).

The BBB restricts ionic and fluid movements between the blood and the brain, allowing specific transporters and channels to regulate ionic traffic, to produce a brain interstitial fluid that provides an optimal medium for neuronal function. The barrier helps to keep separate the pools of neurotransmitters and neuroactive agents that act centrally (in the CNS) and peripherally (in the peripheral tissues and blood) (Abbott et al., 2006).

1.2.1. Anatomical composition of the BBB

The BBB is characterized by Tight Junctions (TJ) between ECs, lack of fenestrations and specific transporters (Kim et al., 2006). The mature BBB is a complex system of different cellular components (Fig. 1.8). Highly specialized microvascular ECs and pericytes are embedded in the basal membrane and surrounded by perivascular macrophages and astrocytic end-feet. The formation of the BBB, called barriergenesis, is the final step during the complex development of the brain vascular system, which is induced by the embryonic neural tube (Rieckmann and Engelhardt, 2003).

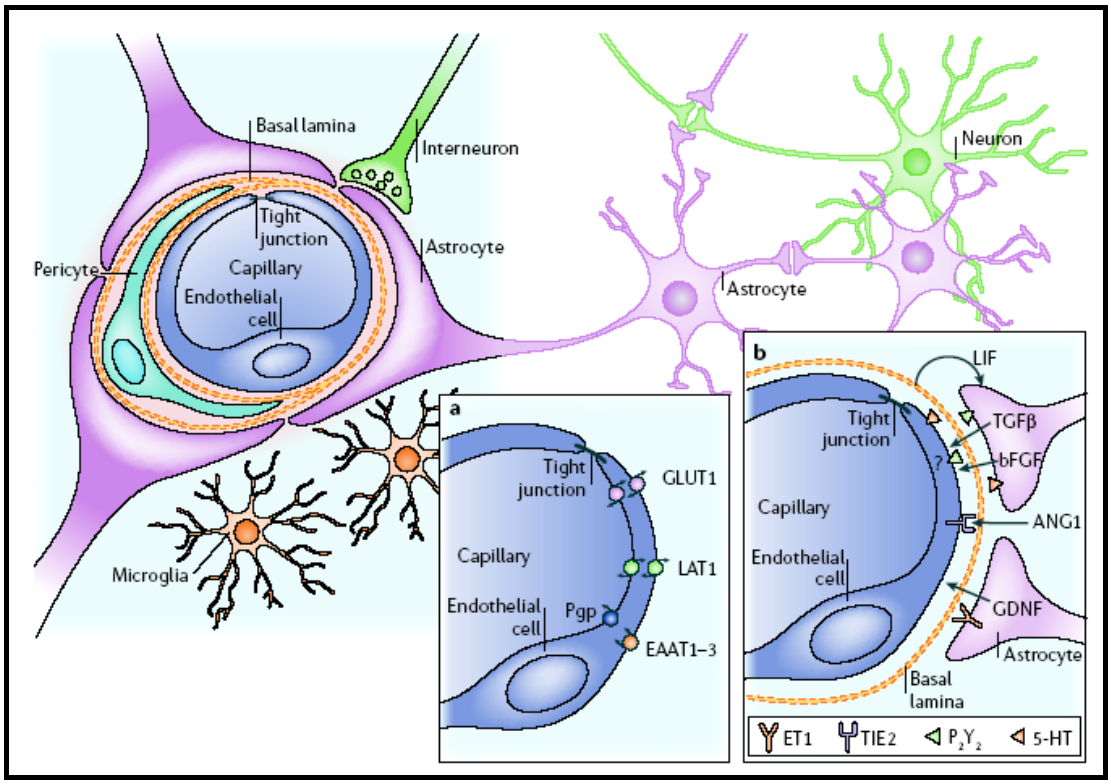

Fig. 1.8: cellular constituents of the BBB: the barrier is formed by capillary ECs, surrounded by basal lamina and astrocytic perivascular end-feet. Astrocytes provide the cellular link to the neurons. (a) brain endothelial cell features are observed in cell culture. The cells express a number of transporters and receptors. (b) Examples of bidirectional astroglial-endothelial induction necessary to establish and maintain the BBB. EAAT1-3, Excitatory Amino Acid Transporters 1-3; ET1, Endothelin 1; GDNP, Glial cell line-Derived Neurotrophic factor; GLUT1, Glucose Transporter 1; LAT1, L-system for large neutral amino acid; LIF, Leukaemia Inhibitory Factor; P_2Y_2, Purinergic receptor; Pgp, P-glycoprotein (Abbott et al., 2006).

ECs

The ECs are different from the ECs of other compartments of the body because of their active metabolism with much mitochondrial content, low number of pinocytotic vessels, lack of fenestration and TJ between ECs. ECs and pericytes are surrounded by a membrane composed of collagen type IV, laminin, fibronectin and heparin sulphate proteoglycan, which is ensheathed by astrocytes end-food (Kim et al., 2006). The ECs of the CNS protect the CNS from the affection of changes in the vascular system and serve the nutritional demands of the CNS. The TJ between ECs serve as a physical blockade to paracellular diffusion of ions, peptides and immune cells from the blood into the CNS. Almost 100% of large-molecules (>400Da) and more than 98% of small molecules do not cross the BBB (Kim et al., 2006).

The main components of junctional complex includes AJ, TJ and gap junctions. Both AJ and TJ act to restrict permeability across the endothelium while gap

junctions, when present at the interendothelial junctions of the BBB, mediate intercellular communication. AJ are ubiquitously expressed in the vasculature and mediate the adhesion of ECs to each other, contact inhibition during vascular growth and remodelling, initiate cell polarity and the regulation of paracellular permeability. The primary component of AJ is VE-cadherin that mediates cell-cell adhesion via homophilic interactions between the extracellular domain of proteins expressed in adjacent cells. The cytoplasmatic tail binds to β-catenin and plakoglobulin, which in turn bind via α-catenin, α-actin and vinculum to the actin cytoskeleton, stabilizing the AJ complex (Hawkins and Davis, 2005).

The TJ result from the triangular relationship among ECs, glial cells and neurons. The TJ complex includes two classes of transmembrane molecules: occludin and claudins which interact with transmembrane proteins on adjacent ECs (Kim et al., 2006). Occludin is a 60-65kDa protein with a carboxy (C)-terminal domain that is capable of linking with Zonula Occludens protein 1 (ZO-1). The main function of occludin appears to be in TJ regulation (Abbott et al., 2006). ZO-1, ZO-2 and ZO-3 are part of the membrane-associated guanylate kinase family and contain multiple domains for association with signalling proteins. ZO-1 and ZO-2, the most widely studied members of the family, interact with both occludin and claudins and the actin cytoskeleton anchoring the transmembrane adhesion proteins to the cytoskeletal scaffold of the ECs (Kim et al., 2006). Junctional Adhesion Molecules (JAM) JAM-A, JAM-B and JAM-C are present in brain ECs and are involved in the formation and maintenance of the TJ. The transmembrane proteins are connected on the cytoplasmatic side to a complex array of peripheral membrane proteins that form large protein complexes, the cytoplasmatic plaques (Abbott et al., 2006).

The brain endothelium transporters that supply the brain with nutrients include the glucose carrier GLUT1, several amino acid carriers (for example LAT1) and transporters for nucleosides, nucleobases and many other substances (Kim et al., 2006; Abbott et al., 2006).

Astrocytes

Astrocytes have been considered the glue of the CNS which play a role as scaffolds in neuronal development and interactions. It has been revealed that astrocytes take part in control of the CNS vascular tone, neurogenesis and synaptogenesis (Kim et

al., 2006). Astrocytes ensheath the ECs and attached pericytes by end-foot processes. In addition, they interconnect ECs with surrounding neurons (Kim et al., 2006). It has also been speculated that astrocytes may act as intermediaries to or in conjunction with neurons in the moment-to moment regulation of cerebral microvascular permeability, in particular via dynamic Ca^{2+} signalling between astrocytes and the endothelium via gap junctions and purinergic transmission (Hawkins and Davis, 2005). In this sense astrocytes and their precursors have been implicated in the induction of BBB (Rieckmann and Engelheardt, 2003).

Pericytes

Pericytes are in close proximity to ECs, separated only by a shared basement membrane. Interaction between ECs and pericytes are mediated by endothelin-1 (Kim et al., 2006). Pericytes seem to be morphologically, biochemically and physiological heterogenous. They express non-muscle actins and they also contain α Smooth Muscle Actin (αSMA) which is a characteristic of the vascular smooth muscle cell. However, they appear to be pluripotent and have the potential to differentiate into osteoblasts, fibroblast-like cells, chondrocytes and adipocytes. In addition macrophage activity is ascribed to CNS pericytes. They embrace the abluminal endothelial surface of almost all arterioles, venules and capillaries. Ultrastructural views show the interdigitating contacts between pericytes and coverage to the vascular ECs. The recruitment and further interaction of pericytes toward the microvascular endothelial wall are essential for the formation, maturation and maintenance of normal microvascular structure and functions (Lai and Kuo, 2005).

Pericytes migrate away from brain microvessels in rapid response to hypoxia and traumatic brain injury; both of these conditions are associated with increased BBB permeability. Whether pericyte migration plays a causative role in BBB failure has not yet been established. However, pericyte-derived angiopoietins can induce endothelial expression of occludin, a major constituent of BBB TJ, indicating that pericytes are involved in the induction and/or maintenance of barrier properties in the cerebral endothelium in a manner similar to glia (Hawkins and Davis, 2005).

Microglia

Microglia originate from blood-borne cells and comigrate with ECs into the CNS, which are regarded as endogenous immune cells in the CNS (Kim et al, 2006). Mi-

croglia are derived from myeloid cells in the periphery and comprise of approximately 12% of cells in the brain. Microglia density varies according to the brains region in the adult human (0.5-16.6%) and in adult mice and they predominate in the grey matter, with the highest concentrations being found in the hippocampus, olfactory telencephalon, basal ganglia and substantia nigra.

During the development they become activated and enforce the programmed elimination of neural cells. Moreover it seems that they enhance neuronal survival through the release of trophic and anti-inflammatory factors.

In the mature brain, microglia typically exist in a resting state characterized by ramified morphology and monitor the brain environment. Activated microglia in response to brain injury or immunological stimuli undergo a dramatic transformation from their resting ramified state into an amoeboid morphology and present an upregulated catalogue of surface molecules such as CD14, MHC molecules, chemokine receptors and several other markers. In their activated state, they can serve diverse beneficial functions essential to neuron survival guiding migration of stem cells to the site of inflammation and injury and furthermore might be involved in neurogenesis (Block et al., 2007). Moreover they are able to induce clearance of apoptotic corposes involving signalling through the low density lipoprotein receptor which binds ligands including apolipoprotein E and activated α2 macroglobulin as well as apoptotic cells (Hauwel et al., 2005).

Neurons

In adult CNS, neurons are not directly in contact with ECs. Instead astrocyte mediate the neurovascular connection, whereas, during development, undifferentiated neurons can be in contact with ECs. Therefore, early neurons may influence the induction of the BBB in ECs (Kim e al., 2006) secreting an array of growth and neurotrophic factors, cytokines, chemokines and neuroactive peptides (Zhao et al., 2006). Communication between neurons and the vasculature may not simply regulate blood flow but BBB permeability as well. Anatomical evidence has been found for direct innervation of the microvascular endothelium and/or associated astrocytic processes by noradrenergic, serotonergic, cholinergic and GABA-ergic neurons as well as others (Hawkins and Davis, 2005).

1.2.2. BBB in neurologic disorders

The disruption of the BBB is closely related with cerebrovascular diseases such as Alzheimer's disease (AD), Parkinson's disease, ischemia, tumors and diabetic retinopathy (Table 1.4). Pro-inflammatory and pro-angiogenic factors can mediate BBB dysfunction characterized by leaky vessels, astrocyte degeneration, recruitment of activated immune cells and neuronal cell death. In several disorders, decreasing nutrients and oxygen levels can induce Nitric Oxide (NO) and free radicals. Astrocyte-derived NO can interact with free radicals, leading to the neurodegenarative process via impairment of mitochondrial function. Deprivation of oxygen and nutrients also induce hypoxia, which then upregulated the expression of growth factors either directly or through Hypoxia Inducible Factor-1 (HIF-1) that induce VEGF that increase BBB permeability (Choi and Kim, 2008).

Stroke
- Astrocytes secrete TGF-β which down-regulate brain capillary endothelial expression of fibrinolytic enzyme tissue plasminogen activator (tPA) and anticoagulant thrombomodulin (TM)
- Proteolysis of the vascular basement membrane/matrix
- Induction of aquaporin 4 (AQP4) mRNA and protein at BBB disruption
- Decrease in BBB permeability after treatment with arginine vasopressin V1 receptor antagonist in a stroke model

Trauma
- Bradykinin, a mediator of inflammation, is produced and stimulates production and release of IL-6 from astrocytes, which leads to opening of the BBB

Infectious or inflammatory process
Examples include bacterial infections, meningitis, encephalitis and sepsis
- The bacterial protein lipopolysaccharide affects the permeability of BBB TJ. This is mediated by the production of free radicals, IL-6 and IL-1β
- Interferon-β prevents BBB disruption

Multiple sclerosis
- Breakdown of the BBB
- Downregulation of laminin in the BM
- Selective loss if claudin 1/3 in experimental autoimmune encephalomyelitis

HIV
- BBB TJ disruption

AD
- Increased glucose transport, upregulation of glucose transporter GLUT1, altered agrin levels, upregulation of AQP4 expression
- Altered cellular relations at the BBB and changes in the basal lamina and β-Amyloid

Parkinson's disease
- Dysfunction of the BBB by reduced efficacy of P-glycoprotein

Epilepsy
- Transient BBB opening in epileptogenic foci and upregulated expression of P-glycoprotein and other drug efflux transporters in astrocytes and endothelium

Brain tumor
× Breakdown of the BBB
× Downregulation of TJ protein claudin 1/3; redistribution of astrocyte AQP4 and Kir4.1 (inwardly reflecting K^+ channel)
Pain
× Inflammatory pain alters BBB TJ protein expression and BBB permeability

Table 1.4: several pathologies of the CNS involve disturbance of BBB function and, in many of these, astrocyte-endothelial cooperation is also abnormal (Abbott et al., 2006).

The development and the progression of several diseases that affect the CNS are strictly linked to the failure of the BBB. In some cases, increased BBB permeability is a consequence of the pathology, such as with ischemic stroke and traumatic brain injury, whereas in other cases the BBB opening may be a precipitating event, such as with multiple sclerosis. In other conditions in which cerebrovascular abnormalities have been noted, such as AD, the relationship between BBB breakdown and pathology is not clear (Hawkins and Davis, 2005). Moreover the disruption of BBB integrity often accompanies pathological changes in cerebral blood flow and perfusion pressure and evidence supports the idea that such BBB opening may be a selective, compensatory event rather then a simple anatomical disruption (Hawkins and Davis, 2005).

A number of studies using in vitro models of the BBB have indicated that hypoxia and hypoxia/reoxygenation lead to increase permeability and/or disruption of BBB TJ although hypoxic stress may increase permeability via the transcellular route as well. Some reports have indicated that BBB ECs are less responsive to hypoxic stress when cocultured with astrocytes or pericytes; nonetheless, in vivo hypoxia/reoxygenation treatments are associated with increased BBB permeability and decreased expression of occludin as well as activation of the transcription factors nuclear factor-κB and HIF-1. Hypoxic reorganization of BBB TJ seems to be mediated in part by VEGF and NO and VEGF antagonism reduces postischemic edema and injury in vivo. In inflammation disease states, such as multiple sclerosis, AD and HIV encephalitis, the major hallmark is the compromised BBB TJ. The meachanism for TJ alterations is still unclear but it seems possible that cytokines circulating from the site of inflammation to the brain may be involved (Hawkins and Davis, 2005).

1.3. The β-Amyloid peptide

In 1906, Dr. Alois Alzheimer first described the amyloid (or Senile) Plaques (SP) and NeuroFibrillary Tangles (NFTs) that represent the definitive pathological features of the disease that bears his name (Fig. 1.9). These hallmarks remain two of the best criteria on which the diagnosis of AD lies (Dries and Yu, 2008).

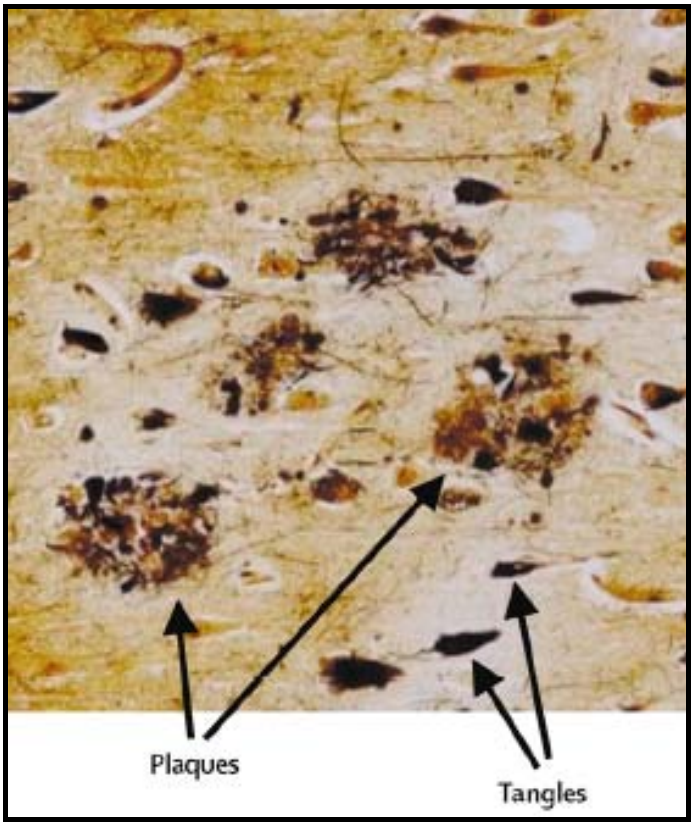

Fig. 1.9: senile plaques and neurofibrillary tangles in the cerebral cortex in AD. Plaques are extracellular deposits of Aβ surrounded by dystrophic neuritis, reactive astrocytes and microglia, whereas tangles are intracellular aggregates composed of a hyperphosphorilated form of the microtubule-associated protein tau (Blennow et al., 2006).

AD is the most common form of dementia in the elderly with half of all individuals over 85 years old developing it. This neurodegenerative disorder is characterized predominantly by initial alteration in recent memory, followed by progressive memory deficits, personality changes and ultimately a complete loss of intellectual ability.

Genetic and epidemiology studies have established that early-onset AD is associated to dominantly inheritable mutations in a least one of three genes (Amyloid Precursor Protein (APP), presenili-1 (PS1) and presenilin-2 (PS2)). Development of

sporadic late-onset AD is associated to age, vascular factors, inflammation and diabetes as well as established susceptibility genes such as apolipoprotein E (ApoE) and the most recently discovered SORL1. In both cases the consequence is the increase in β-amyloid (Aβ) production and deposition respectively (Lacor, 2007).

SP and NFTs, are composed of the Aβ peptide and the tau (τ) protein respectively (Dries and Yu, 2008). Other neuropatological hallmarks of AD include synapse loss, cholinergic and glutamatergic neuronal loss, gliosis and brain atrophy. However NFTs and SP are constantly observed throughout the brain of elderly and centenarian individuals that had not previously met clinical criteria of dementia. In non-demented cases, NFTs are usually restricted to the hippocampal formation, whereas their presence in association areas of the temporal neocortex matches the development of obvious clinical signs of dementia (Lacor, 2007).

1.3.1. Aβ formation

The APP gene is alternatively spliced to yield isoforms of various lengths: the 751- and 770-(longest) amino acid isoforms predominate non-neuronal tissues, while the 695-amino acid form (APP695) is by far the most predominate isoform in neurons. APP and the APP-Like Protein (APLP) have orthologues across nearly all vertebrate and invertebrate animals, and possible roles for APP and its proteolytic products range from axonal transport to transcriptional control and from cell adhesion to apoptosis (Dries and Yu, 2008). APP and its two homologous family members, APLP1 and APLP2, are type I transmembrane proteins, whose extracellular domains contain two conserved sequences (E1 and E2) and whose cytoplasmatic domains contain NPXY sequences important for regulated endocytosis (Hoe and Rebeck, 2008). It is synthesized in the endoplasmatic reticulum, post-trasncriptionally modified in the Golgi (including N- and O-linked glycosylation, sulfation and phosphorilation) and transported to the cell surface via the secretory pathway. APP is also endocytosed from the cell surface and processed in the endosomal-lysosomal pathway, although autophagic vacuoles may also be a site for Aβ production (Sastre et al., 2008).

APP undergoes extracellular cleavage by one of two protease activities, α- or β-secretase, resulting in the release of a large N-terminal extracellular fragment and smaller membrane-bound C-Terminal Fragment (CTF) (Hoe and Rebeck, 2008) (Fig. 1.10).

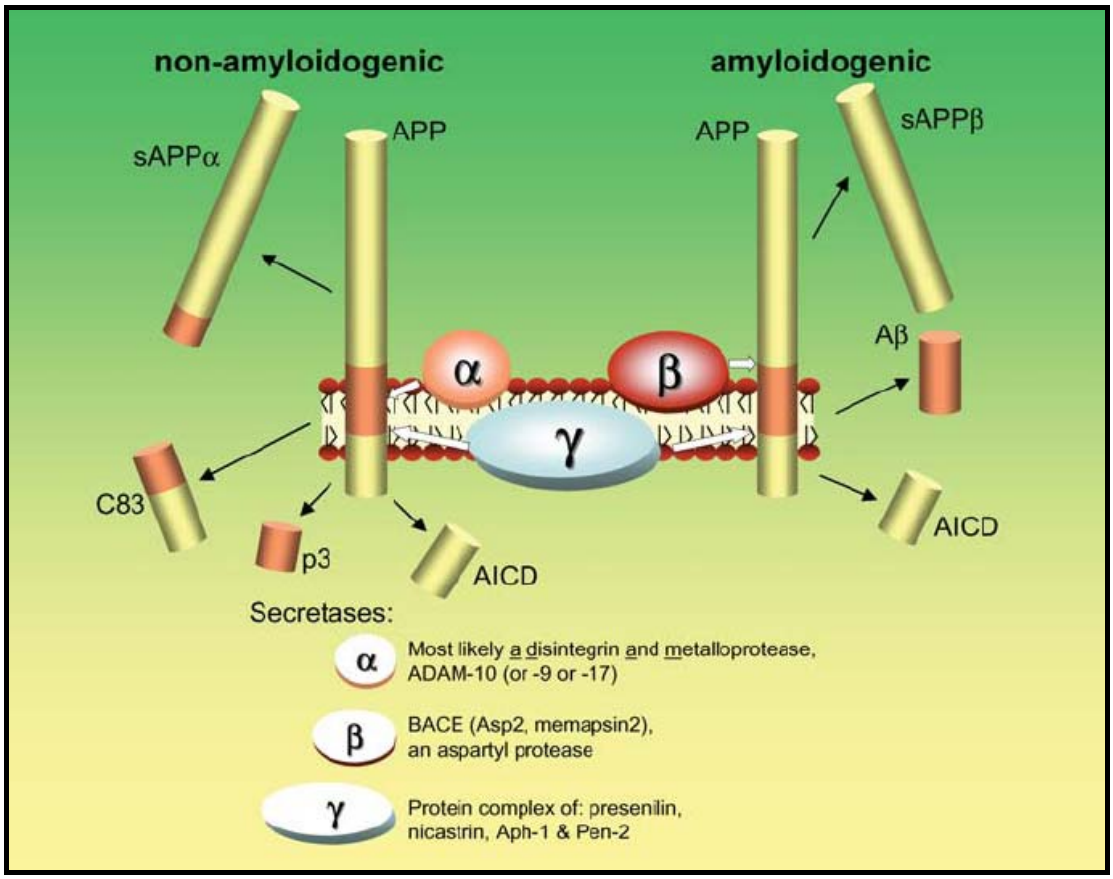

Fig. 1.10: APP processing involves proteolytic cleavage by several secretases. The non-amyloidogenic pathway is initiated by α-secretase cleavage, which occurs in the middle of the amyloid (Aβ) sequence and results in the release of several soluble APP fragments. The amyloidogenic pathway releases Aβ peptides through cleavage by β- and γ-secretases (Pearson and Peers, 2006)•

The α-secretase includes membrane-spanning proteins A disintegrin and metalloproteinase (ADAM)-10 and ADAM-17, and the majority of their activity is thought to occur at the cell surface (Hoe and Rebeck, 2008). The α-secretase cleavage is the first step to the non-amyloidogenic processing pathway of APP molecules. Its cleavage works within the Aβ region (α cleavage site) and precludes the formation of Aβ resulting in the release of a soluble form of APP (sAPPα) and membrane retention of a 83-residue (approximately 10kDa) C-terminal fragment (C83). Subsequent cleavage of C83 by γ-secretase results in an N-terminally truncated and non-toxic Aβ protein of 3kDa (p3).

Aβ is formed from the membrane tethered aspartyl protease β-secretase (BACE 1) cleavage of APP at the Aβ N-terminus (β cleavage site), resulting in a soluble form of APP (sAPPβ) and a 99-residue (approximately 12kDa) C-termini fragment (C99). This C-terminal fragment undergoes subsequent processing by γ-secretase (γ

cleavage site) (Fraering, 2007) resulting in the formation of Aβ peptides from 37 to 49 residues long; these resulting peptides are termed $A\beta_{1-37}$ through $A\beta_{1-49}$, numbered according to the site of cleavage. Two forms are most pertinent to AD etiology: $A\beta_{1-40}$, which is considered "normal" and accounts for approximately 90% of all non-AD Aβ peptides and the more aggregation-prone $A\beta_{1-42}$, which accounts for 5-10% of Aβ peptides in the unaffected, normal brain and it is the first and major peptide to form SP.

The $A\beta_{1-42}$:$A\beta_{1-40}$ ratio has been assimilated as a diagnostic tool for the aberrant processing of APP that leads to AD. The majority of AD-linked mutation in APP occur within the Aβ sequence and the greatest increase is at the $A\beta_{1-42}$:$A\beta_{1-40}$ ratio. The vast number of missense mutations found in the PS1 and PS2 genes either increase the total Aβ peptide load and/or switch the specificity to produce more $A\beta_{1-42}$ and therefore increase the $A\beta_{1-42}$:$A\beta_{1-40}$ ratio *in vitro* and *in vivo* (Dries and Yu, 2008).

1.3.2. Aβ aggregation

Soluble Aβ species found in CSF of AD patients, can be neurotoxic at low concentrations and induce inhibition of long-term potentiation and cognitive dysfunction. The Aβ peptides, in particular the $A\beta_{1-42}$, accumulate into insoluble deposits in fibrillary forms. In this context the misfolding, aggregation and accumulation of the Aβ peptide have been implicated as the primary cause in neuronal death in AD (Deshpande et al., 2006). Nowadays the molecular basis of the early events during the aggregation process and the nature of the structural fluctuations that triggers the misfolding and association of Aβ remain poorly understood (Chi et al., 2008). It has been observed that difference in thermodynamic stability of folded, unfolded and misfolded proteins is not large and the same forces, such as hydrogen bonding, hydrophobic effect, electrostatics, control both native folding and non-native misfolding. It appears reasonable that given modest disturbances, such as a single-point mutation or a change in salt concentration, nearly any polypeptide chain can be driven toward misfolding and aggregation (Murphy, 2007).

It has been shown that $A\beta_{1-40}$ and $A\beta_{1-42}$ peptides have distinct oligomerization pathways. They show different behaviour at the earliest stage of assembly, monomer oligomerization. Studies of the kinetics of Aβ fibril formation have shown that $A\beta_{1-42}$

forms fibrils much faster than $A\beta_{1-40}$ (Kirkitadze and Kowalska, 2005). However increasing evidence from genetics, clinical and cell culture studies suggests that the $A\beta_{1-40}$:$A\beta_{1-42}$ ratio, rather than the total amount of Aβ, is an important determinant of Aβ aggregation, fibrillogenesis and toxicity (Jan et al., 2008).

The fibrillization of Aβ is a complex process involving several discrete steps (Kirkitadze and Kowalska, 2005) (Fig. 1.11).

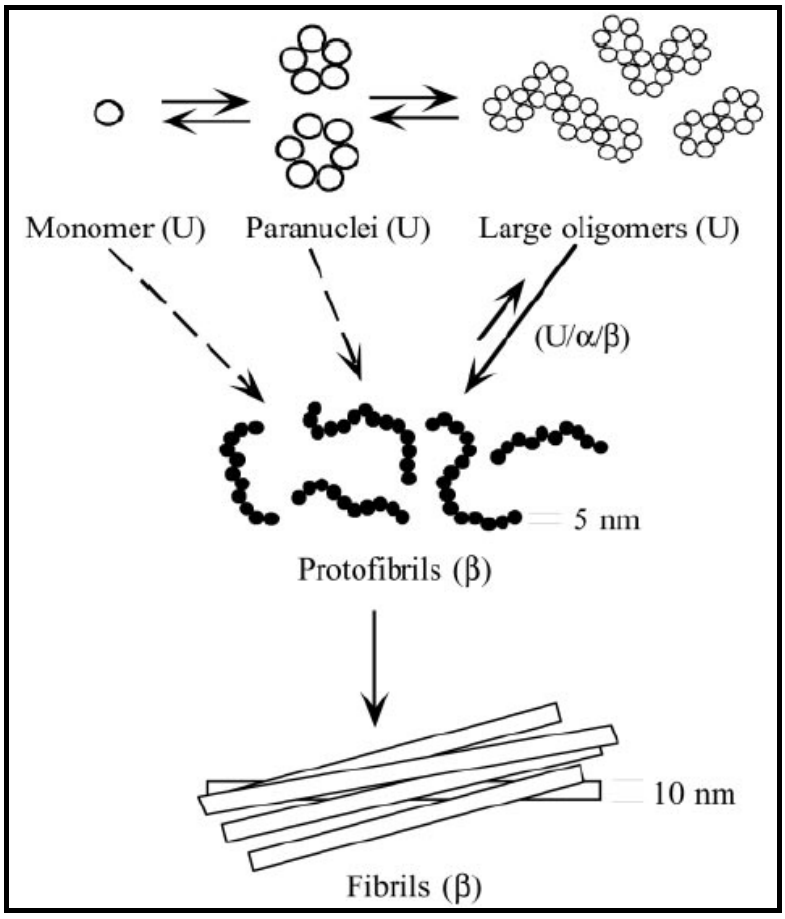

Fig. 1.11: a simple model of $A\beta_{1-42}$ assembly. Monomers rapidly oligomerize into paranuclei. Paranuclei themselves then can oligomerize to form larger, beaded structures. Paranuclei are the initial and minimal structural unit from which $A\beta_{1-42}$ assemblies evolve. The equilibrium between monomer and paranuclei are detectable immediately after peptide dissolution. The conversion to protofibrils is slower but is also reversible. Monomers, paranuclei and large oligomers are predominantly unstructured (U) but do not contain β-sheet/β-turn (β) and helical (α) elements. Protofibril formation involves substantial conformational rearrangements, during which unstructured, α-helix, and β-strand elements (U/α/β)transform into predominantly β-sheet/β-turn structures. Protofibrils may form through the oligomerization of monomers into paranuclei, paranucleus self-association to form larger oligomers and then maturation of these large oligomers into protofibrils. This linear pathway may not be the only one: direct addition of monomers or paranuclei to protofibrils or fibrils can not be ruled out. The final step in the overall pathway is protofibril maturation into fibrils, a process that appears irreversible, at least kinetically. The diameters of the protofibrils and fibrils are indicated but the structures in the scheme are not drawn to scale (Bitan et al., 2003 A).

In vitro, fibril formation occurs readily at concentrations above a "Critical Micelle Concentration" (CMC) that has been found to range from 17.5 and 100μM after which fibrils nucleate within these micelles. The initial phase reflects the energy barrier that must be overcome in order for the otherwise unfolded Aβ to adopt a β-sheet rich conformation and oligomerize into ordered intermediates or protofibrils (Chi et al., 2008). Fibrillization of Aβ is preceded by multiple conformational changes including trimer, pentamer or higher molecular weight complex formation, also known as Aβ-Derived Diffusible Ligands (ADDLs), oligomers composed of 15-20 monomers (AβOs), protofibrils (string oligomers) and dodecameric oligomers Aβ*56 (Deshpande et al., 2006). These intermediate Aβ species are designated collectively as "soluble Aβ" (Glabe, 2004) and they are necessary for fibril elongation (Verdier et al., 2004). The sizes and conformational characteristics of oligomers are quite variable: Aβ peptides form both small spherical oligomers of about 5nm in diameter with molar masses in the 20-50kDa range as well as large spherical oligomers with diameters around 15nm and molar masses approaching 1 million Da (Murphy, 2007).

The initial phase of oligomerization of $A\beta_{1-42}$ monomers involves the formation of pentamer/hexamer units, called paranuclei. They are the initial and minimal structures that can oligomerize to larger forms: large oligomers, protofibrils, fibrils. Monomers, paranuclei and large oligomers are predominately unstructures with only short β-sheet/β-turn and helical elements. During protofibril formation essential conformational changes occur when α-helix and β-strand elements transform into β-sheet/β-turn structures. Differently from $A\beta_{1-42}$, prepared aggregate-free $A\beta_{1-40}$ exists as monomers, dimmers, trimers and tetramers in rapid equilibrium. $A\beta_{1-40}$ oligomerization was particularly sensitive to substitutions of Glu22 or Asp23 and to truncation of the N terminus. $A\beta_{1-42}$ oligomerization, in contrast, is largely unaffected by substitution at position 22 or 23 or by N-terminal truncations, but is affected significantly by substitutions of Phe19 and Ala21. These results reveal that the specific regions and residues that control Aβ oligomerization differ between $A\beta_{1-40}$ and $A\beta_{1-42}$ (Kirkitadze and Kowalska, 2005).

Bitan and co-workers (2003 B) demonstrated that $A\beta_{1-42}$ dipeptide, Ile-41 and Ala-42, mediates formation and self-aggregation of paranuclei. Ile-41 is essential for paranucleus formation whereas Ala-42 is required for paranucleus self-association.

Thus the C-terminal carboxylate group moderates paranucleus self-association and the replacement of the charged carboxylate group by a polar carboxamide function accelerates paranucleus association.

Under normal conditions, brain Aβ is degraded by the peptidases insulin-degrading enzyme, neprilysin and by endothelin-converting enzyme. Aβ is also cleared from the brain in a process balanced by the efflux, mediated by low-density lipoprotein receptor-related protein and the influx, mediated by the Receptor for Advanced Glycation End product (RAGE) of Aβ across the BBB (Blennow et al, 2006). Another mechanism involved in this process is the elimination by bulk flow with interstitial fluid along the perivascular drainage pathway (Boche and Nicoll, 2008). In AD no evidence for any disturbances in these proteolytic enzymes or transport mechanisms have been observed (Blennow et al, 2006).

1.3.3. Aβ effects

Several lines of evidence indicate that physiological levels of Aβ promote cell adhesion, stimulate protein tyrosine phosphorylations and cell proliferation and enhance neurite outgrowth because of its neurotrophic effect (Molnár et al., 2004). Moreover Aβ may play a role in controlling synaptic activity by its depression. In fact increased formation of Aβ and the fragment derived from APP processing provides a negative feedback in hippocampal neurones, since Aβ depresses synaptic activity. Without such depression, synaptic activity could become excessive, leading to excitotoxicity. In primary cultures neurones inhibition of endogenous Aβ production or immunodepletion of Aβ causes neuronal cell death but the same treatment does not affect non-neuronal cells. Perhaps the neuronal cell death in response to secretase inhibition could be restored by the addition of physiological (picomolar) levels of Aβ. Compelling evidence supports a role for Aβ in neuronal survival. The mechanism remains to be determined but may involve altered expression of K^+ channels implicated in neuronal survival or death, in part because they govern excitability and hence the excitotoxicity of released glutamate but also because intracellular concentration of K^+ is a key determinant of apoptosis. The inactivation of K^+ currents of central neurones are suppressed in amplitude by inhibition of the production of endogenous Aβ (Pearson and Peers, 2006). Moreover it has been shown that Aβ peptides stimulate the activity of G

proteins and this activation could be an early step in the molecular mechanism underlying the diverse cellular responses to Aβ (Molnár et al., 2004).

The accumulation of Aβ peptides in SP and in NFTs has been associated with a cascade of neuropathologenic events that induce brain neurodegeneration leading to the cognitive and behavioural decline characteristic of AD (Kirkitadze and Kowalska, 2005). The central hypothesis for the cause of AD is the *amyloid cascade hypothesis* which states that an imbalance between the production and clearance of Aβ in the brain is the initiating event ultimately leading to neuronal degeneration and dementia (Blennow et al, 2006). Hardy and Higgins (1992) hypothesized that neurodegeneration occurring in AD is due to insoluble fibrillar Aβ species that accumulate into SP in the brain. This leads to the formation of NFTs subsequently followed by a massive neuronal loss leading to the observed dementia.

The original amyloid cascade hypothesis was not convincingly able to explain the cellular and molecular mechanisms triggering the full range of neuropathologies associated with AD. Although some reports showed significant correlations of plaque number with dementia, numerous studies have found only weak or no correlation between neocortical plaque densities and clinical severity measures. Moreover the original amyloid cascade hypothesis claimed the fibrillar Aβ ultimately killed neurons, suggesting an irreversibility of the disease (Lacor et al., 2007). Thus in 2002, Hardy and Selkoe proposed a revised amyloid cascade hypothesis, where the small soluble Aβ oligomers, formed prior to fibrillar Aβ deposits and strikingly elevated in the AD brain, play a central role in the pathogenesis of AD. These oligomers are strongly believed to be the “memory-thieves” as they are particularly eager to impact synapse signalling, shape and stability before neuronal death occurs. Many studies have suggested that these oligomers constitute the main causative agent in the pathogenesis of AD, but they do not seem to affect basal synaptic transmission, suggesting that the synaptic alteration observed is initially non-degenerative (Lacor et al., 2007).

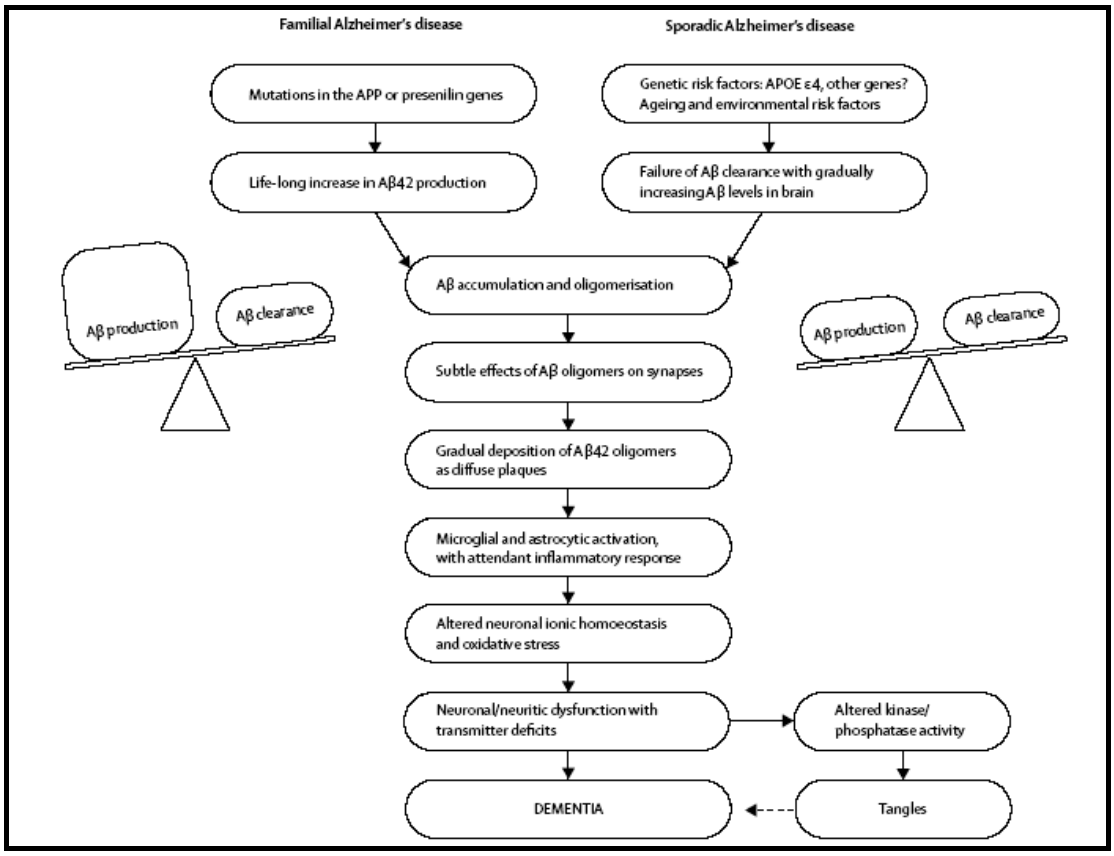

Fig. 1.12: according to the amyloid cascade hypothesis, the central event in the disease pathogenesis is an imbalance between Aβ production and clearance, with increased Aβ production in familial disease and decreased Aβ clearance in sporadic disease. Aβ oligomers could directly inhibit hippocampal long-term potentiation and impairs synaptic function, in addition to the inflammatory and oxidative stress caused by aggregated and deposited Aβ. These processes impair neuronal and synaptic function with resulting neurotransmitter deficits and cognitive symptoms. T pathology with tangle formation is regarded as a downstream event, but could contribute to neuronal dysfunction and cognitive symptoms (Blennow et al., 2006)•

In the last few years another possible mechanism involved in AD has been hypothesized: the *neurovascular hypothesis*. It is based on the observation of neurovascular dysfunctional blood vessels that could contribute to cognitive dysfunction by impairing delivery of nutrients to neurons and by reducing Aβ clearance from the brain. Such cerebrovascular alterations could be initiated by downregulation of the vascular differentiation gene MEOX2, with resulting loss of cerebral microvessels and reduced cerebral blood flow and Aβ efflux from the brain.

Several other hypotheses have been advanced to explain the pathogenesis of AD, including abnormalities in proteins regulating the cell cycle, inflammatory mechanisms, oxidative stress and mitochondrial dysfunction with disruption in neuronal energy metabolism. Although each of these mechanisms could contribute to

disease pathogenesis to what extent they drive the neurodegenerative process is uncertain (Blennow et al., 2006).

AD is characterized by the affection of different types of cells that constitute the BBB such as glial cells and ECs. Aβ peptides seem to play the main role in the pathogenesis of AD even if the mechanisms and the more toxic aggregated form are still uncertain. Some authors support the hypothesis that the insoluble and fibrillary form exerts the more toxic effects while others believe that the insoluble aggregates are the principal cause of the cell death. Recent evidence implicates soluble ADDLs and protofibrils rather than mature amyloid plaques as the most toxic forms of Aβ (Zhao et al., 2006).

Numerous data has established that Aβ-induced neurotoxicity occurs through the induction of apoptotic pathways. It has been observed that $A\beta_{1\text{-}42}$ increases the accumulation of mRNA of the pro-apoptotic gene bax in neuroblastoma cell cultures. Apoptosis is a tightly regulated process, which involves changes in the expression of a distinct set of genes. In particular two of the major genes responsible for regulating apoptosis cell death are bcl-2 and bax: bcl-2 encodes a 26kDa protein that is able to block the apoptotic mechanism while bax promotes apoptosis by traslocation into the mitochondrial membrane and facilitating cytochrome c release, downstreaming apoptotic events (Clementi et al., 2006). Moreover, cell biological studies on neurons on culture and autopsied AD brains demonstrate that Aβ is generated within the neurons, essentially in the ER and Golgi, and then accumulates progressively inside these neurons from where it triggers cell dysfunction before plaque formation and tangle pathology. Thus neuronal dysfunction and degeneration could be caused by and intraneuronal accumulation of Aβ rather than by an extracellular process. In this hypothesis a large amount of evidence suggests that mitochondria could intervene in the mechanisms by which intraneuronal Aβ triggers neuronal dysfunction and degeneration with structural and enzymatic alterations of mitochondria (Aleardi et al., 2005; Zhao et al., 2006).

Some studies suggest that Aβ may interact with redox-active metals such as Ca^{2+}, Fe^{2+}, Zn^{2+} and Al^{3+} that not only promote Aβ peptide aggregation but also release peroxides and other Reactive Oxygen Intermediates (ROIs) that interact with cellular membranes inducing lipid peroxidation and oxidative modification of membrane transporters, receptors and ion channel. This leads to further disruption of

normal physiological cellular metabolism (Zhao et al., 2006) such as calcium homeostasis influx into cytoplasm, which in turn leads to hyperactivation of Ca^{2+}-dependent proteases and kinases and causes free radical generation and various forms of peroxidative injury that activates glia and microglia (Lacor et al., 2007). In fact, immunohistochemical examinations have shown clusters of activated astrocytes and microglia surrounding the Aβ deposits (Heneka and O'Banion, 2007) suggesting that inflammation could play a key role in progression of AD. Thus these lesions could generate chemotactic molecules that mediate astrocyte recruitment which, together with Aβ, could most likely prolong neuroinflammation and contribute to NO-mediated neurotoxicity by expressing the inducible Nitric Oxide Synthase (iNOS) and the L-arginine-supplying enzyme argininosuccinate synthetase (Sastre et al., 2006). Moreover, Aβ deposits could activate microglia to recruit astrocytes by secreting acute-phase proteins such as complement factors and cytokines. Reactive microglia and astrocytes additionally generate proinflammatory mediators, including cytokines, chemokines, prostaglandins, neurotoxic secretory products, Reactive Oxygen Species (ROS) and NO (Choi et al., 2008), all of which can contribute to neuronal dysfunction and cell death, creating a vicious cycle (Heneka and O'Banion, 2007). Chronically activated microglia and astrocytes can kill adjacent neurons by the secretion of highly toxic products. The toxins and inflammatory factors trigger inflammatory cascades, thereby exacerbating conditions in AD (Zhao et al., 2006).

It should be noted that some aspects of microglia function may be beneficial, since activated microglia are able to reduce Aβ accumulation by increasing its fagocytosis, clearance and degradation (Heneka and O'Banion, 2007). If microglial or astrocytic activation fails to clear the toxic forms of Aβ, the innate immune response became chronic and neurotoxic (Man et al., 2007).

Recent evidence suggest that neurons are capable of producing inflammatory mediators supporting the idea that neurons themselves may exacerbate local inflammatory reactions and thus contribute to their own destruction in AD (Heneka and O'Banion, 2007). Moreover an increased occurrence of T cells in the brains of patients with AD has been observed suggesting that T cells may participate in the inflammatory process of the disease. It has also been demonstrated that peripheral T cells of AD patients overexpress Macrophage Inflammatory Protein (MIP)-1α, which binds to its

receptor CCR5 on brain ECs, promoting T cells (Man et al., 2007) and monocytes (Marco and Skaper, 2006) migration through the endothelial TJ.

The accumulation of a significant body of evidence within the last several years indicates that AD is also a vascular disorder whose underlying cause is cerebral hypoperfusion. Chronic overproduction of Aβ and accumulation and/or deposition of Aβ in the matrix of vascular ECs, perivascular cells especially in perivascular space may be an indication of the breakdown of the BBB during the development, progression and maturation of AD. Reduced or low vascular blood flow is a prominent feature if the brain undergoes chronic hypoxia/hypoperfusion and may be a major initiating factor during the development and maturation of AD (Aliev et al., 2004). In particular cerebrovascular pathologies such as structural alterations, atherosclerotic lesions and impaired hemodynamic responses are suggested as early features of AD. It remains unclear whether the reduced cerebral blood flow is a response to neuronal damage or a factor initiating the characteristic neuropathology (Meyer et al., 2008). Hypertension, diabetes, hypercholesterolemia, concentration of cholesterol oxides, neural inflammation and the apolipoproteinE-4 genotype, as well as aging may bring about chronic damage to the brain capillary ECs, which may further result in chronic hypoperfusion and dysregulation of the BBB. The normal ability of the BBB to clear Aβ deposits from brain is compromised and Aβ accumulates in both brain parenchyma and blood vessels, allowing the expression of Aβ peptide neurotoxicity (Zhao et al., 2006). Starting from these observations numerous studies had been performed to determine the effect of Aβ peptides on cultured ECs. The main effects include induction of CD40, phospholipid turnover and overt cell death (Marco and Skaper, 2006). Specifically, it has been observed that Aβ induces loss of EC viability by increasing the degree of apoptosis in HUVECs by DNA condensation, mitochondial dysfunction and activation of caspase-3. Our previously data (Folin et al., 2006) demonstrate that cytotoxic effect induced by Aβ peptides occurs through two different pathways: caspase-8 activation and increase of oxidative stress. Moreover Aβ might also interfere with certain angiogenic and vasomotor homeostatic properties as NO production and VEGF-induced angiogenesis (Suhara et al., 2003). The accumulation of oxidative stress products and misbalance in vasoactive substances (Aliev et al., 2004) and the high levels of inflammatory proteins released by ECs in AD may collectively support neuroinflammatory

cascades, killing neurons and further damaging the integrity of the BBB (Zhao et el., 2006) by disruption of TJ protein complexes (Marco and Skaper, 2006) which in turn induces the progressive release of toxic products and contributes to the neurophatogenesis of AD (Zhao et el., 2006).

1.4. Angiogenesis and AD

The correlation between angiogenesis and AD is still debated. Some reports support the idea that AD is accompanied by increase capillary density, others that AD brains are characterized by decreasing amount of vessels.

A large amount of evidence has supported the hypothesis that AD is mediated by **pathological angiogenesis**. Vagnucci and Li (2003), starting from the observations that putative AD-preventive agents inhibit angiogenesis, hypothesized that brain vascular ECs could have a putative role in AD pathogenesis. Neovascularization in the brain of AD patients occurs in response to impaired cerebral perfusion and vascular injury (Figure 1.13).

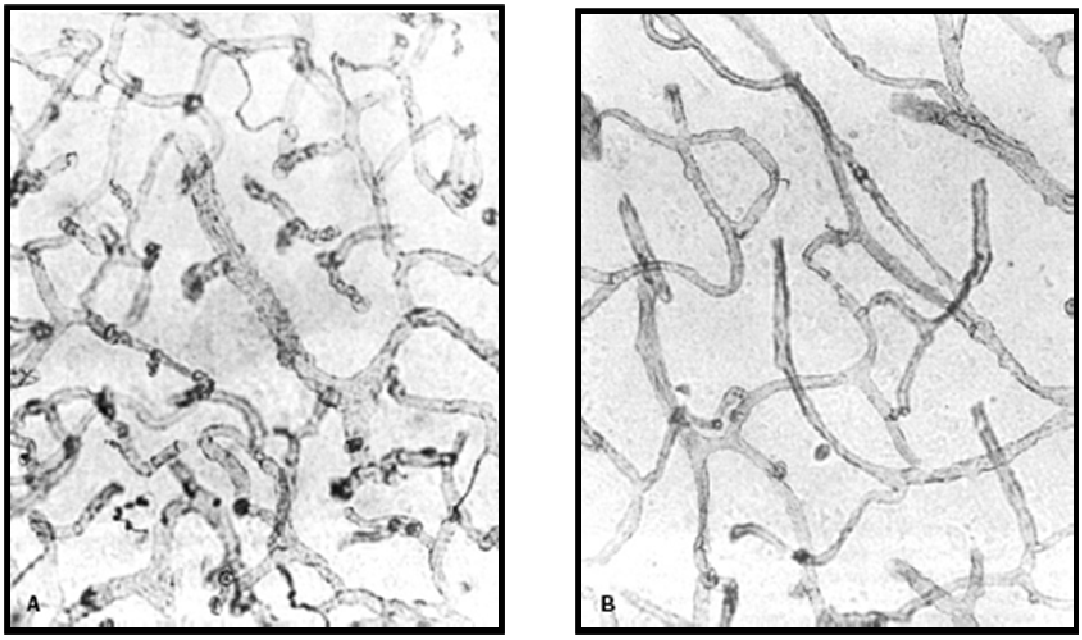

Fig. 1.13: microvascular density in brains in AD (A) and in normal age-matched controls (B) (Vagnucci and Li, 2003).

Morphological and biochemical evidence includes regionally increased capillary density, vascular loop formation, glomeruloid vascular structures formation and

expression of angiogenic factors. In particular significant cerebral microvascular pathology, deficient clearance of Aβ across the BBB and increased density of microvessels in the pathologic lesions are all frequent neuropathological features of AD (Chiappelli et al., 2006).

Differently from normal brain capillaries, in AD the distances between the adjacent capillaries enable rapid diffusion-mediated transport of nutrients and oxygen within brain interstitial fluid from blood to neurons and rapid diffusion of neurotransmitters and metabolic waste products from synapses and neurons back to the microcirculation. In AD the endothelium degenerates, promoting local neuroinflammatory vascular responses, including the activation of brain endothelium, perivascular microglia, pericytes and astrocytes. Activated cells produce pro-inflammatory cytokines and vasoactive substances, which could contribute to cognitive defects (Zlokovic, 2005).

In AD the cerebral microvasculature is in a "pro-angiogenic state" expressing VEGF, Ang-2 and releasing high levels of MMP-2 and MMP-9 (Thirumangalakudi et al., 2006). Moreover the gene expression of stress-related genes that have significant potential to promote angiogenesis are up regulated (Pogue and Lukiw, 2004) while the gene expression of thrombospondin, an endogenous angiogenesis inhibitor, is reduced near focal AD lesions (Vagnucci and Li, 2003). Furthermore it has been demonstrated that VEGF levels are elevated in the CSF and SP regions of the brain and of AD patients (Tarkowski et al., 2002) and that it co-accumulates with Aβ in SP. Most of the VEGF expressed as a compensatory mechanism to hypoperfusion may bind to Aβ deposits without turning over. This situation may result in local deficiency of soluble VEGF that is needed for protection of cerebral vessels and neurons against hypoperfusion. Moreover, Aβ may act as a molecular sink for VEGF expressed in AD brain and could aggravate the progression of AD by blocking the angiogenic and neuroprotective activities of VEGF (Yang et al., 2004).

In vivo observation on rabbit cornea assay shown that Aβ peptides tested at 100 or 200ng/pellet produce angiogenesis accompanied by marked inflammatory reaction. Moreover, i*n vitro* studies demonstrated that Aβ peptides promote EC growth, migration and microtubule network formation when assayed in postcapillary venular ECs (Cantara et al., 2004).

On the other hand many studies demonstrated a decreased microvascular density in AD brain (Jellinger, 2002; Edelberg and Reed, 2003), supporting the idea that the released mediators do not lead to increased vascularity in AD. It has been observed that Aβ peptides exert antiangiogenic effect both *in vivo* and *in vitro* experiments (Paris et al., 2004). Thus it is possible that in response to hypoxia brain ECs become activated, as occurs in inflammation, however unlike the normal inflammatory response this alteration in the endothelium becomes irreversible and leads to an endothelial phenotype characterized by release of numerous mediators (Thirumangalakudi et al., 2006) suggesting a failure of a reparative angiogenic mechanism. In AD microvessels associated with Aβ deposits display non-functional endothelium along with thinning of the basement membrane (Paris et al., 2004).

2 Material and methods

2.1. Cell cultures

2.1.1. Human Cerebral Endothelial Cells (HCECs)

Isolation and culture

Microvascular HCECs were isolated from fresh biopsies of normal human brain. The samples were obtained from surgical procedures on deep seated lesions. Informed consent of the five patients (aged 30-40 years) was obtained and the protocol was approved by the local ethics committee.

Tissue was sectioned into 3 mm^2 fragments and washed with saline solution (PBS) containing 10% of antibiotic-antimycotic solution (penicillin G 100UI/ml, streptomycin 100µg/ml and amphotericin B 0.25µg/ml) (Sigma Aldrich Corp., St. Louis, Mo). The sections were then incubated in 0.1% collagenase B-dispase (Roche Applied Science, Penzberg, Germany) saline solution at 37°C for 25 minutes in Dubnoff shaking water bath (GFL, Burgwedel, Germany). The pre-digested tissue was triturated by a 2 ml pipette for 2 minutes and then filtered through a 100µm strainer (Bencton-Dickson Labware, Franklin Lakes, NJ). Cell suspension was centrifuged and re-suspended in culture medium MV2 supplemented with growth factors and 20% of Foetal Bovine Serum (FBS) (PromoCell, Heidelberg, Germany). Cells obtained were seeded at a density of 10^4 cells/cm^2 on Petri dishes previously coated with fibronectin (1µg/cm^2) (Sigma Aldrich Corp., St. Louis, MO) and grown for 24 hours at 37°C, 5% CO_2. Cells were washed vigorously with PBS to remove unattached cells and fed with fresh Endothelial Cell Growth Medium MV2 (Promocell, Heildelberg, Germany) supplemented with 20% of FBS.

Confluent HCEC primary cultures were purified using Ulex Europaenus Agglutinin I (UEA)-coated (Vector Laboratories, Ltd, Peterborough, UK) Dynabeads M-450 Tosylactivated (Oxoid, Hampshire, UK) as described by Jackson and coworkers (1990). Dynabeads M-450 Tosylactivated are magnetic polystyrene beads coated with a polyurethane layer. The polyurethane surface is activated by p-

toluenesulphonyl chloride to provide reactive groups for covalent binding of proteins or other ligands containing primary amino or sulphydryl groups. Coated procedure of beads consists in a washing step, coating procedure and cell immunoseparation. The first step is necessary to equilibrate beads in appropriate buffer (0.1M phosphate buffer pH 7.4) allowing beads to be ready for coating. During the second step 5μg of pure antibody/10^7 beads were added to beads solution (concentration 4-10 x 10^8 beads per ml final coating solution) and continued to vortex for 24 hours at 37°C. After incubation coated beads were washed in 0.1% BSA (Sigma-Aldrich Corp., St. Louis, MO) saline solution, re-suspended in buffer solution and conserved at 4°C. In the third passage confluent cells were counted in Bürker chamber and suspended in 0.1% BSA (Sigma-Aldrich Corp.) salt solution (10^6cells/ml). Beads were added at cell solution (5 beads per cell). After 30 minutes of incubation at 4°C HCECs bound to the lectin-coated beads were collected with a magnetic particle concentrator and any unbound cells were removed with two washes with buffer solution and re-suspended in culture medium. Cells were seeded on fibronectin-coated Petri dishes (1μg/cm^2) (Sigma Aldrich Corp.) to improve their adhesion and growth. Cultures became confluent within 5-8 days.

Cells that did not interact with beads were seeded and subjected to another immunoseparation.

To obtain subcultures cell culture medium was removed and 0.02% EDTA and 0.25% Trypsin (1:1 v/v) (Sigma Aldrich Corp., St. Louis, MO) saline solution was added to PBS washing cells. Detached cells were re-suspended in a determined volume of cell medium. 0.1ml of cells were added to 0.3ml of Trypan Blue (Sigma Aldrich Corp., St. Louis, MO) and counted in Bürker chamber. Remaining cells were then seeded at desired concentration. In all the experiments II and III passage cells were used.

Characterization

Immunocytochemistry was performed to characterized the isolated cells with rabbit polyclonal anti-human von Willebrand factor (vWf) (Dako Corp., Carpinteria, CA), the most significant endothelial cell marker (Lamszus et al., 1999).

Cells were grown in fibronectin-coated chamber slides (1μg/cm^2) (Sigma Aldrich Corp., St. Louis, MO) until confluence. After three washings with PBS cells

were fixed in ice-cold acetone for 10 minutes at 4°C. Immunostaining was performed at room temperature and cells were washed three times with PBS after each step. 1% BSA (Sigma-Aldrich Corp., St. Louis, MO) PBS solution was used for antibody dilution.

Cells were rehydrated and treated with 1% Triton in PBS for 5 minutes and then incubated with 1% BSA (Sigma-Aldrich Corp.) in PBS for 15 minutes to block non-specific binding sites. The primary antibody rabbit anti-human vWf (dilution 1:300) was added for 1 hour and then the secondary peroxidase conjugated anti-rabbit IgG antibody (Dako Corp., Carpinteria, CA) (diluted 1:150) for 30 minutes. The reaction was developed with avidin-biotin amplified immunoperoxidase method, using the Large Volume Dako LSAB Peroxidase kit (Dako, Glostrup, Denmark). Samples were counterstained with hemotoxylin (Merk KGaA, Darmstadt, Germany). Negative control was performed omitting the primary antibody. Slides were mounted with Eukitt (Fluka, Buchs, Switzerland). Images were captured using a camera connected to Laborlux S microscope (Leitz, Wetzlar, Germany).

Angiogenic capability on *in vitro* Matrigel

To assess the functional characteristic of HCECs, the capability to form capillary-like structures, cells were seeded on Matrigel, soluble basement membrane extract of the Engelbreth-Holm-Swarm tumor that gels at room temperature to form a genuine reconstituted basement membrane. The Matrigel used to perform experiments was Growth factor Reduced Matrigel™ Matrix (Bencton-Dickinson Labware, Bedford, MA) containing a lower quantity of growth factor in comparison to Matrigel Matrix, to decrease the possible interference between the factor to test and the growth factor contained into the Matrigel. Growth factors present in Reduced Matrigel™ Matrix are:

basic Fibroblast Factor	0-0.1pg/ml
Epidermal Growth Factor	<0.5ng/ml
Insulin like Growth factor-1 (IGF-1)	5ng/ml
Nerve Growth Factor	<0.2ng/ml
Platelet Derived Growth Factor (PDGF)	<5pg/ml
Transforming Growth Factor-β (TGF-β)	1.7ng/ml

Matrigel was defrost overnight at 4°C and then 50µl/cm^2 of growth surface were added on ice-cold plates. Plates were incubated for 30 minutes at 37°C to allow Matrigel to became gel. HCECs were seeded (2.5 x 10^4 cells/cm^2) on Matrigel in 500µl of MV2 (Promocell, Heildelberg, Germany) added by 10% FBS (Promocell, Heildelberg, Germany), 1% antibiotic-antimycotic (Sigma-Aldrich Corp., St. Louis, MO) solution and incubated for 24 hours at 37°C, 5% CO_2. At the end of incubation cells were washed with PBS and fixed with 10% formaldehyde in PBS for 24 hours. Cells were observed by Laborlux S microscope (Leitz, Wetzlar, Germany) and images were captured using a camera connected to it.

2.1.2. Rat Cerebral Endothelial Cells (RCECs)

Isolation and culture

Microvascular RCECs were isolated following Abbott and co-workers method (1992) modified by Baiguera and collaborators (2004). Sprague-Dawley male rats (Charles-River, Como, Italy) were used and the experiment protocol was approved by the local Ethics Committee for Animal Studies. The brains were removed and washed in saline solution (PBS) containing 10% of antibiotic-antimycotic solution (penicillin G 100UI/ml, streptomycin 100µg/ml and amphotericin B 0.25µg/ml) (Sigma-Aldrich Corp., St. Louis, MO). External connective share was removed and resting brain was minced. The suspension was washed in saline solution to reduce fat components and then it was incubated in 0.1% collagenase B-dispase (Roche Applied Science, Penzberg, Germany), HEPES (10mM) (Sigma Aldrich Corp., St. Louis, MO) and DNasi (20UI/ml) (Sigma Aldrich Corp., St. Louis, MO) saline solution at 37°C for 1 hour in Dubnoff shaking water bath (GFL, Burgwedel, Germany) to separate microvessels from extracellular matrix and other cellular components. After centrifugation the pellet was re-suspended into 25% BSA (Sigma-Aldrich Corp., St. Louis, MO) density-dependent centrifugation solution in order to separate capillary fragment (heavier) to myelin, neurons, astrocytes and other cellular fragments (lighter). Capillary fragments were re-suspended in MV2 (PromoCell, Heildelberg, Germany) and they were seeded into Petri dishes previously coated with human fibronectin (1µg/cm^2) (Sigma-Aldrich Corp., St. Louis, MO). The medium was changed with new MV2 (PromoCell) every two days until confluence.

In order to separate endothelial cells from contaminant cells, immunoseparation was performed using a modification of the method described by Jackson and coworkers (1990) and Dynabeads M450 Tosylactivated magnetic beads (Oxoid, Hampshire, UK) coated with mouse anti-rat CD31 antibody (AbD Serotec Ltd, Oxford, UK) were used. Beads were prepared following the protocol utilized for Ulex europaenus agglutinin I (UEA)-coated beads.

To obtain subcultures cell culture medium was removed and 0.02% EDTA and 0.25% Trypsin (1:1 v/v) (Sigma Aldrich Corp., St. Louis, MO) saline solution was added to PBS washing cells. Detached cells were re-suspended in a determined volume of cell medium. 0.1ml of cells were added to 0.3ml of Trypan Blue (Sigma Aldrich Corp., St. Louis, MO) and counted in a Bürker chamber. Remaining cells were then seeded at desired concentration. In all the experiments II and III passage cells were used.

Characterization

The phenotype of RCECs was confirmed by means of expression of vWF. Immunocytochemistry was performed using antibody anti-vWf. Cells were seeded on fibronectin (1μg/cm^2)-coated slides (Sigma-Aldrich Corp., St. Louis, MO) and grown until confluence. After three washing with PBS cells were fixed and with HCl and ethanol (1 part of 1% HCl and 99 parts of 70% ethanol). After washing with PBS cells were treated 20 minutes with 0.5% BSA (Sigma-Aldrich Corp., St. Louis, MO) saline solution to block non-specific binding sites and incubated with primary antibody (1:300) in 0.5% BSA (Sigma-Aldrich Corp.) saline solution for 1 hour at room temperature. After three washings with PBS cells were incubated with peroxidase conjugated anti-rabbit IgG antibody (diluted 1:150 in PBS) (Dako Corp., Carpinteria, CA) for 30 minutes at 37°C. The substrate, composed by 0.02% H_2O_2 with 3-amino-9-ethylcarbazole (AEC) dissolved in 20% dimethylformamide (DMF), a chromogenous soluble compound transformed into an insoluble reddish compound by peroxidase enzyme, was added (Vector Laboratories Ltd, Peterborough, UK). Slides were then washed with distilled water to remove the overplus of AEC. Negative control was performed omitting the primary antibody. Slides were mounted with Eukitt (Fluka, Buchs, Switzerland). Images were captured using a camera connected to optical Laborlux S microscope (Leitz, Wetzlar, Germany).

Angiogenic capability on *in vitro* Matrigel

To assess the functional characteristic of RCEC cells were seeded on Matrigel following the procedure used on HCECs.

2.1.3. Rat Hippocampal Astrocytes (RHAs)

Isolation and culture

Primary cultures were obtained using Sprague-Dawley pups of 1-2 days as described by McCarthy and de Vellis (1980). Cerebral hemisphere were removed, meninx were taken out and the obtained hippocampus was chopped into small pieces. Matrix was dissociated in trypsin (0.8mg/ml) (Sigma-Aldrich Corp., St. Louis, MO) saline solution continued vortex for 10 minutes at 37°C. After some centrifugation cells were re-suspended in Basal Medium Eagle (BME) (Sigma Aldrich Corp., St. Louis, MO) added of 2mM glutamine (Sigma-Aldrich Corp., St. Louis, MO), 20mM $NaHCO_3$, 25mM KCl, 10% FBS (PromoCell, Heidelberg, Germany) and 1% antibiotic-antimycotic solution (Sigma Aldrich Corp., St. Louis, MO) and seeded in polylysine-coated Petri dishes (2.5µg/cm^2) (Sigma-Aldrich Corp., St. Louis, MO).

After 14 days of culture, Petri dishes were shaken for 6 hours to remove microglia and oligodendrocytes, and Petri attached astrocytes were then detached using 0.02% EDTA and 0.25% Trypsin (1:1 v/v) (Sigma-Aldrich Corp. St. Louis, MO) saline solution and seeded for the experiment.

Characterization

Immunofluorescence was performed on RHA primary cultures to ensure the pureness of the cultures using antibody anti-Glial Fibrillary Acidic Protein (GFAP), specific cytoplasmatic glial filaments. Cells were seeded in chamber slides (5 x 10^6 cell/cm^2) (Becton-Dickson, Bedford, MA) fixed with ice-cold ethanol, treated with 1% Triton for 5 minutes at room temperature and incubated with 0.5% BSA (Sigma-Aldrich Corp.) saline solution for 30 minutes to block non-specific binding domain. Cells were then incubated with primary monoclonal antibody mouse anti-GFAP (dilution 1:800) (Chemicon International, Temecula, CA) in 0.5% BSA (Sigma-Aldrich Corp., St. Louis, MO) saline solution for 1 hours at 37°C. After three washings with PBS cells were incubated with secondary texas red anti-mouse IgG (1:200) (Vector Laboratories Inc., Burlingame, CA) for 30 minutes and treated with Vectashield®

mounting medium with 4,6-DiAmidino-2-PhenylIndole (DAPI) (Vector Laboratories Inc, Burlingame, CA) to mark nuclei. Negative controls were obtained using the same procedure omitting the primary antibody. Slides were observed using fluorescence Laborlux S microscope (Leitz, Wetzlar, Germany).

2.1.4. Cell culture mediums

Endothelial Cell Growth Medium

The PromoCell Endothelial Cell Growth Medium MV2 (PromoCell, Heidelberg, Germany) was used for culturing endothelial cells, HCECs and RCECs. The medium kit contains the base medium and all supplements required for producing the complete medium. Before the first use the base medium was supplemented with PromoCell Supplement Pack and the complete growth medium was made up of:

Fetal Calf Serum	5%
Epidermal Growth Factor	5.0ng/ml
Hydrocortison	0.2µg/ml
Vascular Endothelial Growth Factor	0.5ng/ml
basic Fibroblast Factor	10ng/ml
R3 Insulin like Growth Factor (R3 IGF-1)	20ng/ml
Ascorbic Acid	1µg/ml

Astrocytes Growth Medium

Astrocytes growth medium used to cultivate RHAs was Basal Medium Eagle (BME) added with:

Fetal Bovine Serum	10%
Streptomycin	0.1mg/ml
Glutamine	0.2mM
Sodium bicarbonate	20mM
Potassium chloride	25mM

Assay Medium

Endothelial Cell Growth Medium MV (PromoCells, Heidelberg, Germany) was used for culturing endothelial cells, HCECs and RCECs, in absence or in presence of different factors to test. Before the first use the base medium was supple-

mented with PromoCell Supplement Pack (PromoCell, Heidelberg, Germany) and the complete growth medium was made up of:

Fetal Calf Serum	2.5%
Epidermal Growth Factor	10ng/ml
Hydrocortison	1μg/ml
Endothelial Cells Growth Supplement/Heparin (ECGS/H)	0.4%
Amphotericin B	50ng/ml
Gentamicin	50μg/ml

Tests on RHAs were performed using BME (Sigma-Aldrich Corp., St. Louis, MO) added with:

Fetal Bovine Serum	2.5%
Streptomycin	0.1mg/ml
Glutamine	0.2mM
Sodium bicarbonate	20mM
Potassium chloride	25mM

2.2. Experimentation with $A\beta_{1-40}$ and $A\beta_{1-42}$ peptides

2.2.1. Preparation of peptides

Rat $A\beta_{1-40}$ and $A\beta_{1-42}$ peptides (Calbiochem, La Jolla, CA) tested on cells were dissolved in sterile distilled water at concentration 10^{-3}M.

Different experimental conditions were assayed:

- non-treated cells (Control)
- cells treated with $A\beta_{1-40}$ 10^{-7}M
- cells treated with $A\beta_{1-42}$ 10^{-7}M

2.2.2. Angiogenic activity *in vivo*. Chorio-Allantoic Membrane (CAM) assay

Fertilized white Leghorn chicken eggs (30 for each series) were incubated under conditions of constant humidity at 37°C. On the third day of incubation a square window was opened in the shell after removal of 2-3ml of albumen to allow detach-

ment of the developing CAM. The window was covered with a transparent glass of the same dimension, sealed with paraffin and the eggs were returned to the incubator.

In a first series of experiments, on incubation day 8, under sterile conditions within laminar flow hood, CAMs were implanted with 1mm^2 sterilized gelatine sponges (Gelfoam Upjohn Co, Kalamazoo, MI) (Ribatti et al., 1997) loaded with 50ng/embryo of Aβ_{1-40} and Aβ_{1-42} peptides (Calbiochem, La Jolla, CA) dissolved in 1μl saline solution (PBS). CAMs implanted with sponges loaded with PBS alone or with 500ng/embryo of human recombinant FGF-2 (R&D Systems, Abindgton, UK) were used as negative and positive controls, respectively. CAMs were examined daily until day 12. CAMs were processed for light microscopy: after the embryos and their membranes were fixed *in ovo* in Bouin's fluid, the sponges and the underlying and immediately adjacent CAM portions were removed, processed for embedding in paraffin. 8μm serial-sections cut along a plane parallel to the CAM surface were stained with 0.5% toluidine blue and observed under a Zeiss Axiophot-2 light microscope (Zeiss S.p.a., Arese, Italy).

Angiogenesis was measured in the sponges by a planimetric "point counting" method (Ribatti et al., 1995) for the computerized image analysis (KS 300 software, Zeiss S.p.a., Arese, Italy) four to six x250 fields covering almost the entire field of every third section within 30 serial sections of at least two sponges per sample were analysed with a superimposed 144-point square reticulum (0.0186mm^2/field and 129.13μm^2/point) to determine the number of microvessels (capillaries and post-capillary venules) both inside the sponges and at the boundary between the sponges and the surrounding CAM mesenchyme. The microvessel area was then measured within the reticulum area as the sum of points that hit microvessels, and recorded as the mean percent-age±standard deviation per sponge and samples.

2.2.3. Angiogenic activity *ex-vivo*. Aortic-ring assay

Sprague-Dawley male rats (1-12 months old) were killed and the experiment protocol was approved by the local Ethics Committee for Animal Studies.

1-2mm vessels ring obtained from aorta were positioned in 24-multiwell plates with the lumen oriented horizontally. 30μl of Matrigel previously defrosted overnight at 4°C were spread onto each aorta section and the organ culture was kept at

37°C in 5% CO_2 to allow the Matrigel to solidify. After 20 minutes of incubation MV in absence or in presence of $A\beta_{1-40}$ or $A\beta_{1-42}$ peptides 10^{-7}M was added. After 12 days, pictures were taken with a Labolux-S microscope (Leitz, Wetzlar, Germany).

2.2.4. Angiogenic activity *in vitro* on HCECs and RCECs

2.2.4.1. Proliferation

To determine the effect of treatment on cellular proliferation Cell Proliferation ELISA BrdU assay (Roche Applied Science, Monza, Italy) was used. The assay is based on the measurement of BrdU incorporation during DNA synthesis. Cells were seeded (1.5 x 10^4 cells/cm^2) in 96 wells plates and cultured for 24 hours. The medium was removed and MV (PromoCell, Heidelberg, Germany) in absence or in presence of $A\beta_{1-40}$ or $A\beta_{1-42}$ 10^{-7}M (Calbiochem, La Jolla, CA) was added for 24 or 48 hours. Three controls were performed:

1. **blank**: has to be performed in each experimental setup. The blank provides information about the unspecific binding of BrdU and anti-BrdU-POD conjugate to the plate. The absorbance value obtained in this control has to be subtracted from all other values.
2. **background control**: it provides information about the unspecific binding of the anti-BrdU-POD conjugate to the cells in absence of BrdU.
3. **control of spontaneous proliferation**: to determine the proliferation degree of non-treated cells.

18 hours before the end of the incubation BrdU was added to the cells. During this labelling period, the pyrimidine analogue BrdU was incorporated in place of thymidine into the DNA of proliferating cells. After removing the culture medium the cells were fixed and the DNA was denaturated by adding FixDenat for 30 minutes at room emperature. This step was essential to improve the accessibility of the incorporated BrdU for detection by the antibody. The anti-BrdU-POD was added to cells for 90 minutes at room temperature. It bound to the BrdU incorporated in newly synthesized endothelial cellular DNA. The immune complexes were detected by the subsequent substrate (TMB) reaction. The reaction product was quantified by measuring the absorbance at the respective wavelength using Microplate Autoreader

ELISA (Bio-Tek Instruments, Winooski, VT) at 405nm, reference wavelength 490nm.

2.2.4.2. Migration

Chemotaxis experiments were performed with the Boyden chamber technique using 24-wells of a chemotaxis chamber with 5μm pore size polycarbonate membranes (Costar, Acton, MA). HCECs or RCECs were seeded (2.5 x 10^4 cells/cm^2) in 100μl of MV (PromoCell, Heidelberg, Germany) into the upper surface of the membrane insert. MV (PromoCell) in absence or in presence of $A\beta_{1-40}$ and $A\beta_{1-42}$ 10^{-7}M (Calbiochem, La Jolla, CA) (300μl final volume) was placed in the lower compartment of the chamber. After 4 hours of incubation at 37°C the upper surface of the filter was gently scraped to remove non-migrated cells. Filters were fixed in 4% formaldehyde and stained with Vectashield® mounting medium with DAPI (Vector Laboratories Inc., Burlingame, CA). The number of cells present in five random field per filter (lower surface) was counted at 10x magnification using Laborlux S fluorescence microscope (Leitz, Wetzlar, Germany).

2.2.4.3. Morphogenesis on Matrigel

HCECs and RCECs were seeded on Matrigel to assess the effect of peptides on functional characteristic of endothelial cells. Growth factor Reduced Matrigel™ Matrix (Bencton-Dickinson Labware, Bedford, MA) was defrosted overnight at 4°C and then 50μl/cm^2 of growth surface was added on ice-cold plates. Plates were incubated 30 minutes at 37°C to allow Matrigel to became gel. Cells were seeded (2.5 x 10^4 cells/cm^2) on Matrigel in 500μl of MV (PromoCell, Heidelberg, Germany) in absence and in presence of $A\beta_{1-40}$ and $A\beta_{1-42}$ 10^{-7}M (Calbiochem, La Jolla, CA) for 24 and 48 hours at 37°C, 5% CO_2. At the end of incubation cells were washed with PBS and fixed with 10% formaldehyde in PBS for 24 hours. Five random fields were captured using a camera connected to Laborlux S microscope (Leitz, Wetzlar, Germany) (magnification 50x).

Image analysis was carried out using the software Leica Imaging System Ltd (Leica Imaging System) and the dimensional (percent area covered by cells and the total length of cell network per field) and the topological parameters (mesh numbers

and branching points per field) were estimated and used to characterized the topological structure of endothelial cells according to Guidolin and co-workers (Guidolin et al., 2004).

2.2.5. EC viability

To measure the viability of HCECs and RCECs after the treatment with $A\beta_{1-40}$ and $A\beta_{1-42}$ 10^{-7}M at 48 hours of incubation, Cell Growth Determination kit MTT based (Sigma Aldrich Corp., St. Louis, MO) was used. In RCECs the effect of peptides was also assessed after 24 hours.

The MTT is based on measuring the activity of living cells via mitochondrial dehydrogenase activity. The component is the 3-(4,5-dimethylthiazol-2-yl)-2,5-diphenyl tetrazolium bromide or MTT. The method was introduced by Mosmann and co-workers (1983) and it is actually used to determine the amount of proliferating cells. Solution of MTT is dissolved in cell culture medium in a yellowish colour. Mitochondrial dehydrogenases of viable cells cleave the tetrazolium ring, yielding purple MTT formazan crystals which are insoluble in aqueous solutions. The crystals are dissolved using acidified isopropanol and the resulting purple solution is spectrophotometrically measured. The increase in cell viability results in an increase in the reduction of MTT and in an increase of absorbance.

HCECs and RCECs were seeded into 96-wells plates (1.5×10^4 cells/cm^2) for 24 hours in MV2 (PromoCell, Heidelberg, Germany). The medium was replaced by 100µl of MV (PromoCell, Heidelberg, Germany) in absence or in presence of $A\beta_{1-40}$ or $A\beta_{1-42}$ 10^{-7}M (Calbiochem, La Jolla, CA). 1 hour and 30 minutes before the end of the incubation with peptides, MTT solution was added in an amount equal to 10% of culture volume. At the end of incubation cell culture medium was removed and MTT crystals were dissolved adding 100µl/well of acidified isopropanol. Plates were gently stirred in a gyratory shaker until the MTT formazan crystals dissolved completely. The reaction product was quantified by measuring the absorbance at wavelength 570nm using Microplate Autoreader ELISA (Bio-Tek Instruments Inc., Winooski, VT).

2.3. Experimentation with $A\beta_{1-42}$ peptide on RCECs and RHAs

2.3.1. VEGF-A release in RCEC and RHA culture mediums

For the quantitative determination of rat Vascular Endothelial Growth Factor (VEGF) concentrations in cell culture mediums, Quantikine® Rat VEGF Immunoassay (R&D Systems, Minneapolis, MN) was used. This assay employs the quantitative sandwich enzyme immunoassay technique. A monoclonal antibody pre-coated onto the microplate react with standard, control and samples pipetted into the wells and any VEGF present is bound to the immobilized antibody. After washing away the unbound substances an enzyme-linked polyclonal antibody is added to the wells. Following a wash to remove any unbound antibody-enzyme reagent, a substrate solution is added to the wells. The enzyme reaction yields a blue poduct that turns yellow when the Stop solution is added. The intensity of the colour measured is in proportion to the amount of VEGF bound in the initial step. The samples values are then read off the standard curve.

RCECs and RHAs were seeded (1.5 x 10^4 cells/cm^2 and 6.25 x 10^4 cells/cm^2 respectively) in 96-well plates for 24 hours in MV2 (PromoCell, Heidelberg, Germany) or in BME (Sigma-Aldrich Corp., St. Louis, MO) 10% FBS. The medium was then replaced with MV (PromoCell, Heidelberg, Germany) or BME (Sigma-Aldrich Corp.) 2.5% FBS (PromoCell, Heidelberg, Germany) in absence or in presence of $A\beta_{1-42}$ 10^{-7}M (Calbiochem, La Jolla, CA) for 3, 24 or 48 hours. At the end of incubation mediums were collected into polypropylene tubes and the particulates were removed by centrifugation. Samples were stored at lower -20°C temperature until use. After adding 50µl of Assay Diluent RD1-41, 50µl of standards (composed of dilution of rat VEGF standard from 2000pg/ml to 31.2pg/ml), control (given with kit) and samples were added to the pre-coated plate. The plate was covered and incubated 2 hours at room temperature on a horizontal microplate shaker. Five washings were performed with 400µl Wash Buffer to ensure the removal of any unbound substances. 100µl of Rat VEGF Conjugate were added to each well and the plate was incubated for 1 hour at room temperature on the shaker. Five washings were performed

and 100µl of Substrate Solution were added to each well. After 30 minutes of incubation at room temperature on the benchtop protected from light, 100µl of Stop solution were added to each well, gently tapping the plate to ensure thorough mixing. The optical density of each well was determine within 30 minutes, using the Microplate Autoreader ELISA (Bio-Tek Instruments Inc., Winooski, VT) set to 450nm, reference wavelength 570nm. Standard curve and quantitative analysis were obtained using the software Microcal Origin 5.0 (Microcal Software Inc., Nothampton, MA).

2.3.2. Expression of VEGF-A mRNA in RCECs and RHAs

The Real Time Retro-Transcriptase-Polymerase Chain Reaction (Real Time RT-PCR) is a high sensitivity and specificity technique to determine the amplification product after each PCR cycle (Higuchi et al., 1993). Two different strategies of quantification can be performed:

- Absolute quantification make it easier to compare expression data between different days and laboratories, because the calibration curve is a non-changing solid and reliable basis;
- Relative quantification is based on the expression ratio of a target gene versus a reference gene and is adequate for most purposes to investigate physiological changes in gene expression levels (Pfaffl et al., 2002).

Relative quantification was performed to investigate expression variations of rat Vascular Endothelial Growth Factor-A (VEG-A) gene in comparison to the housekeeping gene rat hydroximethylbilane synthase (Hmbs).

The isolation of intact RNA requires four essential steps: effective disruption of cells, denaturaion of nucleoprotein complexes, inactivation of endogenous ribonuclease (RNase) activity and removal of contaminating DNA and proteins. The most important step is the immediate inactivation of endogenous RNase that are released from membrane-bound organelles upon cell disruption.

Preparation of samples

RCECs (2.5 x 10^4 cells/cm^2 in 6-well plates) and RHAs (8 x 10^4 cells/cm^2 in 24-well plates, two wells per treatment) were seeded and cultured until confluence. Cell culture mediums were replaced with MV (PromoCell, Heidelberg, Germany) or BME (Sigma-Aldrich Corp., St. Louis, MO) added with 2.5% FBS (PromoCell, Hei-

delberg, Germany) in absence or in presence of $A\beta_{1-42}$ 10^{-7}M (Calbiochem, La Jolla, CA) for 3, 24 or 48 hours. At the end of incubation cells were washed with PBS and lysed with 175µl RNA Lysis Buffer (RLA) (Promega Corporation, Madison, WI) added with 2% β-mercaptoethanol (Promega Corporation, Madison, WI) to inactivate the ribonucleases present in cell extract. The lysate was collected into sterile propylene tubes and stored at -20°C until use.

Extraction and quantification of nucleic acids

RNA was isolated from lysates using SV Total RNA Isolation System (Promega Corporation, Madison, WI) obtaining purified and intact RNA. 350µl of SV RNA Dilution Buffer were added to 175µl of lysate and mixed by inverting the tube 3-4 times. After incubation of 3 minutes at 70°C in a heating block tubes were centrifuged at 13000g for 10 minutes at 4°C. The cleared lysate was transferred to a fresh microcentrifuge tube by pipetting and 200µl 95% ethanol were added to the lysate. After pipetting 3-4 times, the mixture was transferred to the Spin Column Assembly and centrifuged at 13000g for 1 minute. The spin basket was taken from the Spin Column Assembly and the liquid was discarded. The spin basket was replaced in the collection tube and 600µl of SV RNA Wash Solution were added to Spin Column Assembly and centrifuged at 13000g for 1 minute. For each isolation a solution composed by 40µl Yellow Core Buffer, 5µl 0.09M $MnCl_2$ and 5µl DNase I enzyme were prepared in a sterile tube. After discarding the surnatante obtained from the centrifuge, 50µl per sample of solution was added to the membrane inside the spin basket and incubated for 15 minutes at room temperature. At the end of incubation 200µl of SV DNase Stop Solution were added to the membrane and centrifuged for 1 minute at 13000g. After two washings with SV RNA Wash Solution, each spin basket was transferred into a new sterile tube and 100µl of Nuclease-Free Water was added to the membrane and centrifuged for 2 minutes at 13000g. To concentrate the total RNA extracted, samples were dried using the vacuum centrifuge at 4°C Univapo 100 ECH (Stepbio, Bologna, Italy).

The yield of total RNA obtained was determined spectrophotometrically using the spectrophotometer Lambda 11 (Perkin Elmer, Boston, MA). Absorbance values at 260nm (A_{260}) (nucleic acids), 280nm (A_{280}) (proteins) and 320nm (A_{320}) (contaminating material) of 1µl of RNA in 99µl distilled water were determined in quartz cu-

vette with optical space of 10nm. Pure RNA exhibits an A_{260}/A_{280} ratio of 2. However, due to the variations between individual starting materials and in performing procedure, the expected range of A_{260}/A_{280} ratios for RNA are between 1.7and 2.1. RNA concentration was determined using the Lambert-Beer law:

$$RNA\ (\mu g/ml) = A_{260} \times 40 \times D$$

where 40 stands for 40μg/ml, the concentration of RNA when A_{260} has the value of 1 read in 10mm light path cuvette and D is the dilution.

Retro-transcription

Premix, constituted by 1μl oligo dT (Promega Corporation, Madison, WI), sample and nuclease-free solution to obtain a final volume of 5μl, was prepared in a propylene tube and left at 70°C for 5 minutes. 20μl of Mix solution, made up of 0.5mM dNTPs (Sigma Aldrich Corp., MO), 3mM $mgCl_2$, 1U/μl ribonuclease inhibitor, 1U/μl ImProm-II retro-transcriptase and ImProm-II buffer (Promega Corporation, Madison, WI), were added. The obtained mix was incubated 25°C for 15 minutes, 42°C for 60 minutes to allow the copy of mRNA filament to form complementary cDNA and at 70°C for 15 minutes to inactivate retro-transcriptase. Nuclease-free water was processed as samples and used as negative control.

Real Time-PCR

2μl of retro-transcript samples (concentration cDNA 7.5ng/ml) and 12.5μl IQ SYBER-Green Supermix (BioRad Laboratories, Milan, Italy) were mixed. IQ SYBER-Green Supermix is made up of 100mM KCl, 40mM Tris-HCl (pH 8.4), 6mM $MgCl_2$, 0.4mM per dNTPs, SYBER-Green and 50U/ml iTaq DNA polymerase to obtain a final volume of 25μl. The sequences of primers (Promega Corporation, Madison, WI) are reported in Table 2.1.

Rat Hmbs	sense 359-	5'-CCC TTG TGA TGC TGT TGT TGT TTT-3'
	antisense 519-	5'-TGT TGA GGT TTC CCC GAA TA-3'
Rat VEGF-A	sense 2-	5'-TGA ACT TTC TGC TCT CTT GGG TGC-3'
	antisense 121-	5'-TCA CCA CTT CAT GGG CTT TCT GCT-3'

Table 2.1: sequences of rat Hmbs and VEGF-A primers utilized during retro-transcriptase.

Real Time was performed in BioRad I-Cycler iQ detection system using the program that included a denaturation step at 95˚C for 3 min, 40 cycles of two ampli-

fication steps at 95˚C for 10 sec and annealing at 60˚C for 20 sec, and melting curve between 60-90˚C with a heating rate of 0.5˚C/10 sec. During the exponential phase, the fluorescence signal threshold was calculated, and the fraction number of PCR cycles required to reach the cycle threshold (Ct) was determined. Ct values decreased linearly with increasing input target quantity, and were used to calculate relative mRNA expression (Pfaffl, 2001). The principle was used by Pfaffl and co-workers to develop a mathematical model based on the equation

$$\textbf{ratio} = (E_{target})^{\Delta CPtarget\ (control\text{-}sample)} / (E_{ref})^{\Delta CPref\ (control\text{-}sample)}$$

The relative expression ratio of the target gene is computed, based on its real-time PCR efficiencies (E) and the crossing point (CP) difference (Δ) of an unknown sample versus a control ($\Delta CP_{control\text{-}sample}$) (Pfaffl et al., 2002).

The specificity of amplification was tested at the end of each run by melting curve analysis, using the ICycler software 3.0. Initially, detection of the PCR amplification products was controlled by size fractionation on 2% agarose-gel electrophoresis. Each sample was assayed in duplicate and the result was accepted if the difference between duplicates was less than 0.5 cycles. Samples were compared with their own controls. Hmbs was used as reference to normalized data: Ct mean values of VEGF-A of treated cells was normalized with mean values of Hmbs and than compared with the control.

Ideally, during the exponential PCR step the amplification should doubled. In experimental conditions the efficiency of the reaction is variable. Therefore a range linearity values were identified by the determination of a standard curve for each primer. The curve was composed of a serial dilution (1:4) of cDNA starting from 64ng to assess the optimal quantity (Bustin, 2000). Ct values as regards quantity logarithm were inserted into a graph. The straight lines obtained were compared and the quantity of cDNA to use for PCR was a value included in the line where the amplification is linear (Bustin and Nolan, 2004) (Fig. 2.1).

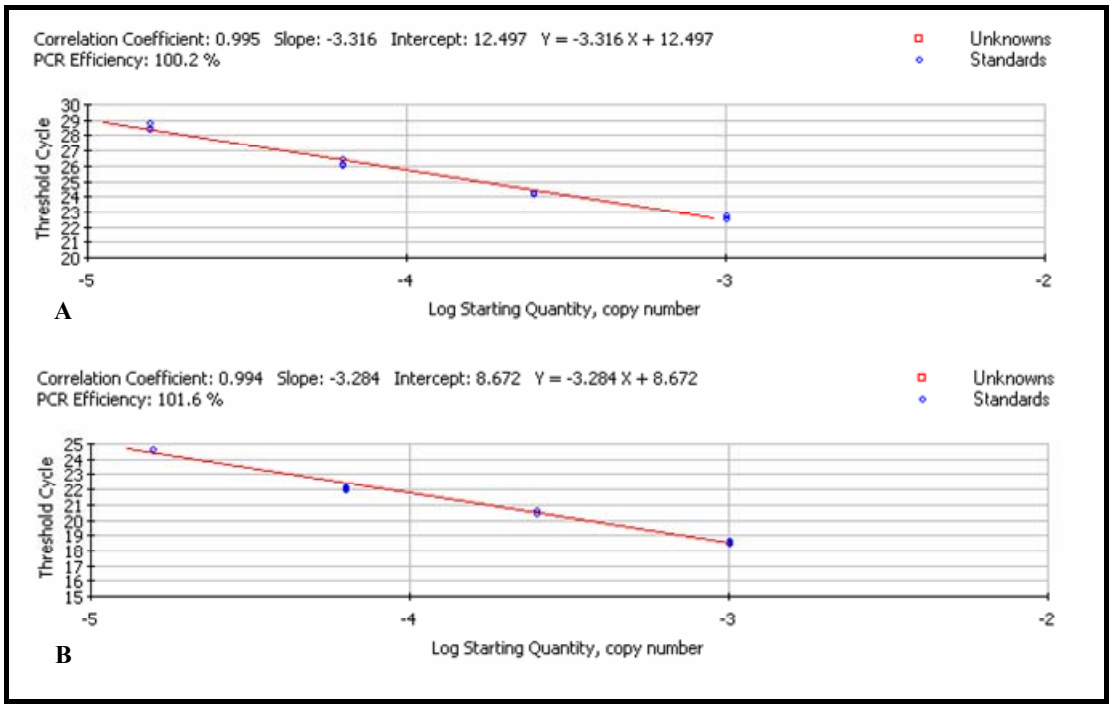

Fig. 2.1: standard straight lines of serial dilution of Hmbs mRNA (A) and VEGF-A mRNA (B).

Agarose gel electrophoresis

2% w/v agarose (SeaKem LE agarose, FMC BioProducts, Rocland, ME) was dissolved in TBE (Tris 89nM, 89mM boric acid, 2mM EDTA, pH 8.3) added with 30µg/ml ethidium bromide (Sigma-Aldrich, St. Louis, MO).

Sample buffer (Sigma-Aldrich, St. Louis, MO), constituted by 0.25% bromophenol blue, 0.25% xilene cianol FF and 40% sucrose, was added to each cDNA sample to increase density. 0.25µg of markers (GeneRuler^{TM} DNA Ladder, Low Range) (Fermentas Gmbh, St. Leon, Germany) were put into wells, as duplicate samples.

After the running in a electronic field of 50-100V gel was put under a UV lamp to observe bands. By the Scanning densitometric gel-Doc XP (BioRad Laboratories, Milan, Italy) imagines were captured and bands were compared.

2.3.3. RHA viability

To measure the viability of RHAs after the treatment with $A\beta_{1-42}$ 10^{-7}M after 3, 24 and 48 hours of incubation, Cell Growth Determination kit MTT based (Sigma Aldrich Corp., St. Louis, MO) was used.

RHAs were seeded into 96-well plates (6.25 x 10^4 cells/cm^2) for 24 hours in BME (Sigma-Aldrich Corp., St. Louis, MO) added with 10% FBS (Promocell, Heidelberg, Germany). The medium was replaced by 100µl of BME (Sigma-Aldrich) 2.5%FBS (PromoCell) in absence or in presence of $A\beta_{1-42}$ 10^{-7}M (Calbiochem, La Jolla, CA). 1 hour and 30 minutes before the end of the incubation, MTT solution was added in an amount equal to 10% of culture volume. At the end of incubation cell culture medium was removed and MTT crystals were dissolved adding 100µl/well of acidified isopropanol. Plates were gently stirred in a gyratory shaker until MTT formazan crystals dissolved completely. The reaction product was quantified by measuring the absorbance at wavelength 570nm using Microplate Autoreader ELISA (Bio-Tek Instruments, Winooski, VT).

2.4. Experimentation with treated RHA culture medium on RCECs

2.4.1. Preparation of samples

RHAs were seeded in polylysine coated plates (2.5µg/cm^2) and grown for 24 hours at 37°C, 5% CO_2 in BME (Sigma-Aldrich, St. Louis, MO) 10% FBS (PromoCell, Heidelberg, Germany). Mediums were replaced with BME (Sigma-Aldrich) 2.5% FBS (PromoCell). Different experimental conditions were assessed:

- well without cells (Control)
- well with non-treated RHAs
- well with $A\beta_{1-42}$ 10^{-7}M-treated RHAs

After 24 or 48 hours mediums were collected into polypropylene tubes and centrifuges to exclude particulates. The mediums were assayed on RCECs to evaluate different *in vitro* angiogenic steps: proliferation, migration and formation of capillary-like structures.

2.4.2. Proliferation

RCEC proliferation was evaluated using Cell Proliferation ELISA BrdU assay (Roche Applied Science, Penzberg, Germany).

RHAs were seeded (6.25 x 10^4 cells/cm^2) in 96-well plates and grown for 24 hours. At the end of incubation with BME (Sigma-Aldrich, St. Louis, MO) 2.5% FBS (PromoCell, Heidelberg, Germany) in absence or in presence of $A\beta_{1-42}$ 10^{-7}M for 24 or 48 hours, mediums were collected, centrifuged and stored at temperatures lower than -20°C until use.

RCECs were seeded in 96-well plates and cultivated for 24 hours in MV2 (PromoCell, Heidelberg, Germany). Mediums were replaced with RHA medium previously collected for 24 or 48 hours. The procedure for the following steps was the same described in 2.2.4.

2.4.3. Migration

RHA mediums was assayed in chemotaxis experiments to evaluate the pro-migratory effect of RHA culture mediums on RCECs.

Chemotaxis was evaluated as described in 2.2.5. RHAs were seeded (6.25 x 10^4 cells/cm^2) in 24-well plates for 24 hours. At the end of the incubation in BME (Sigma-Aldrich, St Louis, MO) 2.5% FBS (PromoCell, Heidelberg, Germany) in absence or in presence of $A\beta_{1-42}$ 10^{-7}M (Calbiochem, La Jolla, CA) for 24 or 48 hours, mediums were collected, centrifuged and stored at -20°C until use. Mediums were placed in the lower chamber and RCECs were seeded in the upper chamber of insert (Costar, Acton, MA) (2.5 x 10^4 cells/cm^2) in 100µl BME (Sigma-Aldrich) 2.5% FBS (PromoCell). The following steps were performed as described in 2.2.5.

2.4.4. Morphogenesis on Matrigel

RHAs were seeded (6.25 x 10^4 cells/cm^2) in 24-well plates in BME (Sigma-Aldrich, St. Louis, MO) 10% FBS (PromoCell, Heidelberg, Germany) and cultivated for 24 hours. After 24 or 48 hours of incubation in absence or in presence of $A\beta_{1-42}$ 10^{-7}M (Calbiochem, La Jolla, CA) in BME (Sigma-Aldrich) 2.5% FBS (PromoCell) mediums were collected in polypropylene tubes, centrifuged and stored at -20°C until use.

Growth factor Reduced Matrigel™ Matrix (Bencton-Dickinson Labware, Bedford, MA) was defrosted overnight at 4°C and then 50µl/cm^2 of growth surface were added on ice-cold plates. Plates were incubated 30 minutes at 37°C to allow Matrigel

to became gel. RCECs were seeded (2.5 x 10^4 cells/cm^2) on Matrigel in 500µl of RHA mediums previously collected for 24 and 48 hours at 37°C, 5% CO_2. The following steps were the same described in 2.2.6.

2.4.5. Determination of cytokines in culture mediums

To determine the amount of Interleukin-1β (IL-1β), Interleukin-6 (IL-6) and Tumor Necrosis Factor-α (TNF-α) contained in cell culture mediums, Rat Cytokine/Chemokine Linco*plex* Kit (Millipore, Milano, Italy) based on Luminex method was used.

RHAs were seeded (6.25 x 10^4 cells/cm^2) in 96-well plates and grown for 24 hours. At the end of incubation with BME (Sigma-Aldrich, St. Louis, MO) 2.5% FBS (PromoCell, Heidelberg, Germany) in absence or in presence of $A\beta_{1-42}$ 10^{-7}M (Calbiochem, La Jolla, CA) (200µl final volume) for 6, 12, 24 or 48 hours, mediums were collected, centrifuged and stored at lower -20°C temperature until use.

RCECs were seeded in 96-well plates and cultivated for 24 hours in MV2 (PromoCell, Heidelberg, Germany). Mediums were replaced with 100µl of RHA mediums previously collected for 6, 12, 24 or 48 hours. At the end of incubation, mediums were collected in polypropylene tubes, centrifuged and stored at -20°C until quantification of cytokines.

Rat Cytokine Standard was reconstitute with 250µl of deionized water to give a 20˙000pg/ml concentration of standard for all analytes except for Leptin, which has a concentration of 100˙000pg/ml after reconstitution. The vial was inverted several times to mix the solution. After 10 seconds in vortex, the vial was set for 10 minutes and the standard was transferred to an appropriately labelled polypropylene microcentrifuge tube. A serial dilution was create adding 120µl of Assay Buffer into each of six polypropylene tubes and 40µl of standard solution in the first vial. 40µl of the first vial were put in the second and mixed. The step was performed until the last vial. The dilutions and the final concentration of each vial is reported in table 2.2 and 2.3.

Standard Concentration (pg/ml)	Volume of Deionized Water to Add	Volume of Standard to Add
Original	250 ml	0

Standard Concentration (pg/ml)	Volume of Assay Buffer to Add	Volume of Standard to Add
1:4	120µl	40µl of Original
1:16	120µl	40µl of 1:4
1:64	120µl	40µl of 1:16
1:256	120µl	40µl of 1:64
1:1,024	120µl	40µl of 1:256
1:4,096	120µl	40µl of 1:1,024

Table 2.2: preparation of standard and diluted vials of Rat Cytokine Standard.

Standard Tube (Dilution)	Concentrations for All Analytes Except Leptin	Concentration for Leptin
Original	20,000pg/ml	100,000pg/ml
1:4	5,000pg/ml	25,000pg/ml
1:16	1,250pg/ml	6,250pg/ml
1:64	312.5pg/ml	1,562.5pg/ml
1:256	78.13pg/ml	390.63pg/ml
1:1,024	19.53pg/ml	97.66pg/ml
1:4,096	4.88pg/ml	24.41pg/ml

Table 2.3: final concentration of standard and diluted vials of Rat Cytokine Standard.

Rat Cytokine Control I and Rat Cytokine Control II were reconstitute with 250µl of deionized water and used as quality control of the kit. The vials were inverted several times to mix the solution. After 10 seconds in vortex, the vials were set for 10 minutes and the controls were transferred to an appropriately labelled polypropylene microcentrifuge tube. The unused portion was stored at -20°C.

Each antibody-bead bottle was sonicated for 30 seconds and mixed in the vortex for 1 minute. 150µl of each antibody bead tube were added to the Mixing Bottle and Assay Buffer was added to obtain a final volume of 3ml. Unused portion was stored at 2-8°C.

The filter plate was blocked by pipetting 200µl of Assay Buffer in each well and the plate was put on a shaker for 10 minutes at room temperature. At the end of incubation the buffer was removed by vacuum. 25µl of Assay Buffer were added to each sample and background well. 25µl of each standard or control was added into the appropriate wells. Then 25µl of the same culture medium utilized on cells were added to background, standard and control wells and 25µl of appropriately diluted samples were added to the each wells. 25µl of vortex-beads were added to each well. The plate was sealed, covered with aluminium foil and incubated with agitation on shaker overnight at 2-8°C. The fluid was gently removed by vacuum filtration and the plate was washed twice with 200µl of Wash Buffer. 25µl of Detection Antibody Cocktail were added into each well and the plate was covered with aluminium foil and put on a shaker at room temperature for 2 hours. At the end of incubation 25µl of Streptavidin-Phycoerythrin were added to each well containing the 25 µL of Detection Antibody Cocktail and the plate was put on a shaker for 30 minutes, protected from light. The plate was then washed twice with Washing Buffer, removing Wash Buffer by vacuum filtration between each wash. 150µl of Sheath Fluid was added to each well and beads were put on the shaker for 5 minutes at room temperature. The plate was run on Bio-plex multi array system based on Luminex technology (BioRad Laboratories, Milan, Italy) and data were obtained by the Bioplex Manager 4.1 software.

2.4.6. RCEC Viability

RHAs were seeded (6.25 x 10^4 cells/cm^2) in 96-well plates and grown in BME (Sigma-Aldrich, St. Louis, MO) 10% FBS (PromoCell, Heidelberg, Germany). After 24 hours mediums were replaced with BME (Sigma-Aldrich) 2.5% FBS (PromoCell) in absence or in presence of $A\beta_{1-42}$ 10^{-7}M (Calbiochem, La Jolla, CA) for 6, 12, 24 or 48 hours. At the end of incubation mediums were collected, centrifuged and stored at temperatures lower than -20°C until use.

RCECs were seeded in 96-well plates and cultivated for 24 hours in MV2 (PromoCell, Heidelberg, Germany). Mediums were replaced with RHA mediums previously collected for 6, 12, 24 or 48 hours. The procedure for the following steps was the same described in 2.2.7.

2.5. Experimentation with $A\beta_{1-42}$ peptide in absence and in presence of $hVEGF_{165}$ on RCECs

2.5.1. Preparation of human Vascular Endothelial Growth Factor ($hVEGF_{165}$)

hVEGF165 (PeproTech Inc., Rocky Hill, NJ) was dissolved in sterile water to a final concentration of 100ng/ml.

Increasing concentrations were tested on RCECs to asses the concentration that has the same effect of non-treated cells:

- 0.1ng/ml
- 0.2ng/ml
- 0.3ng/ml
- 0.4ng/ml
- 0.5ng/ml
- 5ng/ml

The concentration was determined by Trypan Blue exclusion and BrdU assays and resulted in 0.4ng/ml, which was used in all the experiments.

2.5.2. RCEC viability and proliferation with increasing concentration of $hVEGF_{165}$

Trypan Blue exclusion assay is a test based on the evaluation of a cell that possess an intact membrane. In fact Trypan Blue is a colour dye able to penetrate into a cell with damaged membrane. Cells having damaged membrane are blue when observed in optical microscope. It is possible to distinguish between vital cells and non-vital cells (blue) (Phillips and Terryberry, 1957).

RCECs were seeded (2.5×10^4 cells/cm^2) into 24-well plates and cultivated in MV2 (PromoCell, Heidelberg, Germany) for 24 hours. Medium was replaced by MV (PromoCell, Heidelberg, Germany) in absence or in presence of increasing amounts of $hVEGF_{165}$ (PeproTech Inc., Rocky Hill, NJ) for 24 hours. At the end of incubation cells were detached using 0.02% EDTA and 0.25% Trypsin (1:1 v/v) (Sigma-Aldrich Corp. St. Louis, MO) saline solution and counted in Bürker chamber using Trypan Blue (Sigma Aldrich Corp., St. Louis, MO).

BrdU assay was performed on RCECs as described in 2.2.4.

2.5.3. Aggregation kinetics

$A\beta_{1-42}$ (Calbiochem, La Jolla, CA) was dissolved in PBS to a final concentration of 10^{-4}M and incubated at 37°C in absence or in presence of 0.4µg/ml $hVEGF_{165}$ (PrepoTech Inc., Rocky Hill, NJ). Aggregation of $A\beta_{1-42}$ in absence or in presence of $hVEGF_{165}$ was evaluated by Thioflavine T (ThT) fluorescence variation after 0, 24, 96 and 168 hours. 100µl of each sample was added to 3µM ThT solution in 3ml final volume in PBS. ThT fluorescence variation was observed at 550nm (λ_{exc} = 416) using spectrophotofluorimeter LS50B (Perkin Elmer, Boston, MA). The signal due to the free ThT was subtracted.

2.5.4. RCEC viability

$A\beta_{1-42}$ (Calbiochem, La Jolla, CA) was dissolved in PBS to a final concentration of 10^{-4}M and incubated at 37°C in the absence or in presence of 0.4µg/ml $hVEGF_{165}$ (PeproTech Inc., Rocky Hill, NJ) for 24 hours. At the end of incubation, the effect of samples on RCEC viability was assessed by MTT (Sigma Aldrich Corp., St. Louis, MO). RCECs were seeded (1.5 x 10^4 cells/cm^2) in 96-well plates and cultivated for 24 hours in MV2 (PromoCell, Heidelberg, Germany). Mediums were replaced with MV (PromoCell, Heidelberg, Germany) in the absence or presence of factors for 24 hours: non-treated cells, cells treated with freshly solubilised $A\beta_{1-42}$ 10^{-7}M (Calbiochem, La Jolla, CA), cells treated with 24 hours aged $A\beta_{1-42}$ 10^{-7}M (Calbiochem), and cells treated with 24 hours aged $A\beta_{1-42}$ 10^{-7}M (Calbiochem) in presence of $hVEGF_{165}$ 0.4ng/ml (PeproTech Inc.). The following steps were performed as described in 2.2.7.

2.5.5. Morphogenesis on Matrigel

$A\beta_{1-42}$ (Calbiochem, La Jolla, CA) was dissolved in PBS to a final concentration of 10^{-4}M and incubated at 37°C in the absence or presence of 0.4µg/ml $hVEGF_{165}$ (PeproTech Inc., Rocky Hill, NJ) for 24 hours. At the end of incubation the effect of samples on RCEC morphogenesis was evaluated. Growth factor Reduced Matrigel™ Matrix (Bencton-Dickinson Labware, Bedford, MA) was defrosted

overnight at 4°C and then 50µl/cm^2 of growth surface was added on ice-cold plates. Plates were incubated 30 minutes at 37°C to allow Matrigel to became gel. RCECs were seeded (2.5 x 10^4 cells/cm^2) in 24-well plates in MV (PromoCell, Heidelberg, Germany) in the absence or presence of factors for 24 hours: non-treated cells, cells treated with freshly solubilised $A\beta_{1-42}$ 10^{-7}M (Calbiochem) , cells treated with 24 hours aged $A\beta_{1-42}$ 10^{-7}M (Calbiochem), and cells treated with 24 hours aged $A\beta_{1-42}$ 10^{-7}M (Calbiochem) in presence of $hVEGF_{165}$ 0.4ng/ml (PeproTech Inc.). The following steps were performed as described in 2.2.6.

2.6. Statistical analysis

The results were expressed in comparison with the control as mean ± standard deviation. The statistical significance of the difference between mean values was determined by the Student t test for unpaired data or by the comparison of means of more than two groups using one-way ANOVA, followed by POST-HOC Bonferroni-Student Newman Keuls (SNK). A significant level was set at $p<0.05$ and highly significant levels at $p<0.01$.

Each experiment of Real Time RT-PCR was been analysed after Pfaffl (2001) normalization and compared with the basal value 1 by t-test. A significant level was set at $p<0.05$ and highly significant levels at $p<0.01$.

3 Results

3.1. Characterization of cell cultures

3.1.1. Characterization of cerebral endothelial cells (CECs)

To verify that the immunoseparated human and rat cerebral endothelial cells (HCECs and RCECs respectively) were indeed endothelial cells and free from contaminating non endothelial cells, expression of endothelial-specific marker von Willebrandt factor (vWf) was investigated by immunocytochemistry. Both CEC types exhibited positive cytoplasmatic staining with anti-vWf (Fig. 3.1). No background staining was observed omitting the primary antibody.

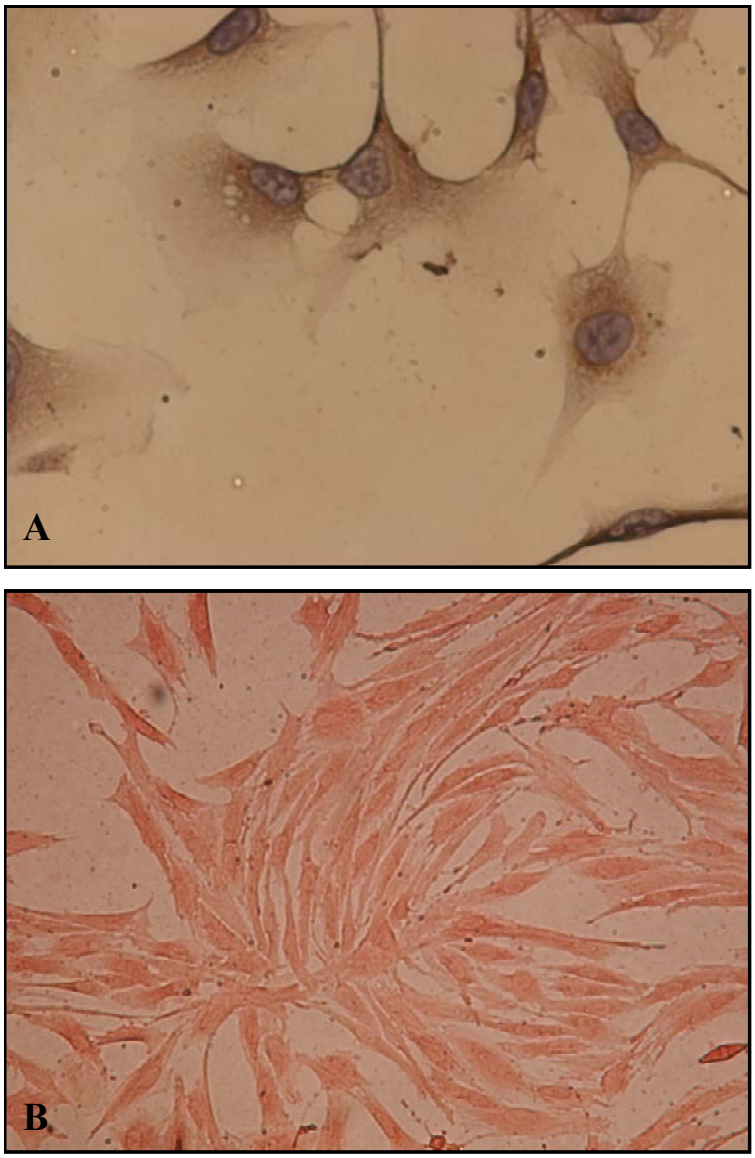

Fig. 3.1: immunocytochemistry of HCECs showing expression of endothelial-specific marker von Willebrandt factor (vWf). Nuclei were contrasted using Merk KGaA, Darmstadt, Germany's hemalum solution. Magnification 400X (A). Immunocytochemistry of RCECs showing the expression of endothelial-specific marker con Willebrandt factor (vWf). RCECs were highlight using 3-amino-9-etil-carbazol (AEC). Magnification 50X (B). No primary antibody was used in negative controls.

Indeed HCECs and RCECs are able to form capillary-like structures on Matrigel, maintaining the functional capability in *in vitro* cultures (Fig. 3.2).

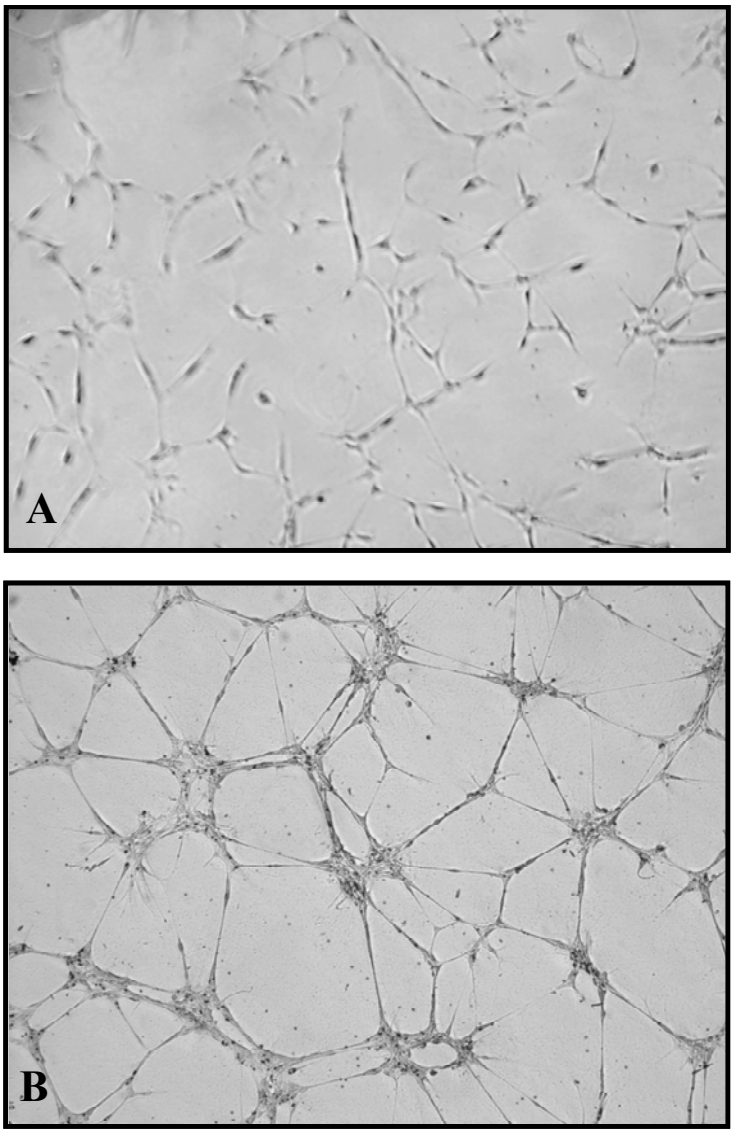

Fig. 3.2: HCECs (A) and RCECs (B) seeded in Matrigel after 24 hours. Both endothelial cell types maintain the ability to form capillary-like structures *in vitro*.

3.1.2. Characterization of rat hippocampus astrocytes (RHAs)

To verify that the isolated rat hippocampus astrocytes (RHAs) were indeed astrocytes and free from contaminating cells, expression of astrocytes-specific marker Glial Fibrillary Acidic Protein (GFAP) was investigated by immunofluorescence. RHAs exhibited positive staining with anti-GFAP antibody (Fig. 3.3 A), consistent with localization of GFAP in glial cytoplasmatic filaments. No background staining was observed omitting the primary antibody (Fig. 3.3 B).

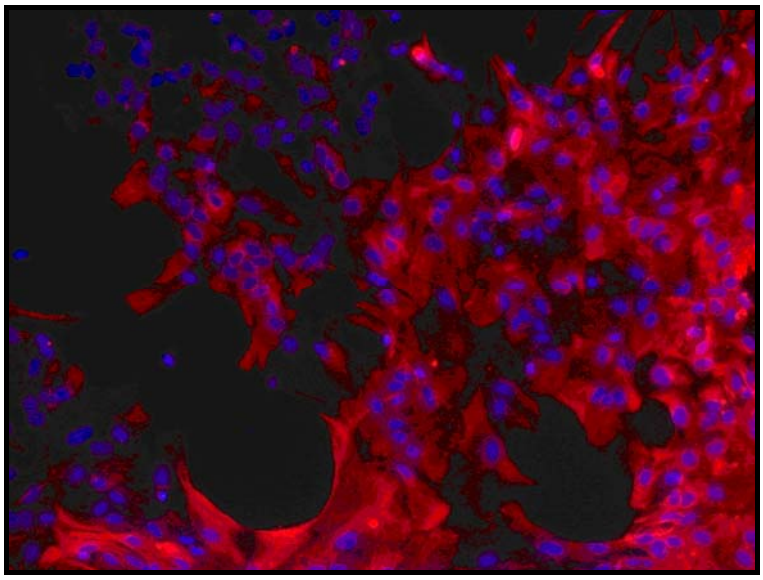

Fig. 3.3: immunofluorescence of RHAs stained with anti-GFAP antibody (red). Nuclei were staining with DAPI. Magnification 100X.

3.2. Experimentation with $A\beta_{1-40}$ and $A\beta_{1-42}$ peptides

3.2.1. Angiogenic activity *in vivo*. Chorio-Allantoic Membrane (CAM) assay

Macroscopic examination of sponges of CAM assay showed that both $A\beta_{1-40}$ and $A\beta_{1-42}$ peptides increased allantoic vessels around sponges after 12 days of incubation. Vessels developed radially towards the implant in a spoke and wheel pattern (Fig. 3.4 A and C). A similar result was produced by sponges loaded with FGF-2 (not shown). No vascular response was detected around the sponges treated with PBS alone (Fig. 3.4 B).

Histological examination of the sponges treated with both $A\beta_{1-40}$ and $A\beta_{1-42}$ peptides showed numerous small blood vessels inside the sponge trabeculae (Fig. 3.4 D and E) in comparison to PBS treated sponges (F). Table 3.1 showing microvessel counts 96 hours after sponge implants, confirms macroscopic observations: statistical difference between $A\beta_{1-40}$ and $A\beta_{1-42}$ peptides and PBS-loaded specimens in microvessel counts in the CAM area under the implant. The angiogenic response induced by both Aβ peptide implants was comparable to that obtain with FGF-2.

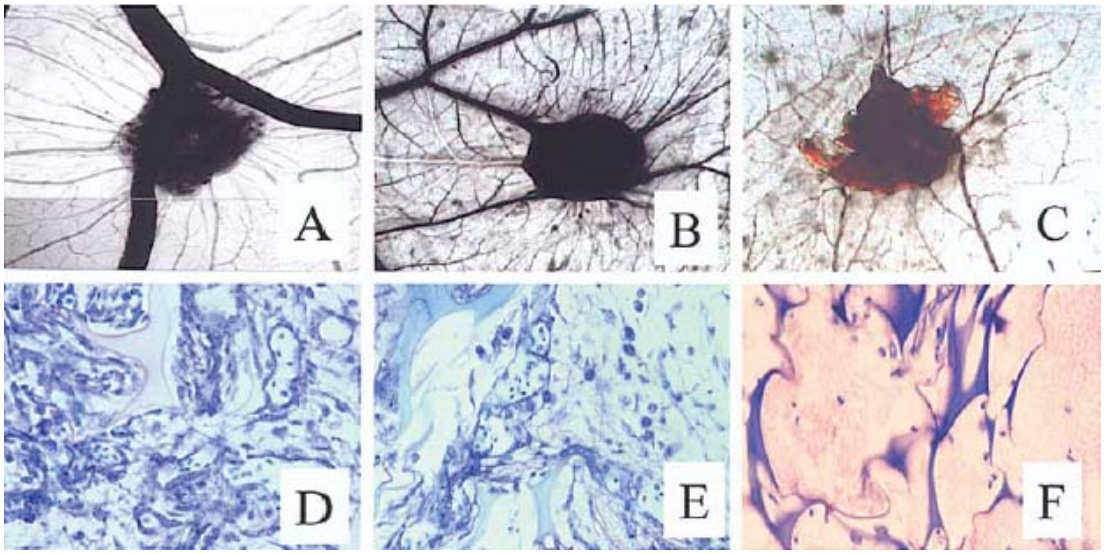

Fig. 3.4: angiogenic activity of Aβ peptides *in vivo* in CAM assay 96 hours after the $A\beta_{1-40}$ (A) and $A\beta_{1-42}$ (B) peptide-treated sponges were implanted. Increased allantoic vessels grew around sponges in comparison to sponges treated with PBS alone (C). Magnification 50X. Histological pictures of CAM treated with $A\beta_{1-40}$ (D), $A\beta_{1-42}$ (E) and PBS (F). In D and E numerous microvessels inside sponges, while in the control specimens (F) no blood vessels are recognizable. Magnification 250X.

Specimen	Microvessel density %	Mean±SD
$A\beta_{1-40}$	19.4	28±4 **
$A\beta_{1-42}$	18.4	26±3 **
PBS	4.2	6±2
FGF-2	20.8	30±5 **

Table 3.1: quantification of angiogenic response in the CAM assay at microscopic level at 96 hours after sponge implants. ** $p<0.01$ to PBS implants. Statistical analysis was determined by Student's t test unpaired data between mean values.

3.2.2. Angiogenic activity *ex-vivo*. Aortic-ring assay

The pro-angiogenic effect of $A\beta_{1-40}$ and $A\beta_{1-42}$ peptides in *ex-vivo* model was assayed observing the formation of microvessel network from rat aorta explants. When tested at 10^{-7}M concentration both Aβ peptides allowed endothelial tubes to sprout from aorta rings (Fig. 3.5 A and B). Otherwise no tube formation has been observed in control specimens (Fig. 3.5 C).

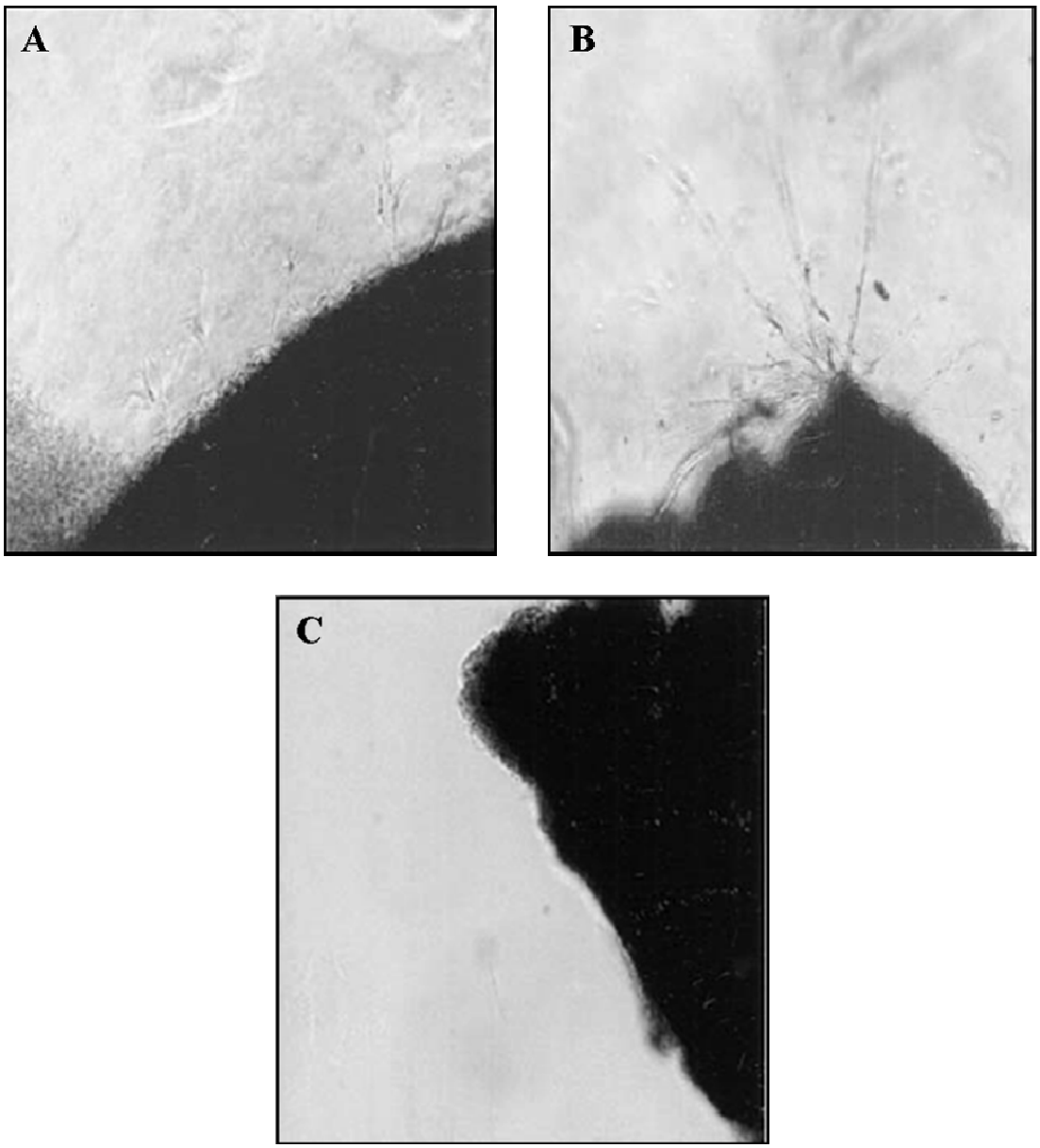

Fig. 3.5: effect of Aβ peptides on new vessels formation in rat aortic ring assay. Increased formation of vessels sprouting from aorta were the result of the treatments with $A\beta_{1-40}$ (A) and $A\beta_{1-42}$ (B) at concentration 10^{-7}M after 12 days of incubation. No tubes formation in control rings (C). Original magnification 10X.

3.2.3.Angiogenic activity *in vitro* on HCECs and RCECs

3.2.3.1. Proliferation

To assess the effect of $A\beta_{1-40}$ and $A\beta_{1-42}$ at concentration 10^{-7}M on HCECs and RCECs on proliferation, BrdU experiments were assessed. Exposure of HCECs to both Aβ peptides induced them to proliferate following 24 and 48 hours in compari-

son to control. No effects were detectable in RCECs were both Aβ peptides did not affect proliferation in comparison to non treated cells (Fig. 3.6).

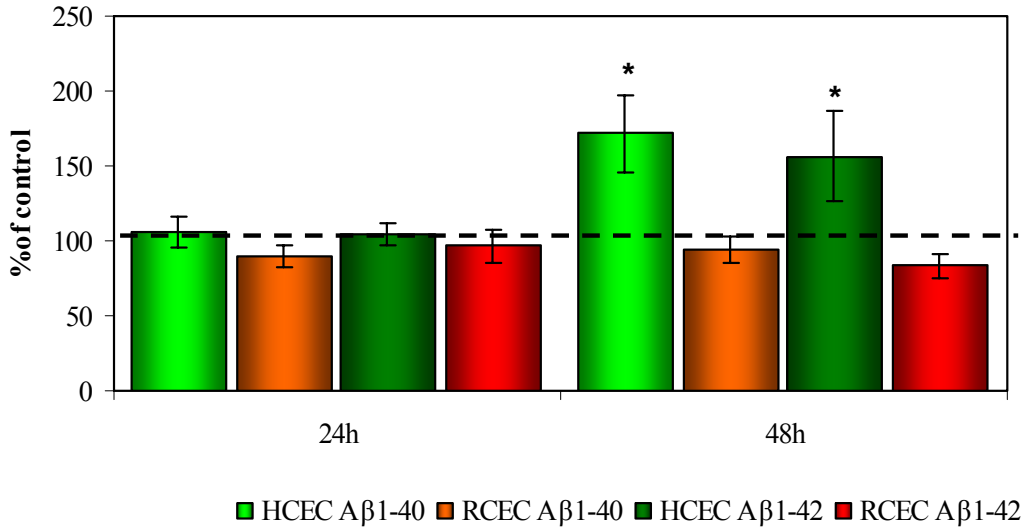

Fig. 3.6: BrdU assay performed on HCECs and RCECs after 24 or 48 hours of treatments with $A\beta_{1-40}$ and $A\beta_{1-42}$ at 10^{-7}M concentration. Both Aβ peptides did not affect proliferation rate of RCECs while on HCECs they increased significantly ($p<0.05$) the proliferation in comparison to non treated cells. * $p<0.05$ to control. Statistical analysis was determined by Student's t test unpaired data between mean values. Bars are means±standard deviation of four separate experiments.

3.2.3.2. Migration

Migration is another step of the angiogenic process. To assess the chemotaxis effect of $A\beta_{1-40}$ and $A\beta_{1-42}$ at concentration 10^{-7}M on HCEC and RCEC migration assay had been performed using the Boyden chamber technique. $A\beta_{1-40}$ and $A\beta_{1-42}$ increased respectively the migration of HCECs 3 and 6-fold in comparison to non treated cells. No effect were detectable in RCECs (Fig. 3.7).

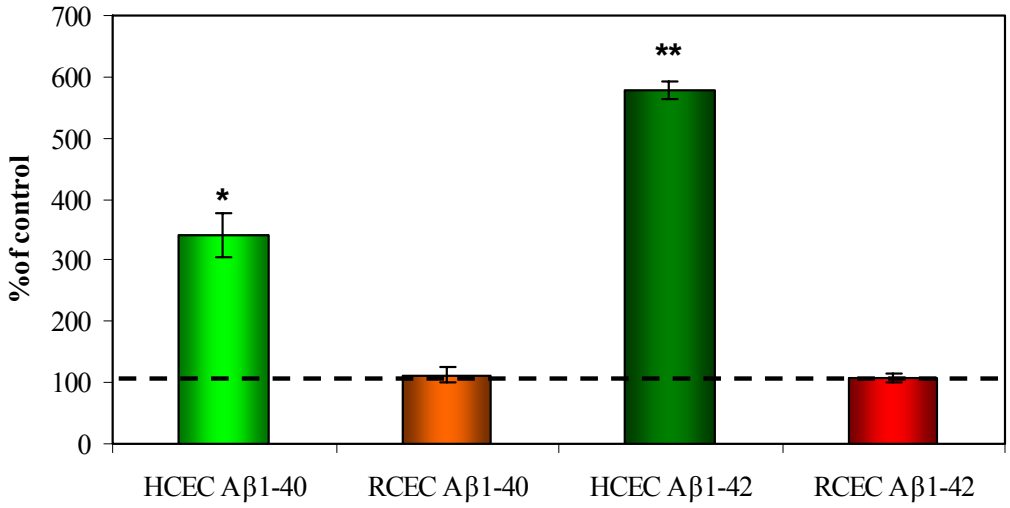

Fig. 3.7: migration assay performed using the Boyden chamber technique to assess chemotaxis of Aβ peptides after 4 hours of incubation on HCECs and RCECs. HCECs are induced to migrate toward $A\beta_{1-40}$ and $A\beta_{1-42}$ at 10^{-7}M concentration in comparison to control. * p<0.05 and ** p<0.001 to control. Statistical analysis was determined by Student's t test unpaired data between mean values. Bars are means±standard deviation of five separate experiments.

3.2.3.3. Morphogenesis on Matrigel

To determine whether $A\beta_{1-40}$ and $A\beta_{1-42}$ peptides at concentration 10^{-7}M possess pro-angiogenic proprieties in HCEC and RCEC cultures after 24 and 48 hours, capillary-like structures formation was assessed by seeding cells on growth factor-reduced Matrigel. Qualitative analysis of imagines showed increasing formation of capillary-like structures on Matrigel in HCECs after 24 (Fig. 3.8 A, B, C) and 48 hours (Fig. 3.9 A, B, C) by both Aβ peptides. Diversely to RCECs Aβ peptides decreased tube formation at 24 hours (Fig. 3.8 D, E, F) and no effect was detectable after 48 hours (Fig. 3.9 D, E, F).

Quantitative analysis indicated that both Aβ peptides after 24 and 48 hours of treatment at concentration 10^{-7}M increased dimensional parameters, such percent area covered by cells and the total length of cell network per field, and topological parameters, such as mesh number and branching points per field as compared to non treated cells. Diversely in RCECs Aβ peptides decreased in all considered parameters in comparison to the control after 24 hours of treatment. After 48 hours no effects were detectable in RCECs (Fig. 3.10).

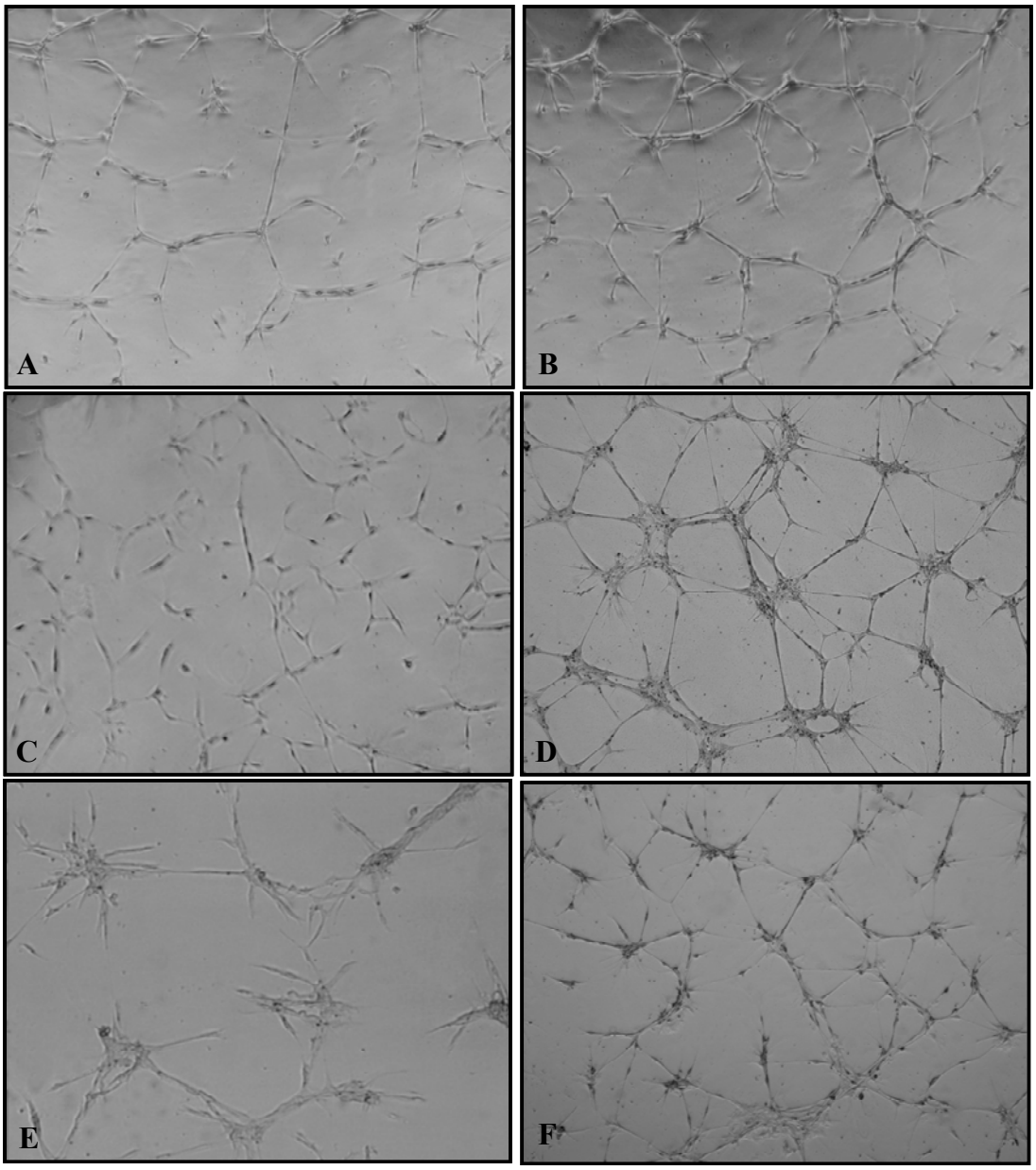

Fig. 3.8: Aβ peptide-induce tube formation by HCECs and RCECs seeded in Matrigel after 24 hours of treatments. (A) and (E) $A\beta_{1-40}$ 10^{-7}M effect respectively on HCECs and RCECs; (B) and (F) $A\beta_{1-42}$ 10^{-7}M effect respectively on HCECs and RCECs; (C) and (D) control cell respectively on HCECs and RCECs.

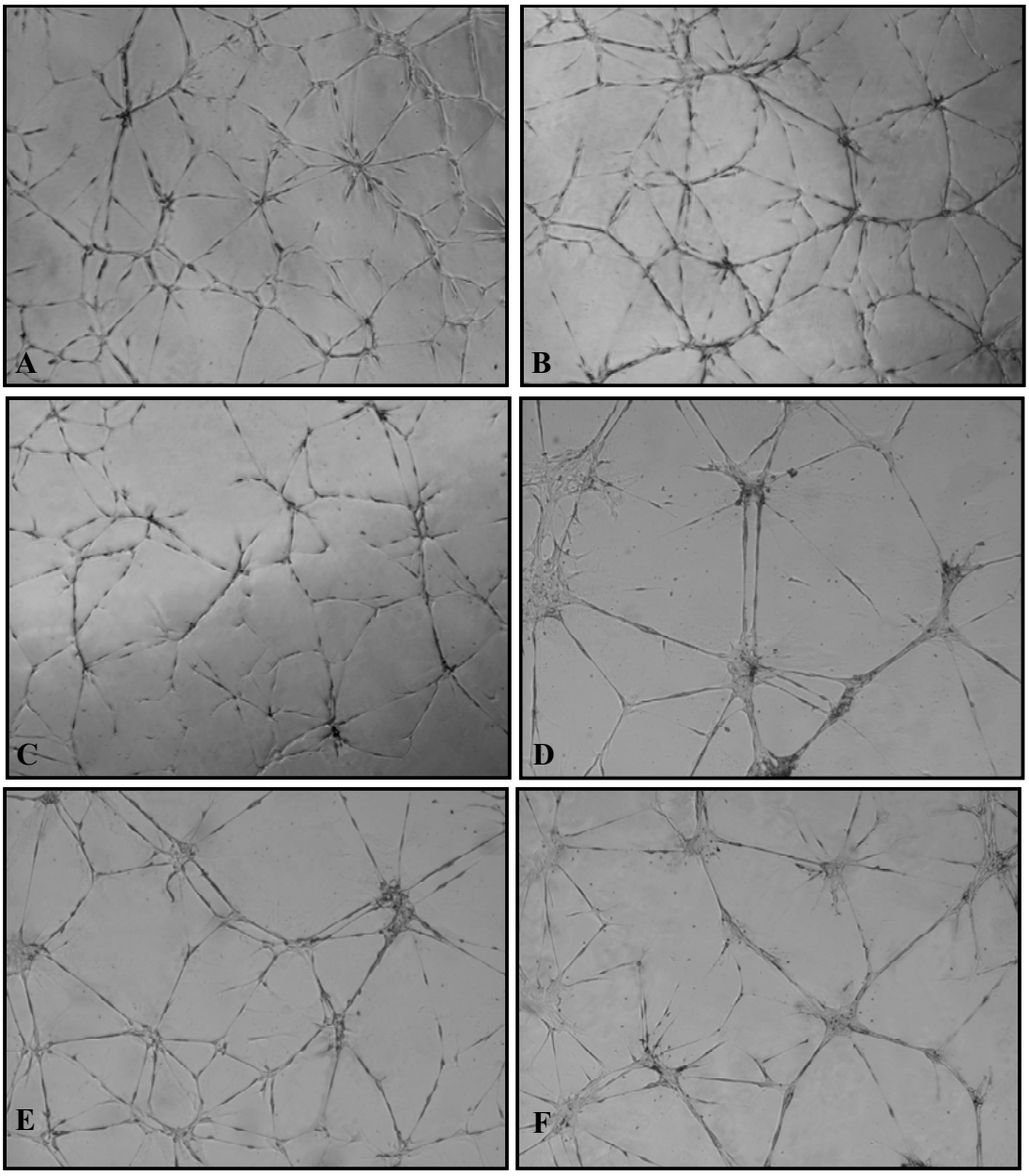

Fig. 3.9: Aβ peptide-induce tube formation by HCECs and RCECs seeded in Matrigel after 48 hours of treatments. A and E $A\beta_{1-40}$ 10^{-7}M effect respectively on HCECs and RCECs; B and F $A\beta_{1-42}$ 10^{-7}M effect respectively on HCECs and RCECs; C and D control cell respectively on HCECs and RCECs.

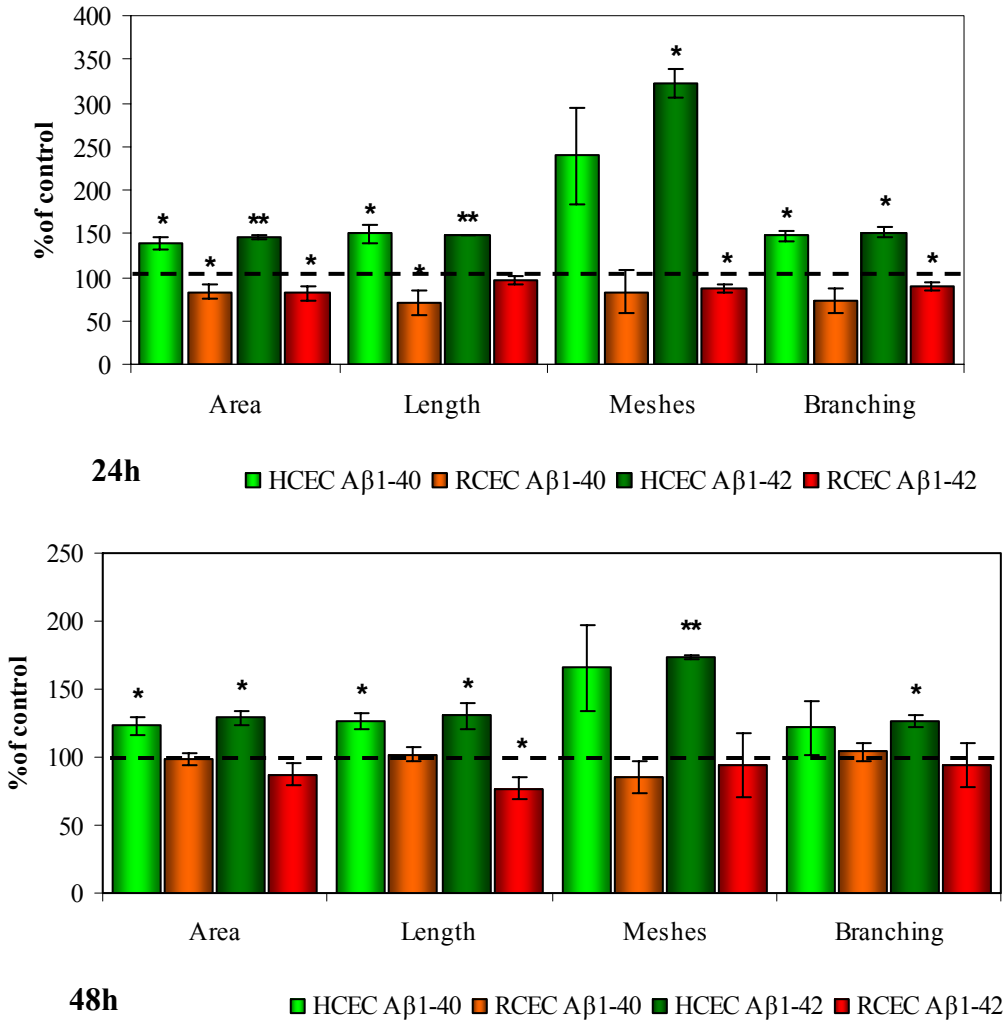

Fig. 3.10: quantitative analysis of tube formation estimated as dimensional (percent of area covered by cells and total length of cell network per filed) and topological (mesh number and branching point per field) parameters indicates that both Aβ peptides increased the formation of capillary-like structure formation after 24 and 48 hours in HCECs in comparison to non treated cells while they decreased all considered parameters in RCECs after 24 hours in comparison to control and they did have effects after 48 hours. * $p<0.05$ and ** $p<0.01$ to control. Statistical analysis was determined by Student's t test unpaired data between mean values. Bars are means±standard deviation of five separate experiments.

3.2.4. Endothelial cells viability

To assess the effect of $A\beta_{1\text{-}40}$ and $A\beta_{1\text{-}42}$ peptides at concentration 10^{-7}M on HCEC and RCEC viability MTT assay was performed after 48 hours of treatment. Redox activity of HCECs had significantly increased with similar efficiency by both $A\beta_{1\text{-}40}$ and $A\beta_{1\text{-}42}$ peptides. No effect was observable in RCECs (Fig. 3.11). MTT assay was performed in RCECs after 24 hours to assess the effect of Aβ peptides be-

fore 48 hours of treatment: $A\beta_{1-40}$ and $A\beta_{1-42}$ decreased viability of RCECs in comparison to the control (Fig. 3.12).

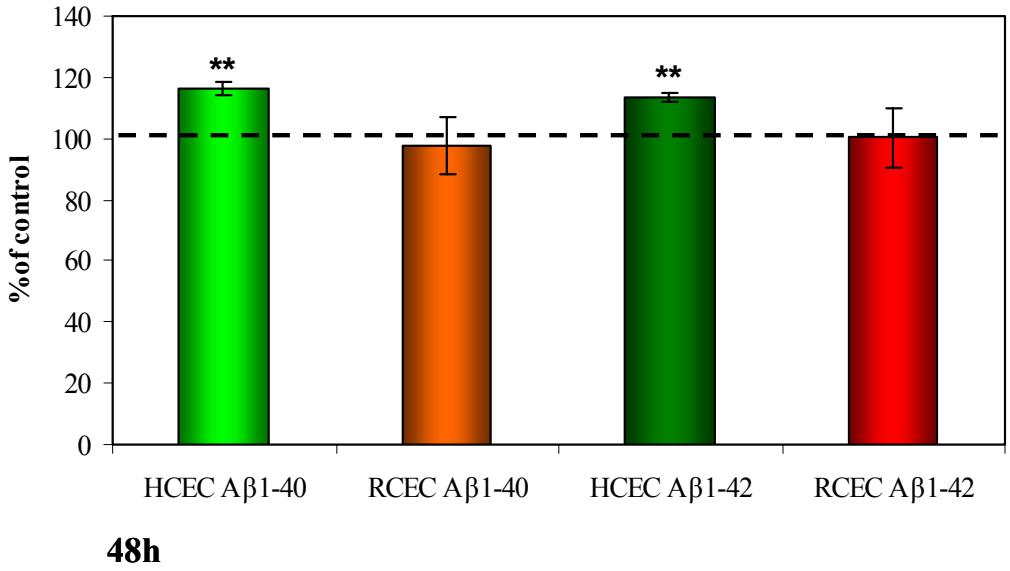

Fig. 3.11: effect of $A\beta_{1-40}$ and $A\beta_{1-42}$ peptides at concentration 10^{-7}M on the viability of cultured HCECs and RCECs, as measured by MTT-reduction assay after 48h. ** p<0.01 to control. Statistical analysis was determined by Student's t test unpaired data between mean values. Bars are means±standard deviation of five separate experiments.

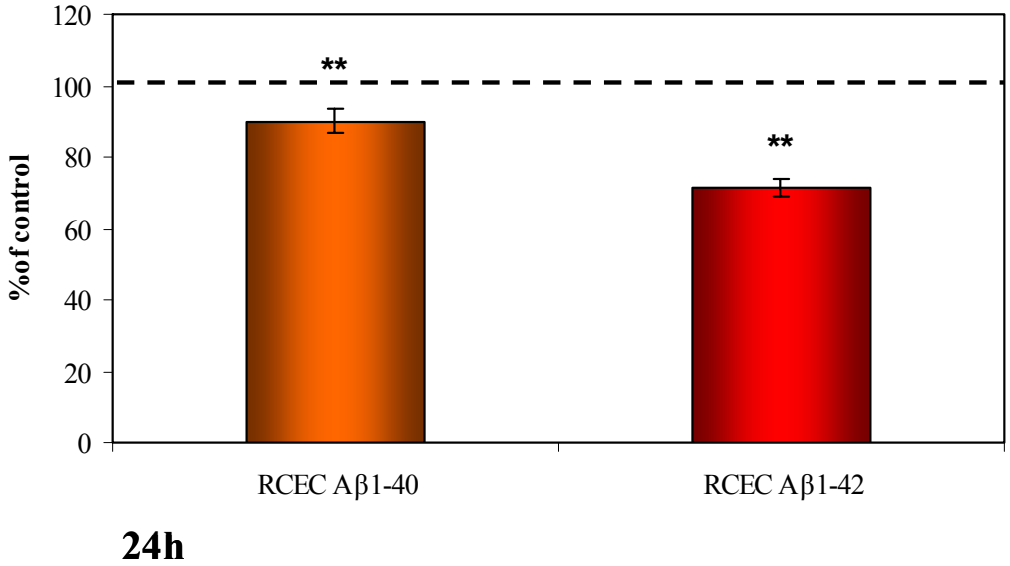

Fig. 3.12: effect of $A\beta_{1-40}$ and $A\beta_{1-42}$ peptides at concentration 10^{-7}M on the viability of cultured RCECs, as measured by MTT-reduction assay after 24h. * p<0.05 to control. Statistical analysis was determined by Student's t test unpaired data between mean values. Bars are means±standard deviation of five separate experiments.

3.3. Experimentation with $A\beta_{1-42}$ peptide on RCECs and RHAs

3.3.1. VEGF-A release in RCEC and RHA cell culture mediums

The effect of $A\beta_{1-42}$ at concentration 10^{-7}M in VEGF release by RCECs and RHAs after 3, 24 or 48 hours of treatment was evaluated analysing cell culture mediums. No variations between treated and non treated cells were detected neither in RCECs nor in RHAs in all considered incubation periods (Fig. 3.13).

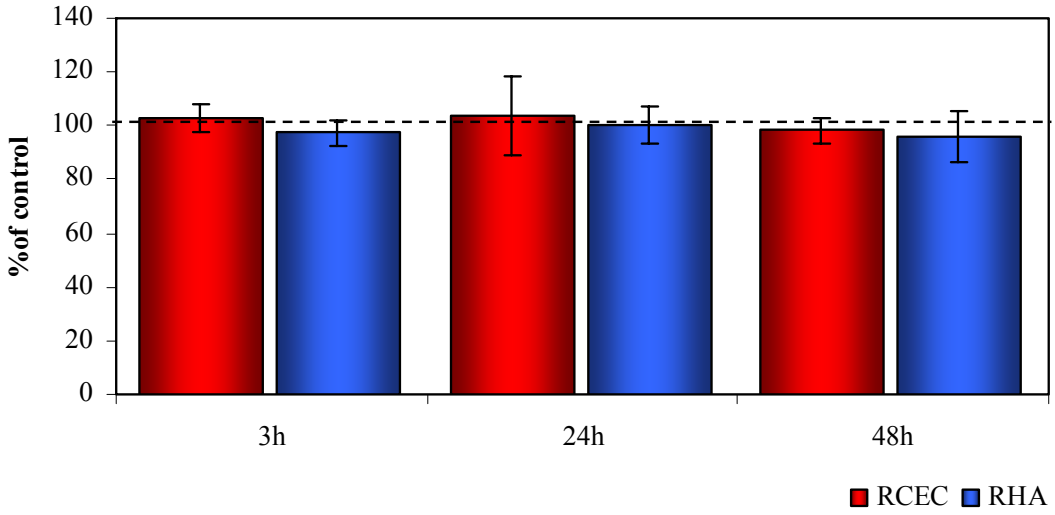

Fig. 3.13: VEGF release in cell culture medium from RCECs and RHAs treated with $A\beta_{1-42}$ peptide at concentration 10^{-7}M after 3, 24 or 48 hours. No variations were observed. Statistical analysis was determined by Student's t test unpaired data between mean values. Bars are means±standard deviation of four separate experiments.

3.3.2. Expression of VEGF-A mRNA in RCECs and RHAs

To assess if $A\beta_{1-42}$ at concentration 10^{-7}M affected the expression of VEGF mRNA in RCECs and RHAs, relative quantification of VEGF mRNA expression in comparison to Hmbs mRNA expression was performed by Real Time RT-PCR after 3, 24 or 48 hours of treatment. During Real Time RT-PCR fluorescence signalling was captured by ICycler iQ Optical System (version 3, Bio-Rad Laboratories) software. The resulting curves produced by the software were utilized to obtain a Ct value for every specimen. Fig. 3.14 shows an example of Ct curves of 24 hours treated RCECs (A) and RHAs (B). Amplification specificity of Hmbs and VEGF-A

primers were evaluated at the end of every Real Time RT-PCR observing the melting curves and also performing agarose gel electrophoresis (Fig. 3.16) in both RCECs and RHAs. Fig. 3.15 shows an example of melting curves in 24 hours treated RCECs (A) and RHAs (B).

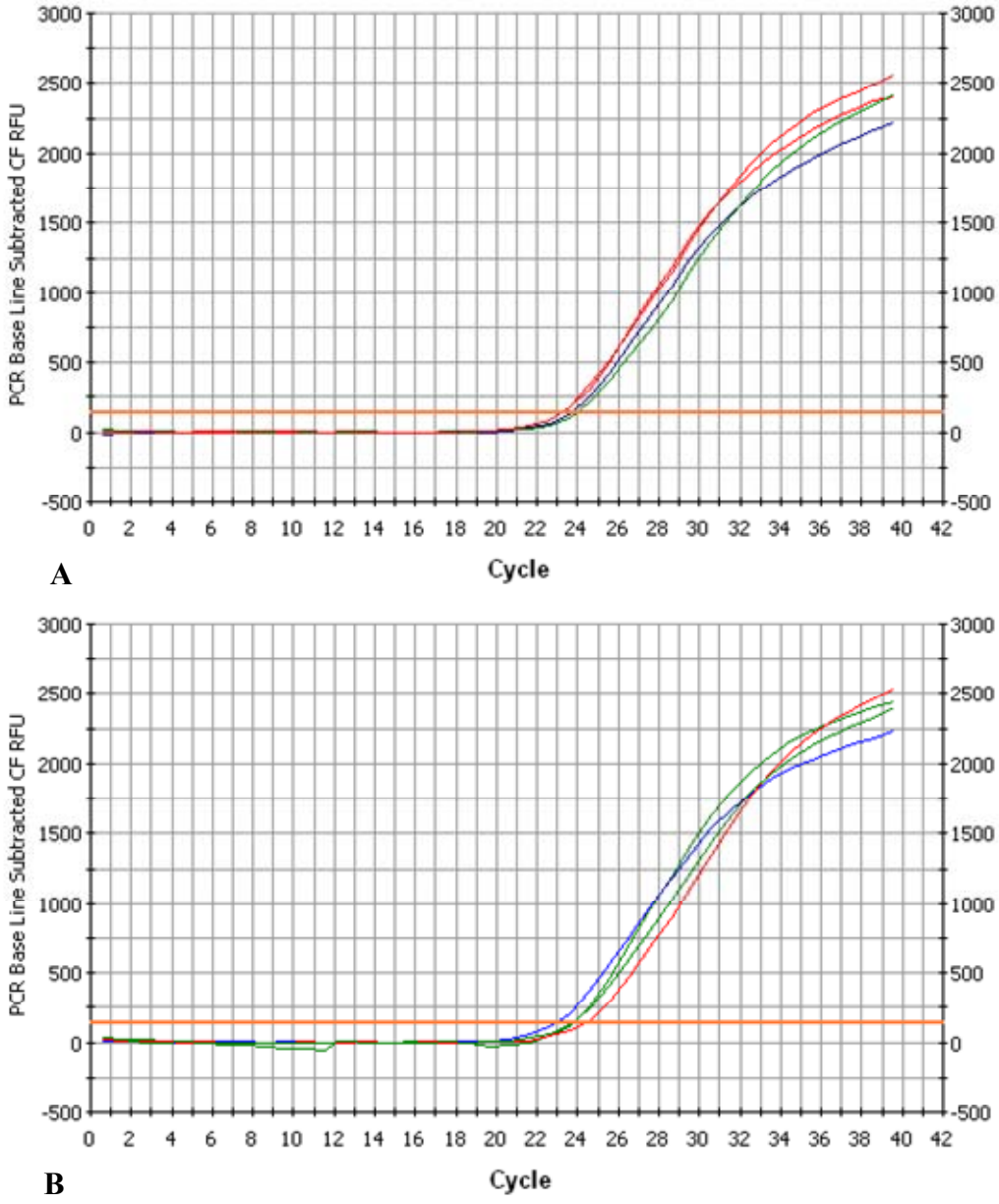

Fig. 3.14: example of Ct curves of 24 hours control and treated RCECs (A) and RHAs (B).

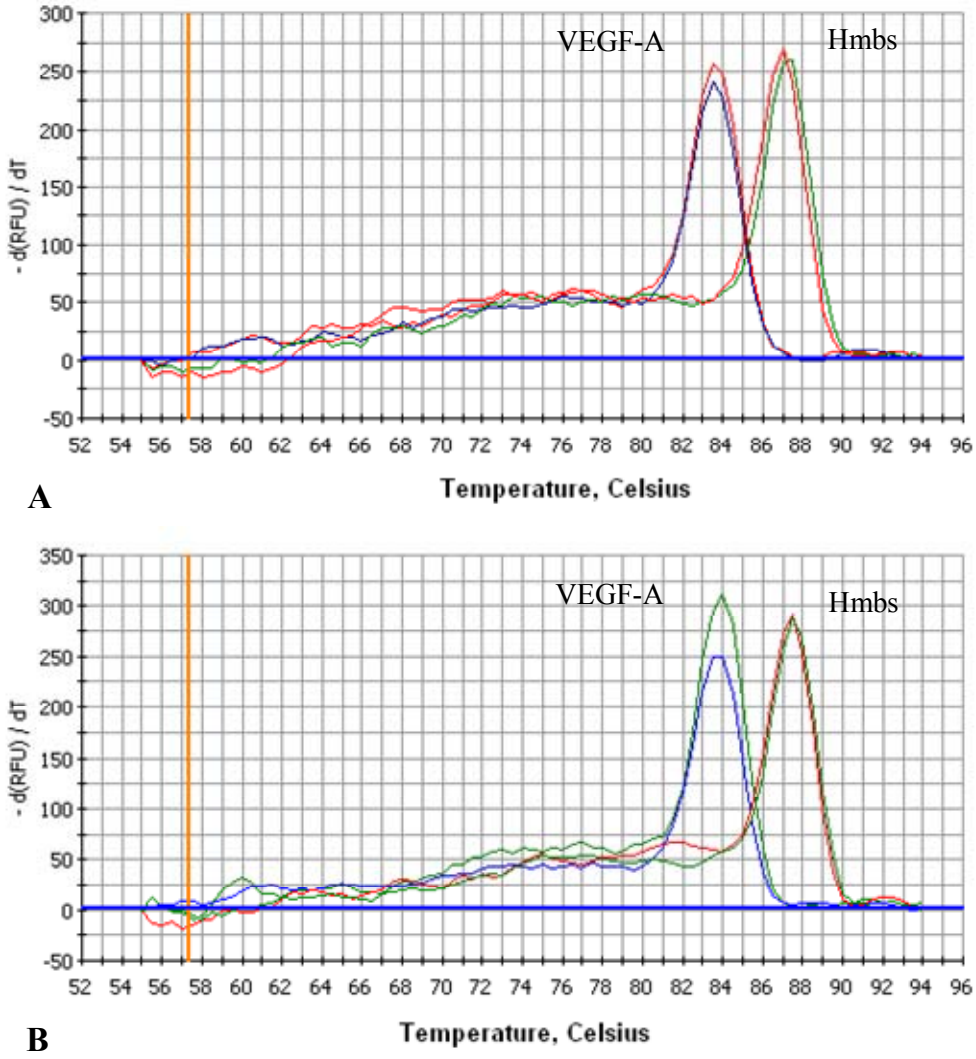

Fig. 3.15: example of melting curves of 24 hours control and treated RCECs (A) and RHAs (B). Melting temperatures of Hmbs primer (83°C) and VEGF-A primes (87°C).

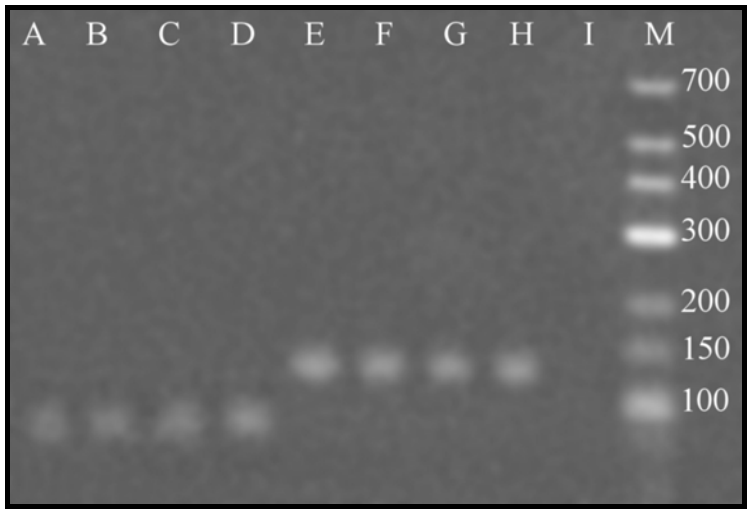

Fig. 3.16: agarose gel (2%) electrophoresis stained with Ethidium Bromide showing amplified cDNA with Hmbs and VEGF rat specific primers confirmed the specificity of amplification products as for Hmbs(95bp) as for VEGF-A (119bp). (A) and (E) expression of 24 hours non treated RCEC Hmbs and VEGF respectively; (B) and (F) expression of 24 hours $A\beta_{1-42}$ 10^{-7}M treated RCEC Hmbs and VEGF respectively; (C) and (G) expression of 24 hours non treated RHA Hmbs and VEGF respectively; (D) and (H) expression of 24 hours $A\beta_{1-42}$ 10^{-7}M treated RHA Hmbs and VEGF respectively; (I) water as negative control did not show amplification; (L) markers (GeneRuler™ DNA Ladder, Low Range, Fermentas).

Data obtained by Pfaffl's normalization (2001) demonstrated that $A\beta_{1-42}$ peptide at concentration 10^{-7}M did not affect expression of VEGF-A mRNA in both RCECs and RHAs at any considered time (3, 24 or 48 hours) (Fig. 3.17).

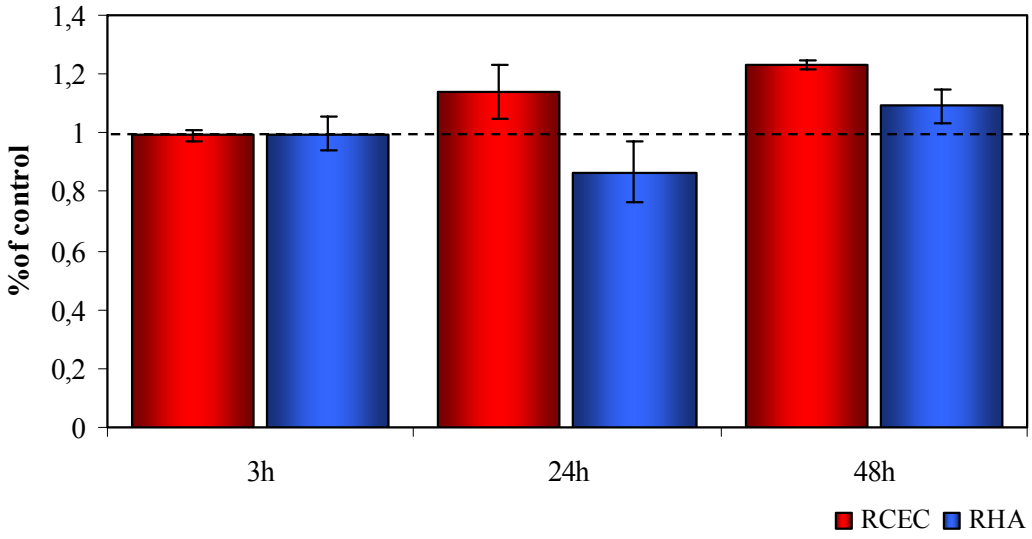

Fig. 3.17: semiquantitative Real Time RT-PCR analysis of VEGF-A mRNA expression after 3, 24 and 48 hours of treatment with $A\beta_{1-42}$ at concentration 10^{-7}M on RCECs and RHAs. Statistical analysis was determined by Student's t test unpaired data between mean values. Bars are means±standard deviation of three separate experiments.

3.3.3. RHA viability

RHA viability was evaluated using MTT assay, based on dehydrogenase reduction of MTT from mitochondria in living cells, after 3, 24 and 48 hours of treatment. $A\beta_{1-42}$ did not affect RHA viability at any time (Fig. 3.18).

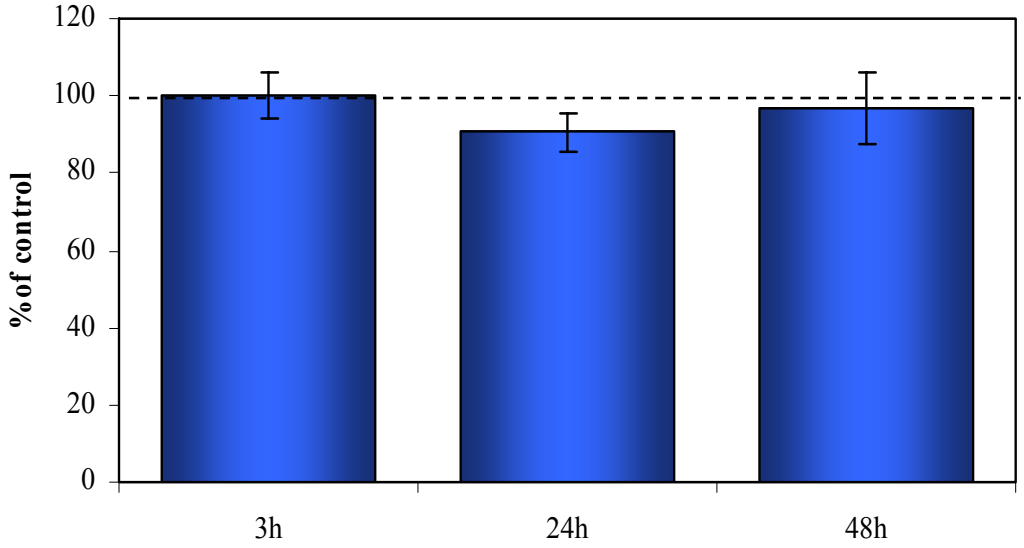

Fig. 3.18: effect of $A\beta_{1-42}$ peptides at concentration 10^{-7}M on the viability of cultured HCECs and RCECs, as measured by MTT-reduction assay after 3, 24 and 48h. ** p<0.01 to control. Statistical analysis was determined by Student's t test unpaired data between mean values. Bars are means±standard deviation of five separate experiments.

3.4. Experimentation with treated RHA culture medium on RCECs

3.4.1. Proliferation

Proliferation effect of 24 and 48 hours control and $A\beta_{1-42}$ 10^{-7}M RHA cell culture mediums on RCECs after 24 and 48 hours of treatment was assessed by BrdU assay. Treatment with 24 hours RHA culture medium did not affect RCEC proliferation in the following 24 hours. 48 hours of exposure of 48 hours control RHA culture medium increased proliferation rate in comparison to new RHA culture medium of RCECs while $A\beta_{1-42}$ 10^{-7}M treated RHA culture medium did not affect proliferation (Fig. 3.19).

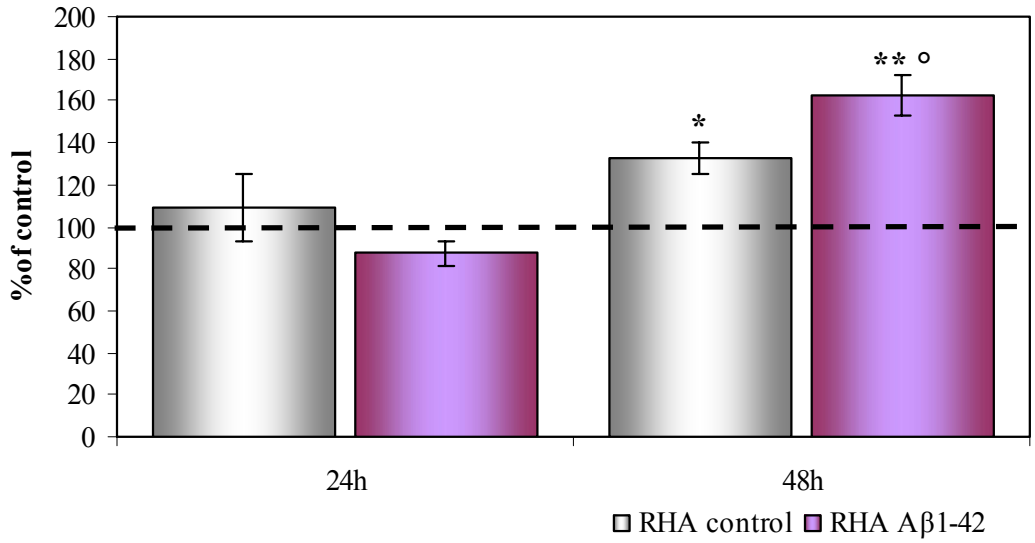

Fig. 3.19: BrdU assay performed on RCECs after 24 or 48 hours of treatment with 24 and 48 hours control and $A\beta_{1-42}$ 10^{-7}M treated RHA culture mediums. 24 hours RHA medium did not affect proliferation rate of RCECs after 24 hours while 48 hours control culture medium increased proliferation of RCECs after 48 hours in comparison to new RHA culture medium. * $p<0.05$ to control. Statistical analysis was performed by ANOVA followed by the t-test of Student-Newman-Keuls as post-hoc test. Bars are means±standard deviation of six separate experiments.

3.4.2. Migration

Collected cell culture mediums of 24 and 48 hour control and $A\beta_{1-42}$ 10^{-7}M treated RHAs were used to assess chemotaxic effect on RCECs. After 4 hours of incubation no effects were observable using 24 and 48 hours control and treated RHA culture medium (Fig. 3.20).

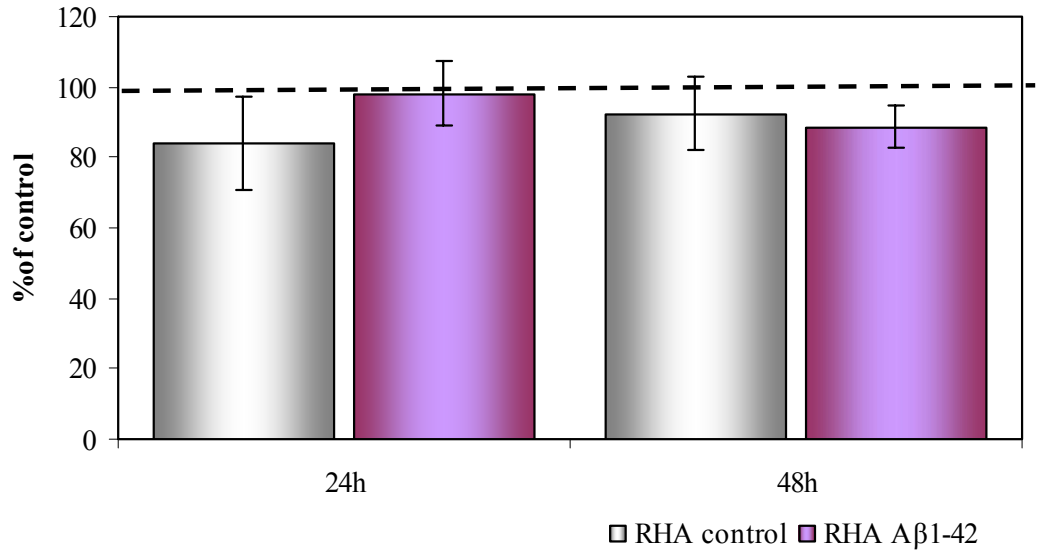

Fig. 3.20: migration assay performed using the Boyden chamber technique to assess chemotaxis of 24 and 48 hours control and $A\beta_{1-42}$ treated RHA cell culture medium after 4 hours of incubation on RCECs. No effects were observable in all considered cases. Statistical analysis was performed by ANOVA followed by the t-test of Student-Newman-Keuls as post-hoc test. Bars are means±standard deviation of three separate experiments.

3.4.3. Morphogenesis on Matrigel

To assess whether 24 and 48 hours control and $A\beta_{1-42}$ 10^{-7}M RHA culture medium affected capillary-like structures formation after 24 and 48 hours, cells were seeded on growth factor-reduced Matrigel. Qualitative analysis of imagines showed increasing formation of capillary-like structures in RCECs in both specimens in comparison to new RHA medium (Fig. 3.21).

Quantitative analysis confirmed that 24 and 48 hours RHA control medium increased dimensional parameters, such percent area covered by cells and the total length of cell network per field, and topological parameters, such as mesh number and branching points per field as compared to new RHA culture medium. $A\beta_{1-42}$ treated RHA mediums increased all considered parameters in comparison to new culture medium after 24 and 48 hours of treatment (Fig. 3.22).

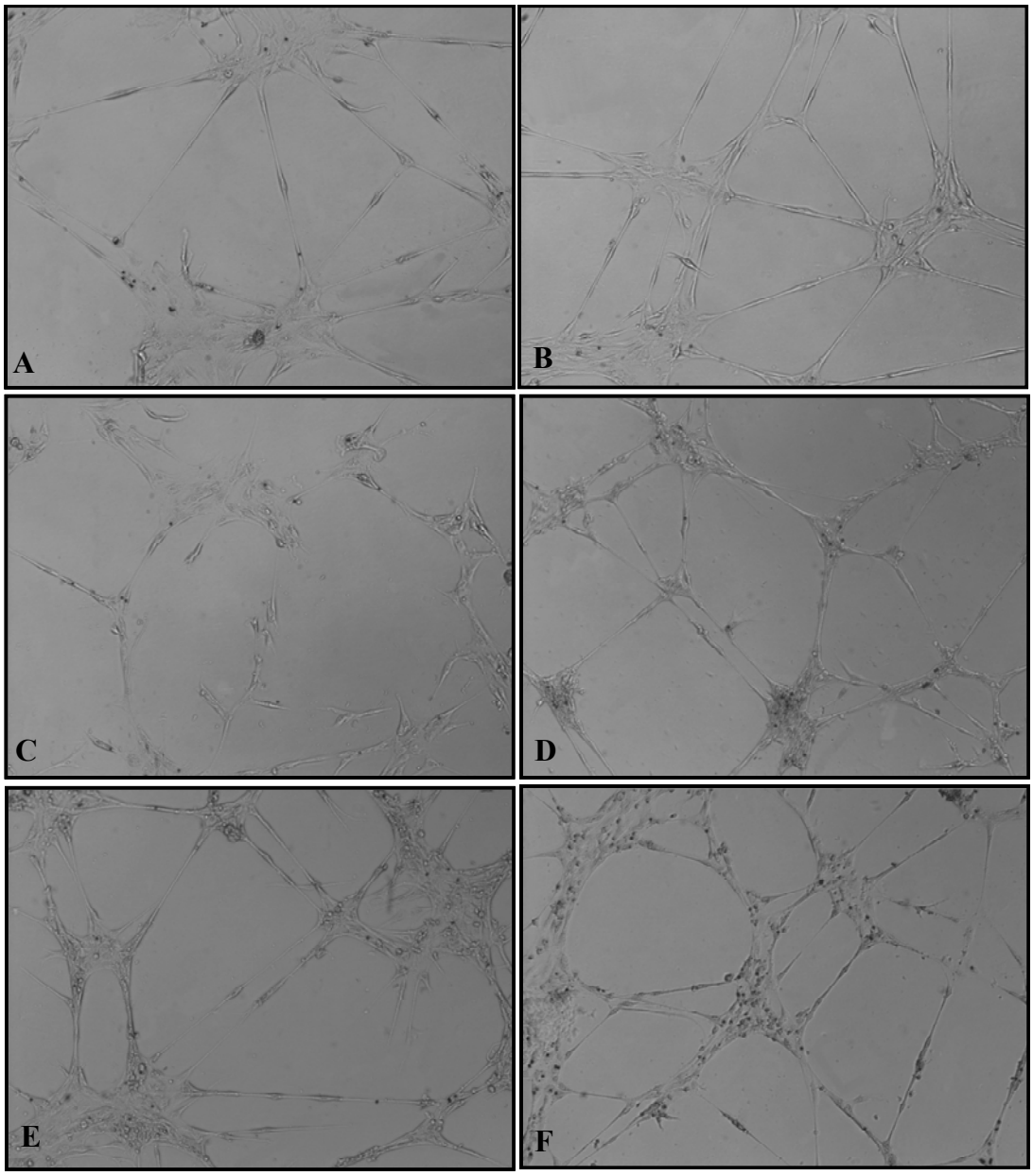

Fig. 3.21: Aβ peptide-induce tube formation by RCECs seeded in Matrigel after 24 and 48 hours of treatments with 24 (A, B, C) and 48 (D, E, F) hours control and $A\beta_{1-42}$ 10^{-7}M RHA culture mediums. (A) and (E) effect of control RHA culture medium on RCECs respectively after 24 and 48 hours of incubation; (B) and (F) effect of $A\beta_{1-42}$ 10^{-7}M RHA culture medium on RCECs respectively after 24 and 48 hours of incubation; (C) and (D) effect of new RHA culture medium on RCECs respectively after 24 and 48 hours of incubation.

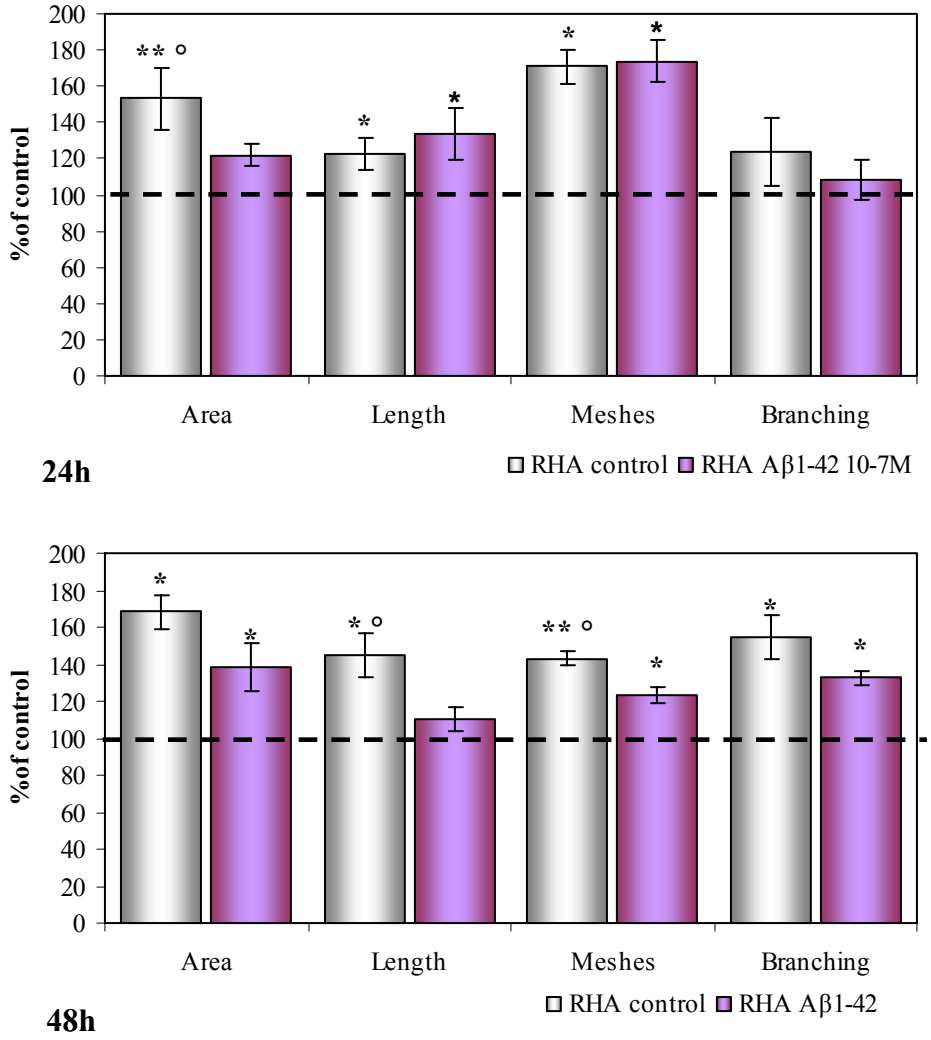

Fig. 3.22: quantitative analysis of tube formation estimated as dimensional (percent of area covered by cells and total length of cell network per filed) and topological (mesh number and branching point per field) parameters indicates that both 24 and 48 hours RHA control and $A\beta_{1-42}$ 10^{-7}M culture medium increased the formation of capillary-like structure formation after 24 and 48 hours in RCECs in comparison to new culture medium. The treatment with control RHA culture medium incubated 24 and 48 hours increased all considered parameters also in comparison to $A\beta_{1-42}$ 10^{-7}M culture medium. * $p<0.05$ and ** $p<0.01$ to new RHA culture medium; ° $p<0.05$ to $A\beta_{1-42}$ 10^{-7}M RHA culture medium. Statistical analysis was determined by Student's t test unpaired data between mean values. Bars are means±standard deviation of five separate experiments.

3.4.4. Determination of cytokines in culture mediums

To determine the levels of three cytokines (IL-1β, IL-6 and TNF-α) in 6, 12, 24 and 48 hour non-treated and $A\beta_{1-42}$ treated RHA culture mediums before and after the exposure on RCECs for 6, 12, 24 and 48 hours respectively, Rat Cytokine/Chemokine Linco*plex* Kit (Millipore, Milano, Italy) based on Luminex method

was used. Both non-treated RHAs and RCECs release low levels of the cytokines. RHA non-treated mediums were used as control.

After 6 and 12 hours the level of IL-1β significantly increases in all the mediums in comparison to control. Moreover the medium of RCECs cultured in $A\beta_{1-42}$ treated RHA medium presents significantly higher levels of IL-1β in comparison to medium of RCECs cultured in non-treated RHA medium. No differences were observed after 24 and 48 hours of treatment in comparison to control.

The level of IL-6 increases in non-treated and $A\beta_{1-42}$ treated RHA mediums after the exposure on RCECs. No differences were observed in $A\beta_{1-42}$ treated RHA medium in comparison to control at all the considered times. After 6 hours in the medium of RCECs cultured on $A\beta_{1-42}$ treated RHA medium the increasing in the levels of IL-6 is higher in comparison to all the other mediums.

After 6, 12 and 48 hours the level of TNF-α significantly increases in $A\beta_{1-42}$ treated RHA mediums and decreases in the other mediums in comparison to control. No effects were observed after 24 hours of treatment.

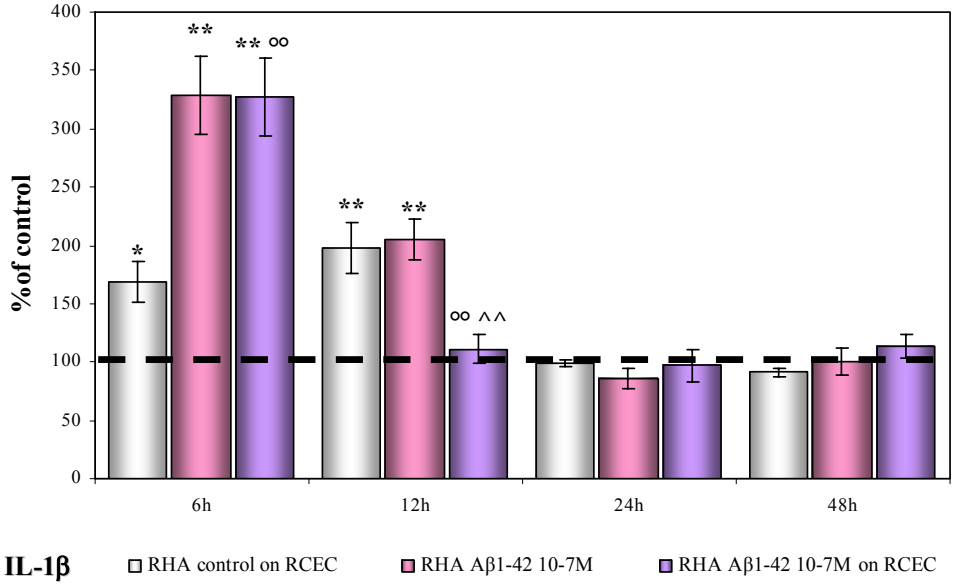

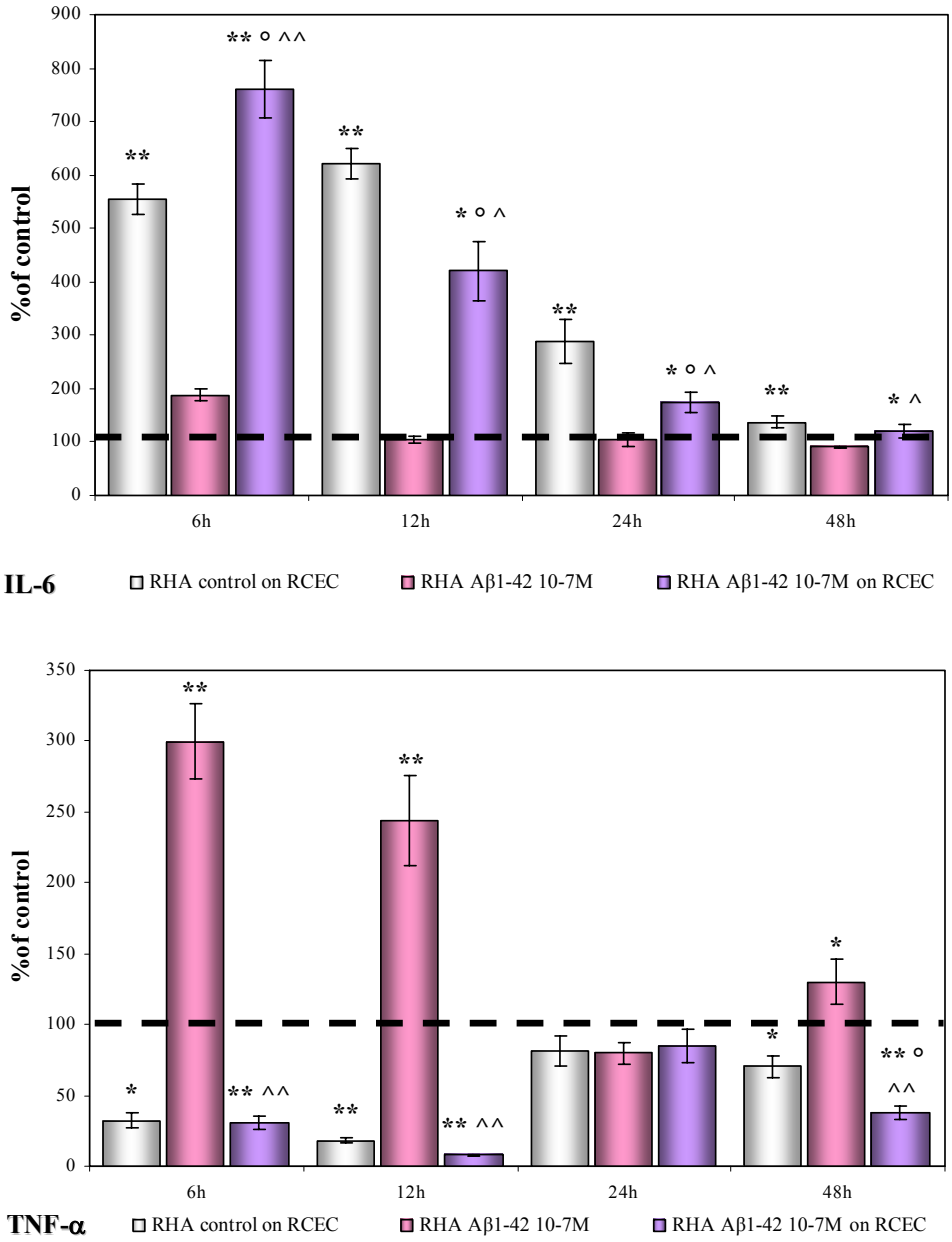

Fig. 3.23: effect of 6, 12, 24 and 48 hours of non-treated and $A\beta_{1-42}$ 10^{-7}M treated RHA culture medium on the release of IL-1α, IL-6 and TNF-α before and after the contact of RCECs, as measured by Luminex technique. * p<0.05 to control; ** p<0.01 to control; ° p<0.05 to $A\beta_{1-42}$ 10^{-7}M RHA culture medium; °° p<0.01 to $A\beta_{1-42}$ 10^{-7}M RHA culture medium; ^ p<0.05 to RCEC medium treated with non-treated RHA medium; ^^ p<0.01 to RCEC medium treated with non-treated RHA medium. Statistical analysis was performed by ANOVA followed by the t-test of Student-Newman-Keuls as post-hoc test. Bars are means±standard deviation of four separate experiments.

3.4.5. Viability

MTT assay was performed to assess whether 6, 12, 24 and 48 hours control and $A\beta_{1-42}$ 10^{-7}M treated RHA culture mediums affected RCEC viability after 6, 12, 24

and 48 hours respectively. No effects were observed after 6 and 24 hours of treatment with 6 and 24 hours mediums respectively while after 12 hours control and treated cell culture mediums redox activity of RCECs increased in comparison to new 12 hours RHA medium assayed. The incubation of 48 hours RHA treated culture medium for 48 hours on RCECs decreased redox activity in comparison to new RHA medium and the 48 hours RHA control culture medium increased viability in comparison to new $A\beta_{1\text{-}42}$ treated RHA medium (Fig. 3.24).

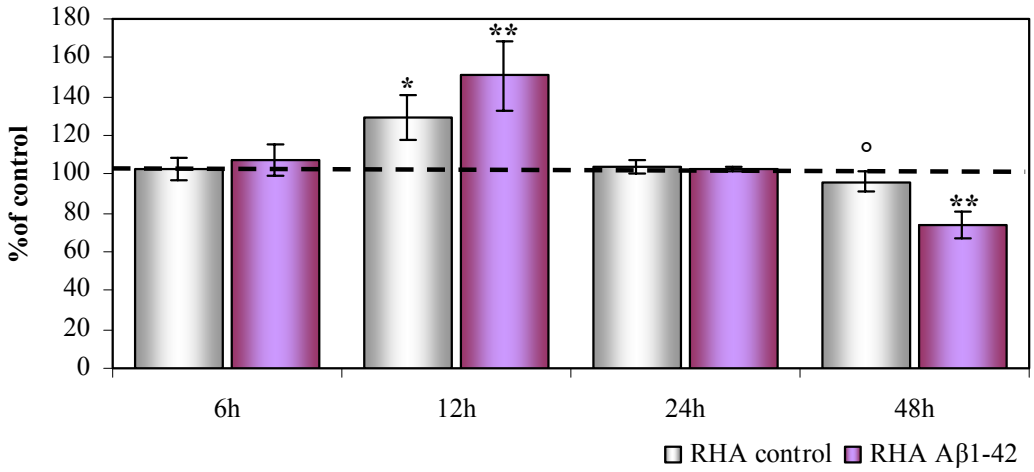

Fig. 3.24: effect of 6, 12, 24 and 48 hours of control and $A\beta_{1\text{-}42}$ 10^{-7}M treated RHA culture medium on the viability of cultured RCECs, as measured by MTT-reduction assay after 6, 12, 24 and 48h. * $p<0.05$ to control; ** $p<0.01$ to control; ° $p<0.05$ to to $A\beta_{1\text{-}42}$ 10^{-7}M RHA culture medium. Statistical analysis was performed by ANOVA followed by the t-test of Student-Newman-Keuls as post-hoc test. Bars are means±standard deviation of four separate experiments.

3.5. Experimentation with $A\beta_{1\text{-}42}$ peptide in absence and in presence of $hVEGF_{165}$ on RCECs

3.5.1. RCEC viability and proliferation with increasing concentration of $hVEGF_{165}$

To assess the concentration of $hVEGF_{165}$ that does not affect viability and proliferation of RCECs increasing concentration of $hVEGF_{165}$ (0,1; 0,2; 0,3; 0,4; 0,5 and 5 ng/ml) were tested at 24 hours of incubation by Trypan Blue exclusion assay and proliferation, using BrdU assay. The concentration that satisfied the condition in both tests was 0,4ng/ml of $hVEGF_{165}$ (Fig. 3.25).

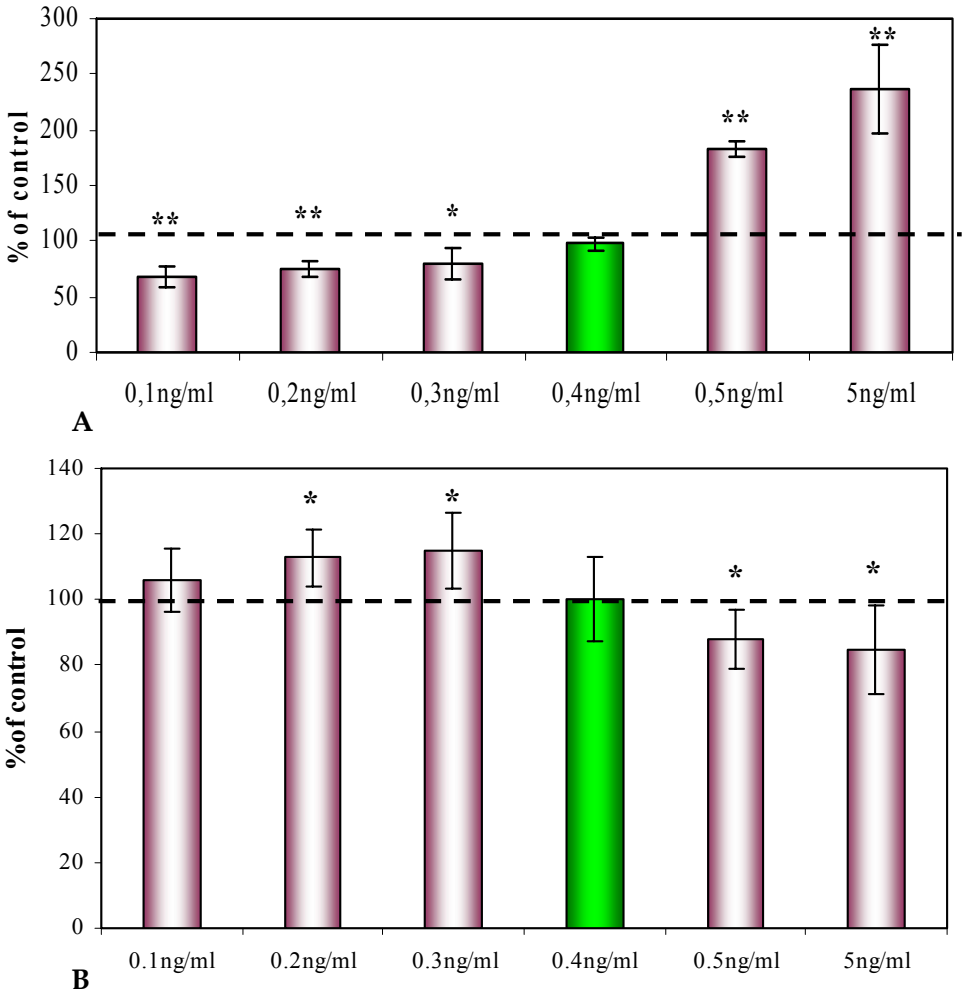

Fig. 3.25: increasing concentration of $hVEGF_{165}$ to assess the concentration that has the same effect of control in RCEC Trypan Blue exclusion assay (A) and proliferation (B). The satisfied concentration in both assays resulted 0,4ng/ml. * $p<0.05$ and ** $p<0.01$ to control. Statistical analysis was determined by Student's t test unpaired data between mean values. Bars are means±standard deviation of four separate experiments.

3.5.2. Aggregation kinetics

Tioflavin T (ThT) rapidly associates in β-sheet-rich aggregates giving rise to a new λ_{max} excitation at 416nm and enhances emission λ_{max} at 550nm, as opposed to the 385nm (ex) and 445nm (em) λ values of the free dye. This change is dependent on the aggregational state, in that monomeric or dimeric peptides do not react with ThT (LeVine et al., 1993). Aggregation kinetics of $A\beta_{1-42}$ in absence or in presence of $hVEGF_{165}$ was studied following ThT fluorescence at 0, 24, 96 and 168 hours. As shown in Fig. 3.26, $A\beta_{1-42}$ self-aggregation increased, remaining unchanged, after 24 hours of incubation in PBS at 37°C. When incubated in presence of $hVEGF_{165}$, $A\beta_{1-}$

$_{42}$ aggregation decreased in comparison to Aβ$_{1-42}$ alone resulting similar to the peptide at time 0. The aggregation state of co-incubation did not vary during the aggregation kinetics.

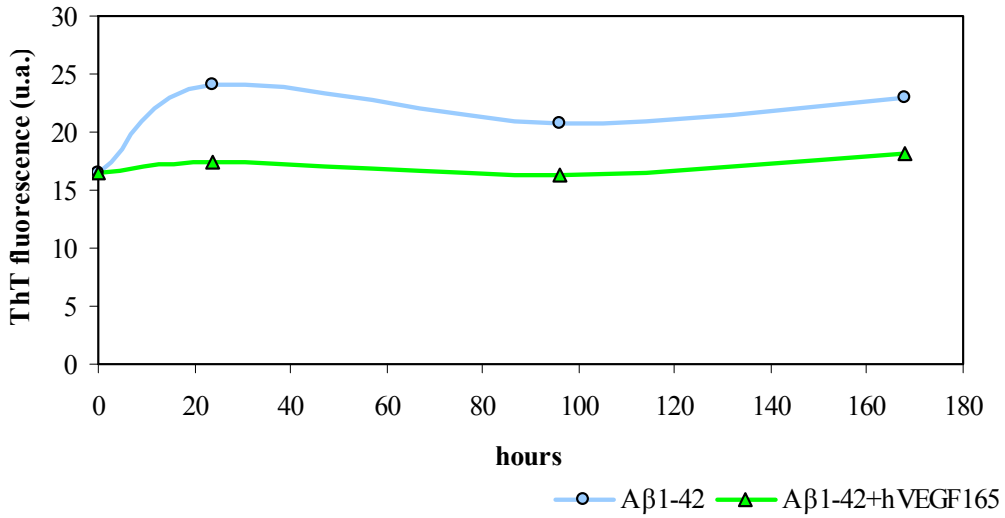

Fig. 3.26: aggregation kinetics of Aβ$_{1-42}$ peptide in absence and in presence of hVEGF$_{165}$ studied by variation of Tioflavin T (ThT) fluorescence emission intensity. ThT fluorescence was collected at 550nm (λexc = 416nm) with a dye concentration of 3μM. The concentration of Aβ$_{1-42}$ was 10^{-4}M and hVEGF$_{165}$ was 0,4μg/ml. The signal due to ThT alone was subtracted.

3.5.3. RCEC viability

The effect of freshly solubilised Aβ$_{1-42}$ and 24 hours aged Aβ$_{1-42}$ in absence or in presence of hVEGF$_{165}$ on 24 hours treated RCEC viability was assayed by MTT. Aβ$_{1-42}$ peptides were tested at concentration 10^{-7}M and hVEGF$_{165}$ at concentration 0,4ng/ml. Redox activity was significantly decreased by both freshly solubilised Aβ$_{1-42}$ and 24 hours aged Aβ$_{1-42}$ in comparison to non treated cells. 24 hours aged Aβ$_{1-42}$ in presence of hVEGF$_{165}$ increased RCEC viability in comparison to control and both Aβ peptides (Fig. 3.27).

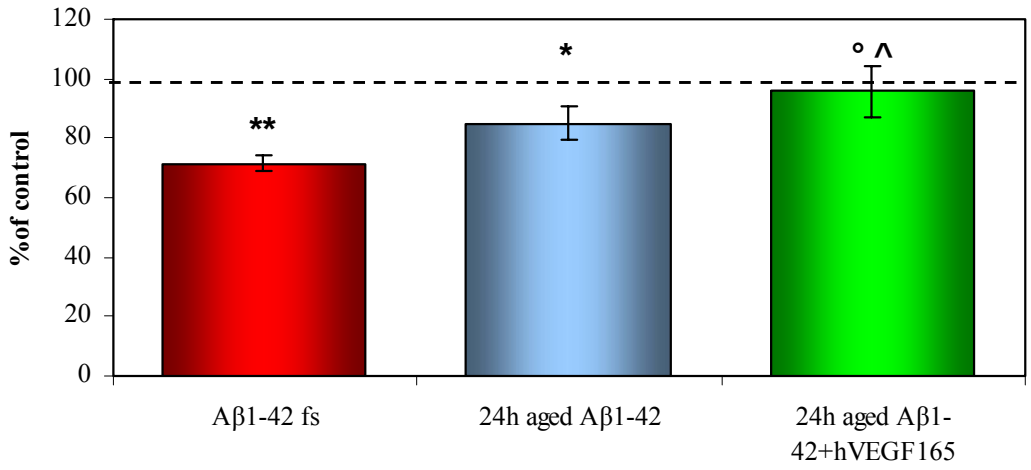

Fig. 3.27: effect of freshly solubilised $A\beta_{1-42}$ and 24 hours aged $A\beta_{1-42}$ in absence or in presence of $hVEGF_{165}$ at concentration 10^{-7}M on the viability of cultured RCECs, as measured by MTT-reduction assay after 48h. * p<0.05 and ** p<0.01 to control; ° p<0.05 and °°p<0.01 freshly solubilised $A\beta_{1-42}$; ^^ p<0.01 24 hours aged $A\beta_{1-42}$. Statistical analysis was performed by ANOVA followed by the t-test of Student-Newman-Keuls as post-hoc test. Bars are means±standard deviation of three separate experiments.

3.5.4. Morphogenesis on Matrigel

To assess whether 24 hours aged $A\beta_{1-42}$ in absence or in presence of $hVEGF_{165}$ and freshly solubilised $A\beta_{1-42}$ affected capillary-like structures formation after 24 hours, cells were seeded on growth factor-reduced Matrigel. Qualitative analysis of imagines showed decreasing formation of capillary-like structures in RCECs treated with freshly solubilised $A\beta_{1-42}$ and 24 hours aged $A\beta_{1-42}$ at concentration 10^{-7}M in comparison to control (Fig. 3.28). RCECs treated with 24 hours aged $A\beta_{1-42}$ in presence of $hVEGF_{165}$ showed increased formation of structures in comparison to freshly solubilised $A\beta_{1-42}$, 24 hours aged $A\beta_{1-42}$ and control.

Quantitative analysis confirmed that as freshly solubilised as 24 hours aged $A\beta_{1-42}$ after 24 hours of treatment at concentration 10^{-7}M decreased dimensional parameters, such percent area covered by cells and the total length of cell network per field, and topological parameters, such as mesh number and branching points per field as compared to non treated cells. 24 hours aged $A\beta_{1-42}$ in presence of $hVEGF_{165}$ increased all considered parameters in comparison to soluble and aggregated $A\beta_{1-42}$ after 24 hours of treatment. (Fig. 3.29).

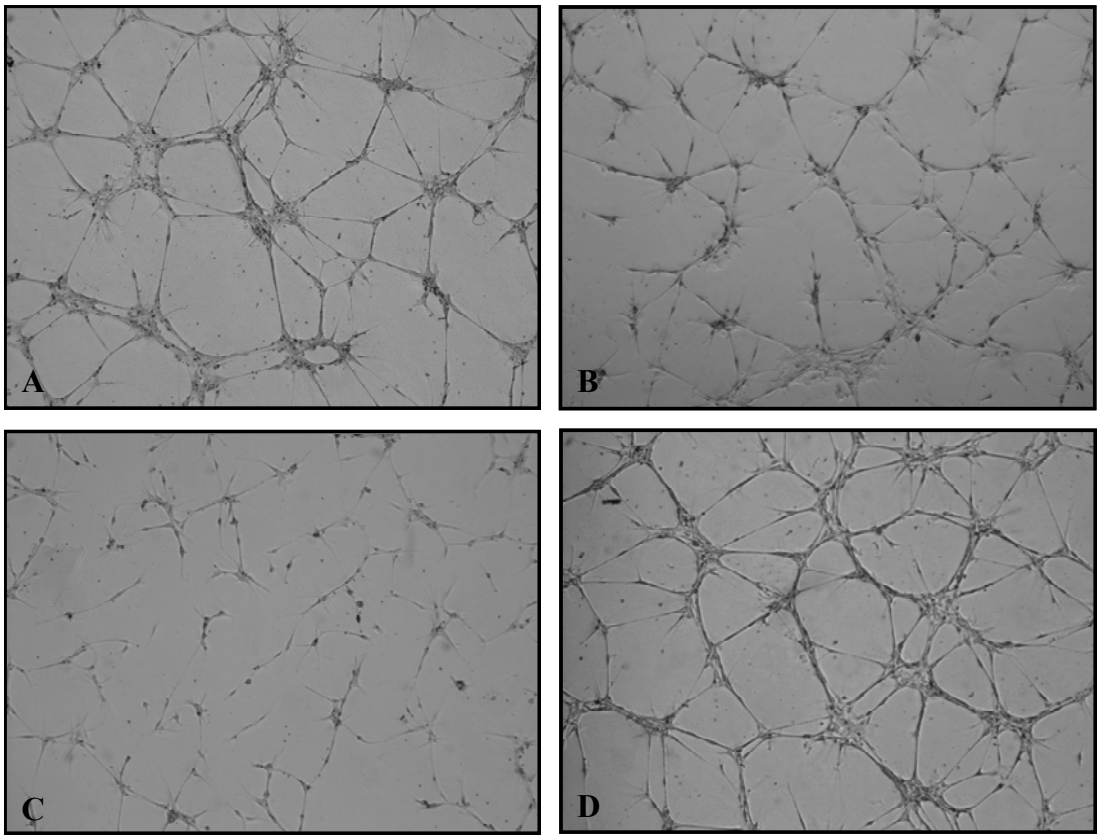

Fig. 3.28: Aβ peptide-induce tube formation by RCECs seeded in Matrigel after 24 hours of treatments. (A) control cell; (B) freshly solubilised $A\beta_{1-42}$ 10^{-7}M; (C) 24 hours aged $A\beta_{1-42}$ 10^{-7}M; (D) 24 hours aged $A\beta_{1-42}$ in presence of $hVEGF_{165}$.

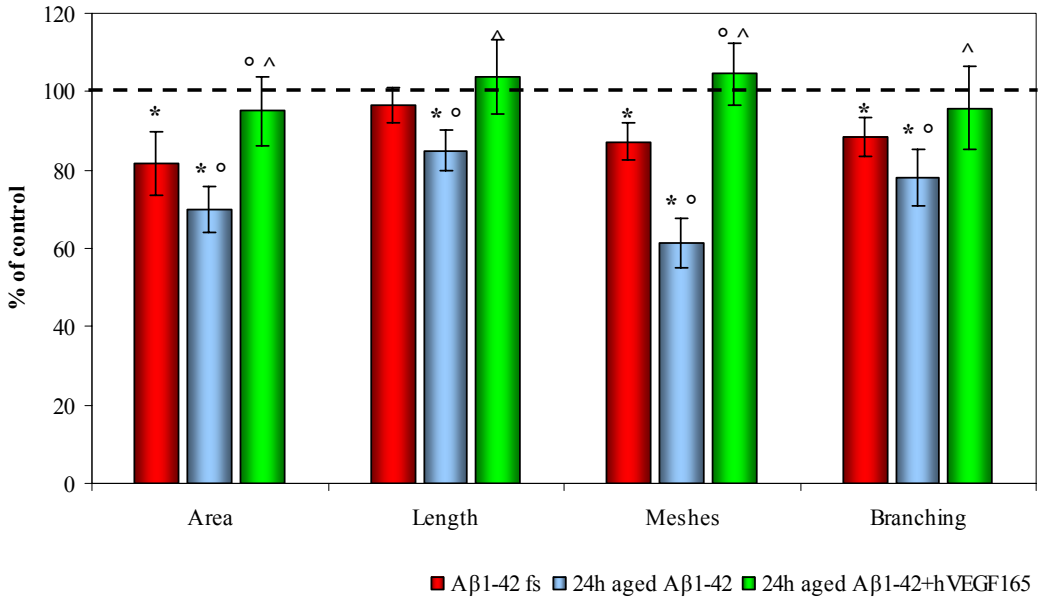

Fig. 3.29: quantitative analysis of tube formation estimated as dimensional (percent of area covered by cells and total length of cell network per filed) and topological (mesh number and branching point per field) parameters indicates that both freshly solubilised $A\beta_{1\text{-}42}$ and 24 hours aged $A\beta_{1\text{-}42}$ at concentration 10^{-7}M decreased the formation of capillary-like structure formation after 24 in RCECs in comparison to non treated cells. The treatment with 24 hours aged $A\beta_{1\text{-}42}$ in presence of $hVEGF_{165}$ increased all considered parameters in comparison to both freshly solubilised $A\beta_{1\text{-}42}$ and 24 hours aged $A\beta_{1\text{-}42}$. * $p<0.05$ to control; ° $p<0.05$ to freshly solubilised $A\beta_{1\text{-}42}$; ^ $p<0.05$ to 24 hours aged $A\beta_{1\text{-}42}$. Statistical analysis was determined by ANOVA followed by the t-test of Student-Newman-Keuls as post-hoc test. Bars are means±standard deviation of five separate experiments.

4 Discussion

Angiogenesis, the formation of new vessels from pre-existing vasculature, is a highly complex and coordinated series of events that involves the degeneration of vascular BM, the proliferation of ECs and the targeting, maturation and expansion of neovasculature (Pogue and Lukiv, 2004). Angiogenesis takes place in various physiological and pathological conditions, such as embryonic development, chronic inflammation and tumors (Bouïs et al, 2006). In both cerebral vascular disease and AD, amyloid is associated with angiopathy that includes irregularities in arterial wall structure, such as alterations of BM, loss of smooth muscle cells and weakening of the vessel wall (Vinters et al., 1996), and increased microcapillary density in the region of Aβ deposits (Hoozemans et al., 2002; McGeer and McGeer, 2003). Thirumangalakudi and co-workers (2006) comparing the expression of the angiogenic mediators VEGF, Ang and MMPs in the microcirculation of AD patients and age-matched controls demonstrated that Ang-2 and VEGF are expressed by AD- but not control-derived microvessels.

The understanding of mechanisms that promote angiogenesis could allow for the realization of clinical applications for the formation of new vessels in tissue and organ transplantation assuring constant and stable supply of nutrients and oxygen, two of the major limiting factor for the success of a transplant, on one hand and, at the same time, for the reduction of angiogenesis-dependent pathologies. In that context the **aim** of the present work is an attempt to understand angiogenic mechanisms activated during AD analysing the effect of two of the major components of vascular deposits and SP, $A\beta_{1-40}$ and $A\beta_{1-42}$ peptides, *in vivo* by the CAM assay, *ex-vivo* by the aortic ring assay and *in vitro* using two endothelial cell culture models, the Human Cerebral Endothelial Cells (HCECs) and the Rat Cerebral Endothelial Cells (RCECs), by the analysis of their effect on proliferation, migration and capillary-like structure formation on Matrigel.

Our results demonstrate that both $A\beta_{1-40}$ and $A\beta_{1-42}$ peptides stimulate the *in vivo* formation of capillary vessels in the chick embryo CAM, an extraembryotic membrane which serves as a gas network and is widely utilized as a target for angiogenic and anti-angiogenic compounds. Moreover *ex-vivo* experiments performed on

rat aortic-ring confirmed that both Aβ peptides concentration 10^{-7}M increase the formation of vessel structures. These data are in accord with those previously published by Cantara and co-workers (2004; 2005) showing that $A\beta_{1-40}$ peptide stimulate ECs to acquire an angiogenic phenotype through interaction with endogenous FGF-2 and induction of its synthesis. Conversely, experiments performed by Paris and co-workers (2004) using concentration higher than ours, demonstrated dose-dependent inhibition of angiogenesis by $A\beta_{1-40}$ and $A\beta_{1-42}$ peptides as by CAM and rat aortic-ring assays. Thus Aβ peptides show different effect *in vivo* and *ex-vivo* on the angiogenic process in relation to concentration.

Our *in vitro* experiments performed on RCECs and, for the first time, on normal HCEC cultures demonstrated the $A\beta_{1-40}$ and $A\beta_{1-42}$ 10^{-7}M promote angiogenesis on HCECs increasing proliferation, migration and formation of capillary-like structures on Matrigel and decreasing the formation of capillary-like structures on RCECs after 24 hours of treatment. The peptides on these cells show an anti-angiogenic. The anti-angiogenic effect of Aβ peptides on RCECs after 24 hours of treatment is the result of decreased viability observed at the same incubation time. Our results corroborate those obtained by other researchers: the effect of Aβ peptides is strictly linked to the animal model utilized and to cell organ origin (Paris et al., 2004; Cantara et al., 2004). However literature data showed that Aβ peptides *in vitro* express dual role in angiogenesis depending on concentration of the peptide. In particular nanomolar concentrations of Aβ peptides increase microvessels outgrowth within Matrigel of human middle cerebral arteries ECs while micromolar concentrations decrease formation of capillary-like structures (Paris et al, 2004). Thus Aβ peptides exert pro-angiogenic effects at low concentration while higher concentrations inhibit the process. It has been demonstrated that Aβ peptides induce apoptosis in neurons, ECs, cerebrovascular smooth muscle cells, oligodendrocytes and astrocytes (Hsu et al., 2007). Experimental evidence on HUVECs and bovine aortic ECs (BAECs) demonstrated that Aβ peptides inhibit two endothelial responses critical to angiogenesis, EC migration and proliferation, and affect the viability of ECs (Magrane et al., 2006). Exposure of quiescent capillary venular ECs from bovine hearth to $A\beta_{1-40}$ peptide in concentration ranging from nanomolar to micromolar greatly affects their ability to proliferate: nanomolar concentrations of Aβ stimulate cell growth while micromolar concentrations inhibit the proliferation

probably as consequence of cell death (Cantara et al., 2004; Cantara et al., 2005). It has been hypothesized that during early phases of the development of AD, Aβ stimulates ECs to acquire an angiogenic phenotype through interaction with endogenous FGF-2 and induction of its synthesis. This could be a protective mechanism to counteract hypoxia or the diminished vascular function close to the site of inflammation, or, instead, may facilitate the inflammatory process. Later Aβ starts to accumulate, becoming toxic for ECs and its aggregation contributes to exacerbating the inflammation (Cantara et al., 2005). As no differences were observed between the two Aβ isoforms, the following experiments were performed using $A\beta_{1\text{-}42}$ 10^{-7}M peptide.

To evaluate if $A\beta_{1\text{-}42}$ is anti-angiogenic on RCECs altered the release and the production of VEGF-A, the amount of VEGF-A released by RCECs and mRNA for VEGF-A in RCECs were evaluated respectively by ELISA kit and semiquantitative Real Time-RT PCR after 3, 24 or 48 hours of treatment. VEGF is known to be the major pro-angiogenic factor and prime regulator of EC proliferation. Enhanced VEGF immunoreactivity has been found in the neurocortex of patients with AD and the expression of this compound has been shown in reactive astrocytes and ECs surrounding amyloid deposits in brains with AD (Chiappelli et al., 2006). No differences between treated and no treated cells were observed in the release of VEGF-A in culture mediums and the transcription of mRNA for VEGF-A. These results confirm previous data obtained by Park and Chae (2007). They observed that cytotoxic concentrations of $A\beta_{1\text{-}42}$ does not affect VEGF synthesis and expression in an immortalized cell line derived from a somatic cell fusion of mouse hippocampal neurons and neuroblastoma cells. Moreover they demonstrated that Aβ reduces the production H_2O_2, a stimulator of VEGF, and thus the expression of VEGF. *In vivo* experiments performed by Zand and co-workers (2005) demonstrate considerable angiogenesis and up-regulation of VEGF expression 7 days post-injection of $A\beta_{1\text{-}42}$ in rat hippocampus. Furthermore, immunoreactivity was associated with astrocytes, but not with ECs, suggesting roles for these cells as a source of VEGF to promote proliferation and activation of ECs. Starting from these observations the effect of $A\beta_{1\text{-}42}$ 10^{-7}M on Rat Hippocampal Astrocytes (RHAs) release of VEGF-A and expression of mRNA for VEGF-A after were evaluated. No differences between treated and not treated cells for the release of VEGF-A and the production of mRNA for VEGF-A after 3,

24 or 48 hours were observed. Moreover $A\beta_{1-42}$ does not affect RHA viability at the same incubation times contrary to reports in literature, where the exposition of RHAs to $A\beta_{1-42}$ peptide decrease cell viability in absence of cell death and increase proliferation (Kerokoski et al., 2001). Thus in rat cell culture models, $A\beta_{1-42}$ 10^{-7}M decreases angiogenesis capability as consequence of toxic effect on RCECs without affecting VEGF release.

Trying to explain the different *in vivo* and *in vitro* effect of Aβ peptide on RCECs and assuming that Aβ acts as an indirect factor on promoting angiogenesis, 24 and 48 hour control and $A\beta_{1-42}$ treated RHA culture mediums were tested on RCECs for 24 and 48 hours respectively and proliferation, migration and capillary-like structure formations were evaluated. The results demonstrate that both 48 hour RHA mediums increase the proliferation of RCECs but the $A\beta_{1-42}$ treated RHA mediums' effect is high in comparison to control medium. Moreover both 24 and 48 hour mediums increase the formation of capillary-like structures on Matrigel but RHA control mediums are more angiogenic than $A\beta_{1-42}$ 10^{-7}M treated RHA mediums. Based on these results we assume that RHAs are necessary for brain angiogenesis and $A\beta_{1-42}$ peptide does not affect that process.

Many studies report high levels of several inflammatory cytokines in serum or plasma of AD patients. In particular increased levels of IL-1β, IL-6 and TNF-α have been found in both peripheral blood and autopsy specimens of patients with mild to moderate late-onset AD (Guerreiro et al., 2007). In the last few years it has been hypothesised that Aβ activates microglia that releases various inflammatory mediators including a whole array of neurotoxic cytokines. Once activated, microglia cells may also recruit astrocytes that actively enhance the inflammatory response to extracellular Aβ deposits, explaining the pro-inflammatory state and damage founded on AD brains (Heneka and O'Banion, 2007). AD microvessels express high levels of IL-1β, IL-6, TNF-α and TGF-β and are therefore an important source of inflammatory proteins (Christov et al., 2004). As inflammation is a process that can activate angiogenesis, trying to understand what factors could be interesting in that process, the quantification of levels of IL-1β, IL-6 and TNF-α on control and Aβ treated RHA culture mediums before and after exposure to RCECs have been evaluated using the Multiplex technique. 24 and 48 hour RHA culture mediums increase release of IL-6 from RCECs

after 25 and 48 hours even if it is independent of Aβ treatment. It is known that the release of IL-6 occurs as consequence of stimulation of IL-1β. Thus levels of the IL-1β, IL-6 and TNF-α were analysed on control and Aβ treated RHA culture mediums before and after theexposure on RCECs for 6 and 12 hours. The levels of all the cytokines increase. In particular IL-1β level increases in all the mediums while IL-6 level increases only in RCEC medium treated with both control and RHA treated mediums. Interestingly level of TNF-α increases only in the Aβ treated RHA medium. Thus RHA mediums stimulate the secretion of IL-1β and TNF-α from RCECs within 24 hours while the secretion of IL-6 is stimulated at all the considered times. The major effect is observable at 6 hours where the release is higher for all the cytokines. A large amount of literature data suggest that TNF-α inhibits *in vitro* angiogenesis phases such as endothelial proliferation and tube formation suggesting that TNF-α may induce angiogenesis indirectly by activating other regulators of angiogenesis. In particular Hangai and co-workers (2006) demonstrated that TNF-α induces the sequential upregulation of Ang-2 and then Ang-1 and VEGF mRNA and protein expression in choroidal microvascular endothelial cells and in HUVECs *in vitro*, exerting its profound angiogenic action *in vivo* by stimulating the appropriate sequence of endothelial-specific angiogenic factors. Recent evidence (Maisonpierre et al., 1997) suggests that angiogenesis requires initial inactivation of, or at least weakening of, constitutive Tie2 signalling in endothelial cells. It has been postulated that Ang-2 cooperate with VEGF at the leading edge of the vascular sprout by blocking the stabilizing or maturing function of Ang-1, thus allowing vessels to revert to, and remain in, a plastic state where they are more responsive to a sprouting signal by VEGF. These data provide support for the importance of TNF-α and Ang-1/Ang-2 and their autocrine regulatory loops in neovascularisation. (Hangai et al., 2006). The pro-angiogenic effect of RHA mediums can be the result of the stimulation of different substances that act together to promote angiogenesis. TNF-α could act as an activator of RCECs and subsequently other cytokines released by RHAs or by RCECs could promote angiogenesis. The evaluation of RCEC viability has demonstrated increasing after 12 hours of treatment with both control and RHA treated medium and decreasing after 48 hours. It seems possible that RHAs secrete pro-angiogenic factors that induce RCECs to secrete pro-inflammatory cytokines. The over-production of inflammatory

cytokines results in decreased viability of RCECs as reported in literature where high concentration of pro-inflammatory cytokines increase oxidative stress, down-regulate endothelial NOS (eNOS) bioactivity and induce EC apoptosis (Kofler et al., 2005). Apoptotic signals have been reported to be implicated in a variety of cellular functions, including cell proliferation, survival, differentiation and inflammatory response (Izumi et al., 2005). However more studies are necessary to understand the effect and consequences of RHA mediums on RCECs.

A growing number of *in vitro* and *in vivo* studies support the notion that soluble oligomeric peptides with high β-sheet content are toxic to neuronal cells and cause their dysfunction and death. In contrast, the aggregation of these peptides in the form of fibrillar amyloid may represent a protective response that delays neurodegeneration by sequestering soluble Aβ into amyloid fibrils or into amorphous aggregates (Watson et al., 2005). Moreover it has been observed that VEGF is heavily accumulated and co-localized with Aβ plaques in the brain of patients with AD. In vitro experiments have shown that VEGF binds to Aβ with high affinity and is co-aggregated with Aβ (Yang et al., 2004). Aβ interact with $VEGF_{165}$ but not with $VEGF_{121}$ as consequence of the binding of Aβ with the Heparin-Binding Domain (HBD) of $VEGF_{165}$ (the C-terminal HBD encoded by exon 7 and 8 and thus not present in $VEGF_{121}$). The core binding of Aβ appears to be between 25 and 35 amino acid, the region known to be responsible for the toxicity of Aβ. In fact the binding between VEGF and Aβ protect cells from Aβ-induced neurotoxicity by the inhibition of Aβ aggregation (Yang et al., 2005). Starting from these observations the effect of freshly solubilised $Aβ_{1-42}$ and 24 hours aged $Aβ_{1-42}$ in absence or in presence of $hVEGF_{165}$ on RCEC viability was evaluated. In agreement with Yang and co-workers (2005) results on pheochromocytoma cell cultures the presence of $hVEGF_{165}$ increases RCEC viability in comparison to control, to freshly solubilised and 24 hours aged $Aβ_{1-42}$. Thus the aggregation kinetics of $Aβ_{1-42}$ in absence and in presence of $hVEGF_{165}$ was performed following ThT fluorescence at 0, 24, 96 and 168 hours. The presence of $hVEGF_{165}$ disfavours the formation of Aβ β-sheet structures and thus the possibility to form aggregates. Moreover the presence of $hVEGF_{165}$ restores the cell capability of capillary-like tubule formation on Matrigel probably as consequence of the recovery of viability.

In conclusion it is possible to assert that Aβ peptides are equally angiogenic *in vivo*, *ex-vivo* and *in vitro* on HCECs while they are anti-angiogenic on RCECs, probably as consequence of their reduction on viability. This anti-angiogenic effect is not due to interference on VEGF production and secretion on RCECs and neither on RHAs. Moreover Aβ peptide does not affect the secretion of pro-inflammatory cytokines on RHAs. Non-treated and treated RHA culture mediums induce the formation of capillary-like structure formation suggesting a pivotal role of RHAs on the angiogenic process. Moreover $A\beta_{1\text{-}42}$ stimulate the secretion of TNF-α from RHAs. The cytokine could act as activator of RCECs to promote an activated state. Subsequently other cytokines contained in the mediums could promote angiogenesis. The increased production of VEGF in AD brains could be a protective mechanism to reduce the aggregated and more toxic forms of Aβ peptide. In fact $hVEGF_{165}$ binds $A\beta_{1\text{-}42}$ disfavouring its aggregation and its toxic effects on RCECs.

References

Aase K, von Euler G, Li X, Pontén A, Thorén P, Cao R, Cao Y, Olofsson B, Gebre-Medhin S, Pekny M, Alitalo K, Betsholtz C, Eriksson U, *Vascular endothelial growth factor-B-deficient mice display an atrial conduction defect*, Circulation. 2001 Jul 17;104(3):358-64

Abbott NJ, Hughes CC, Revest PA, Greenwood J, *Development and characterisation of a rat brain capillary endothelial culture: towards an in vitro blood-brain barrier*, J Cell Sci. 1992 Sep;103 (Pt 1):23-37

Abbott NJ, Rönnbäck L, Hansson E, *Astrocyte-endothelial interactions at the blood-brain barrier*, Nat Rev Neurosci. 2006 Jan;7(1):41-53, Review

Albini A, Sporn MB, *The tumour microenvironment as a target for chemoprevention*, Nat Rev Cancer. 2007 Feb;7(2):139-47, Review

Aleardi AM, Benard G, Augereau O, Malgat M, Talbot JC, Mazat JP, Letellier T, Dachary-Prigent J, Solaini GC, Rossignol R, *Gradual alteration of mitochondrial structure and function by beta-amyloids: importance of membrane viscosity changes, energy deprivation, reactive oxygen species production, and cytochrome c release*, J Bioenerg Biomembr. 2005 Aug;37(4):207-25

Aliev G, Smith MA, de la Torre JC, Perry G, *Mitochondria as a primary target for vascular hypoperfusion and oxidative stress in Alzheimer's disease*, Mitochondrion. 2004 Sep;4(5-6):649-63

Asahara T, Murohara T, Sullivan A, Silver M, van der Zee R, Li T, Witzenbichler B, Schatteman G, Isner JM, *Isolation of putative progenitor endothelial cells for angiogenesis*, Science. 1997 Feb 14;275(5302):964-7

Auerbach R, Lewis R, Shinners B, Kubai L, Akhtar N, *Angiogenesis assays: a critical overview*, Clin Chem. 2003 Jan;49(1):32-40, Review

Bach F, Uddin FJ, Burke D, *Angiopoietins in malignancy*, Eur J Surg Oncol. 2007 Feb;33(1):7-15. Epub 2006 Sep 7, Review

Baiguera S, Conconi MT, Guidolin D, Mazzocchi G, Malendowicz LK, Parnigotto PP, Spinazzi R, Nussdorfer GG, *Ghrelin inhibits in vitro angiogenic activity of rat brain microvascular endothelial cells*, Int J Mol Med. 2004 Nov;14(5):849-54

Benelli R, Albini A, Noonan D, *Neutrophils and angiogenesis: potential initiators of the angiogenic cascade*, Chem Immunol Allergy. 2003;83:167-81, Review

Bitan G, Kirkitadze MD, Lomakin A, Vollers SS, Benedek GB, Teplow DB, *Amyloid beta -protein (Abeta) assembly: Abeta 40 and Abeta 42 oligomerize through dis-*

tinct pathways, Proc Natl Acad Sci U S A. 2003 Jan 7;100(1):330-5, Epub 2002 Dec 27 **(A)**

Bitan G, Vollers SS, Teplow DB, *Elucidation of primary structure elements controlling early amyloid beta-protein oligomerization*, J Biol Chem. 2003 Sep 12;278(37):34882-9, Epub 2003 Jul 2 **(B)**

Blennow K, de Leon MJ, Zetterberg H, *Alzheimer's disease*, Lancet. 2006 Jul 29;368(9533):387-403, Review

Block ML, Zecca L, Hong JS, *Microglia-mediated neurotoxicity: uncovering the molecular mechanisms*, Nat Rev Neurosci. 2007 Jan;8(1):57-69, Review

Boche D, Nicoll JA, *The role of the immune system in clearance of Abeta from the brain*, Brain Pathol. 2008 Apr;18(2):267-78, Review

Bouïs D, Kusumanto Y, Meijer C, Mulder NH, Hospers GA, *A review on pro- and anti-angiogenic factors as targets of clinical intervention*, Pharmacol Res. 2006 Feb;53(2):89-103, Review

Bustin SA, *Absolute quantification of mRNA using real-time reverse transcription polymerase chain reaction assays*, J Mol Endocrinol. 2000 Oct;25(2):169-93, Review

Bustin SA, Nolan T, *Pitfalls of quantitative real-time reverse-transcription polymerase chain reaction*, J Biomol Tech. 2004 Sep;15(3):155-66, Review

Byrne AM, Bouchier-Hayes DJ, Harmey JH, *Angiogenic and cell survival functions of vascular endothelial growth factor (VEGF)*, J Cell Mol Med. 2005 Oct-Dec;9(4):777-94, Review

Cantara S, Donnini S, Morbidelli L, Giachetti A, Schulz R, Memo M, Ziche M., *Physiological levels of amyloid peptides stimulate the angiogenic response through FGF-2*, FASEB J. 2004 Dec;18(15):1943-5, Epub 2004 Sep 24

Cantara S, Ziche M, Donnini S, *Opposite effects of beta amyloid on endothelial cell survival: role of fibroblast growth factor-2 (FGF-2),* Pharmacol Rep. 2005;57 Suppl:138-43

Cao Y, Lundwall A, Gadaleanu V, Lilja H, Bjartell A, *Anti-thrombin is expressed in the benign prostatic epithelium and in prostate cancer and is capable of forming complexes with prostate-specific antigen and human glandular kallikrein 2*, Am J Pathol. 2002 Dec;161(6):2053-63

Chi EY, Ege C, Winans A, Majewski J, Wu G, Kjaer K, Lee KY, *Lipid membrane templates the ordering and induces the fibrillogenesis of Alzheimer's disease amyloid-beta peptide*, Proteins. 2008 Jul;72(1):1-24

Chiappelli M, Borroni B, Archetti S, Calabrese E, Corsi MM, Franceschi M, Padovani A, Licastro F, *VEGF gene and phenotype relation with Alzheimer's disease and mild cognitive impairment*, Rejuvenation Res. 2006 Winter;9(4):485-93

Choi K, Zhuang H, Crain B, Doré S, *Expression and localization of prostaglandin transporter in Alzheimer disease brains and age-matched controls*, J Neuroimmunol. 2008 Mar;195(1-2):81-7, Epub 2008 Mar 18

Choi YK, Kim KW, *Blood-neural barrier: its diversity and coordinated cell-to-cell communication*, BMB Rep. 2008 May 31;41(5):345-52, Review

Christov A, Ottman JT, Grammas P, *Vascular inflammatory, oxidative and protease-based processes: implications for neuronal cell death in Alzheimer's disease*, Neurol Res. 2004 Jul;26(5):540-6

Clark ER, Clark EL, Growth and behavior of epidermis as observed microscopically in observation chambers inserted in the ears of rabbits, Am J Anat. 1953 Sep;93(2):171-219, *

Clementi ME, Pezzotti M, Orsini F, Sampaolese B, Mezzogori D, Grassi C, Giardina B, Misiti F, *Alzheimer's amyloid beta-peptide (1-42) induces cell death in human neuroblastoma via bax/bcl-2 ratio increase: an intriguing role for methionine 35*, Biochem Biophys Res Commun. 2006 Mar 31;342(1):206-13, Epub 2006 Feb 3

Daly C, Pasnikowski E, Burova E, Wong V, Aldrich TH, Griffiths J, Ioffe E, Daly TJ, Fandl JP, Papadopoulos N, McDonald DM, Thurston G, Yancopoulos GD, Rudge JS, *Angiopoietin-2 functions as an autocrine protective factor in stressed endothelial cells*, Proc Natl Acad Sci U S A. 2006 Oct 17;103(42):15491-6, Epub 2006 Oct 9

D'Andrea LD, Del Gatto A, Pedone C, Benedetti E, *Peptide-based molecules in angiogenesis*, Chem Biol Drug Des. 2006 Feb;67(2):115-26, Review

de Boer AG, Gaillard PJ, Blood-*brain barrier dysfunction and recovery*, J Neural Transm. 2006 Apr;113(4):455-62, Review

Deshpande A, Mina E, Glabe C, Busciglio J, *Different conformations of amyloid beta induce neurotoxicity by distinct mechanisms in human cortical neurons*, J Neurosci. 2006 May 31;26(22):6011-8

Dries DR, Yu G, *Assembly, maturation, and trafficking of the gamma-secretase complex in Alzheimer's disease*, Curr Alzheimer Res. 2008 Apr;5(2):132-46, Review

Edelberg JM, Reed MJ, *Aging and angiogenesis*, Front Biosci. 2003 Sep 1;8:s1199-209, Review

Fiedler U, Augustin HG, *Angiopoietins: a link between angiogenesis and inflammation*, Trends Immunol. 2006 Dec;27(12):552-8. Epub 2006 Oct 12, Review

Folin M, Baiguera S, **Fioravanzo L**, Conconi MT, Grandi C, Nussdorfer GG, Parnigotto PP, *Caspase-8 activation and oxidative stress are involved in the cytotoxic effect of beta-amyloid on rat brain microvascular endothelial cells*, Int J Mol Med. 2006 Mar;17(3):431-5

Folkman J, Haudenschild C, *Angiogenesis in vitro*, Nature. 1980 Dec 11;288(5791):551-6, *

Folkman J, Shing Y, *Angiogenesis*, J Biol Chem. 1992 Jun 5;267(16):10931-4, Review

Fraering PC, *Structural and functional determinants of γ-secretase, an intramembrane protease implicated in Alzheimer's disease*, Curr. Genomics, 2007, 8, 531-549

Gagnon E, Cattaruzzi P, Griffith M, Muzakare L, LeFlao K, Faure R, Béliveau R, Hussain SN, Koutsilieris M, Doillon CJ, *Human vascular endothelial cells with extended life spans: in vitro cell response, protein expression, and angiogenesis*, Angiogenesis. 2002;5(1-2):21-33

Garmy-Susini B, Varner JA, *Circulating endothelial progenitor cells*, Br J Cancer. 2005 Oct 17;93(8):855-8, Review

Gerhardt H, Golding M, Fruttiger M, Ruhrberg C, Lundkvist A, Abramsson A, Jeltsch M, Mitchell C, Alitalo K, Shima D, Betsholtz C, *VEGF guides angiogenic sprouting utilizing endothelial tip cell filopodia*, J Cell Biol. 2003 Jun 23;161(6):1163-77, Epub 2003 Jun 16, *

Gill M, Dias S, Hattori K, Rivera ML, Hicklin D, Witte L, Girardi L, Yurt R, Himel H, Rafii S, *Vascular trauma induces rapid but transient mobilization of VEGFR2(+)AC133(+) endothelial precursor cells*, Circ Res. 2001 Feb 2;88(2):167-74

Gimbrone MA Jr, Cotran RS, Folkman J, *Endothelial regeneration: studies with human endothelial cells in culture*, Ser Haematol. 1973;6(4):453-5, *

Glabe CG, *Conformation-dependent antibodies target diseases of protein misfolding*, Trends Biochem Sci. 2004 Oct;29(10):542-7, Review

Guerreiro RJ, Santana I, Brás JM, Santiago B, Paiva A, Oliveira C, *Peripheral inflammatory cytokines as biomarkers in Alzheimer's disease and mild cognitive impairment*, Neurodegener Dis. 2007;4(6):406-12, Epub 2007 Oct 9

Guidolin D, Vacca A, Nussdorfer GG, Ribatti D, *A new image analysis method based on topological and fractal parameters to evaluate the angiostatic activity of docetaxel by using the Matrigel assay in vitro*, Microvasc Res. 2004 Mar;67(2):117-24

Hangai M, He S, Hoffmann S, Lim JI, Ryan SJ, Hinton DR, *Sequential induction of angiogenic growth factors by TNF-alpha in choroidal endothelial cells*, J Neuroimmunol. 2006 Feb;171(1-2):45-56, Epub 2005 Nov 8

Hanna J, Goldman-Wohl D, Hamani Y, Avraham I, Greenfield C, Natanson-Yaron S, Prus D, Cohen-Daniel L, Arnon TI, Manaster I, Gazit R, Yutkin V, Benharroch D, Porgador A, Keshet E, Yagel S, Mandelboim O, *Decidual NK cells regulate key developmental processes at the human fetal-maternal interface*, Nat Med. 2006 Sep;12(9):1065-74, Epub 2006 Aug 6

Hardy J, Selkoe DJ, *The amyloid hypothesis of Alzheimer's disease: progress and problems on the road to therapeutics*, Science. 2002 Jul 19;297(5580):353-6, Review; Erratum in: Science 2002 Sep 27;297(5590):2209

Hardy JA, Higgins GA, *Alzheimer's disease: the amyloid cascade hypothesis*, Science. 1992 Apr 10;256(5054):184-5, Review, *

Hauwel M, Furon E, Canova C, Griffiths M, Neal J, Gasque P, *Innate (inherent) control of brain infection, brain inflammation and brain repair: the role of microglia, astrocytes, "protective" glial stem cells and stromal ependymal cells*, Brain Res Brain Res Rev. 2005 Apr;48(2):220-33, Review

Hawkins BT, Davis TP, *The blood-brain barrier/neurovascular unit in health and disease*, Pharmacol Rev. 2005 Jun;57(2):173-85, Review

Heneka MT, O'Banion MK, *Inflammatory processes in Alzheimer's disease*, J Neuroimmunol. 2007 Mar;184(1-2):69-91, Epub 2007 Jan 12, Review

Heryanto B, Girling JE, Rogers PA, *Intravascular neutrophils partially mediate the endometrial endothelial cell proliferative response to oestrogen in ovariectomised mice*, Reproduction. 2004 May;127(5):613-20

Higuchi R, Fockler C, Dollinger G, Watson R, *Kinetic PCR analysis: real-time monitoring of DNA amplification reactions*, Biotechnology (N Y). 1993 Sep;11(9):1026-30

Hoe HS, Rebeck GW, *Regulated proteolysis of APP and ApoE receptors*, Mol Neurobiol. 2008 Feb;37(1):64-72. Epub 2008 Apr 15. Review

Holderfield MT, Hughes CC, *Crosstalk between vascular endothelial growth factor, notch, and transforming growth factor-beta in vascular morphogenesis*, Circ Res. 2008 Mar 28;102(6):637-52, Review

Hoozemans JJ, Veerhuis R, Rozemuller AJ, Eikelenboom P, *The pathological cascade of Alzheimer's disease: the role of inflammation and its therapeutic implications*, Drugs Today (Barc). 2002 Jun;38(6):429-43, Review

Hsu MJ, Hsu CY, Chen BC, Chen MC, Ou G, Lin CH, *Apoptosis signal-regulating kinase 1 in amyloid beta peptide-induced cerebral endothelial cell apoptosis*, J Neurosci. 2007 May 23;27(21):5719-29

Hung SC, Pochampally RR, Chen SC, Hsu SC, Prockop DJ, *Angiogenic effects of human multipotent stromal cell conditioned medium activate the PI3K-Akt pathway in hypoxic endothelial cells to inhibit apoptosis, increase survival, and stimulate angiogenesis*, Stem Cells. 2007 Sep;25(9):2363-70, Epub 2007 May 31

Izumi Y, Kim-Mitsuyama S, Yoshiyama M, Omura T, Shiota M, Matsuzawa A, Yukimura T, Murohara T, Takeya M, Ichijo H, Yoshikawa J, Iwao H, *Important role of apoptosis signal-regulating kinase 1 in ischemia-induced angiogenesis*, Arterioscler Thromb Vasc Biol. 2005 Sep;25(9):1877-83, Epub 2005 Jun 23

Jackson CJ, Garbett PK, Nissen B, Schrieber L, *Binding of human endothelium to Ulex europaeus I-coated Dynabeads: application to the isolation of microvascular endothelium*, J Cell Sci. 1990 Jun;96 (Pt 2):257-62

Jan A, Gokce O, Luthi-Carter R, Lashuel HA, *The ratio of monomeric to aggregated forms of Abeta40 and Abeta42 is an important determinant of amyloid-beta aggregation, fibrillogenesis, and toxicity*, J Biol Chem. 2008 Oct 17;283(42):28176-89, Epub 2008 Aug 11

Jellinger KA, *Alzheimer disease and cerebrovascular pathology: an update*, J Neural Transm. 2002 May;109(5-6):813-36, Review

Jones EA, le Noble F, Eichmann A, *What determines blood vessel structure? Genetic prespecification vs. hemodynamics*, Physiology (Bethesda). 2006 Dec;21:388-95, Review

Kalluri R, *Basement membranes: structure, assembly and role in tumour angiogenesis*, Nat Rev Cancer. 2003 Jun;3(6):422-33, Review

Kanzawa S, Endo H, Shioya N, *Improved in vitro angiogenesis model by collagen density reduction and the use of type III collagen*, Ann Plast Surg. 1993 Mar;30(3):244-51

Karamysheva AF, *Mechanisms of angiogenesis*, Biochemistry (Mosc). 2008 Jul;73(7):751-62, Review

Keck PJ, Hauser SD, Krivi G, Sanzo K, Warren T, Feder J, Connolly DT, *Vascular permeability factor, an endothelial cell mitogen related to PDGF*, Science. 1989 Dec 8;246(4935):1309-12

Kerokoski P, Soininen H, Pirttilä T, *Beta-amyloid (1-42) affects MTT reduction in astrocytes: implications for vesicular trafficking and cell functionality*, Neurochem Int. 2001 Feb;38(2):127-34

Kim JH, Kim JH, Park JA, Lee SW, Kim WJ, Yu YS, Kim KW, *Blood-neural barrier: intercellular communication at glio-vascular interface*, J Biochem Mol Biol. 2006 Jul 31;39(4):339-45, Review

Kirkitadze MD, Kowalska A, *Molecular mechanisms initiating amyloid beta-fibril formation in Alzheimer's disease*, Acta Biochim Pol. 2005;52(2):417-23, Epub 2005 May 31

Kofler S, Nickel T, Weis M, *Role of cytokines in cardiovascular diseases: a focus on endothelial responses to inflammation*, Clin Sci (Lond). 2005 Mar;108(3):205-13, Review

Kurz H, *Physiology of angiogenesis*, J Neurooncol. 2000 Oct-Nov;50(1-2):17-35, Review

Lacor PN, Buniel MC, Furlow PW, Clemente AS, Velasco PT, Wood M, Viola KL, Klein WL, *Abeta oligomer-induced aberrations in synapse composition, shape, and density provide a molecular basis for loss of connectivity in Alzheimer's disease*, J Neurosci. 2007 Jan 24;27(4):796-807

Lai CH, Kuo KH, *The critical component to establish in vitro BBB model: Pericyte*, Brain Res Brain Res Rev. 2005 Dec 15;50(2):258-65, Epub 2005 Sep 30. Review

Lamszus K, Schmidt NO, Ergün S, Westphal M, *Isolation and culture of human neuromicrovascular endothelial cells for the study of angiogenesis in vitro*, J Neurosci Res. 1999 Feb 1;55(3):370-8

Laschke MW, Menger MD, *In vitro and in vivo approaches to study angiogenesis in the pathophysiology and therapy of endometriosis*, Hum Reprod Update. 2007 Jul-Aug;13(4):331-42, Epub 2007 Mar 8, Review

Lejeune FJ, Liénard D, Matter M, Rüegg C, *Efficiency of recombinant human TNF in human cancer therapy*, Cancer Immun. 2006 Mar 22;6:6, Review

Leng T, Miller JM, Bilbao KV, Palanker DV, Huie P, Blumenkranz MS, *The chick chorioallantoic membrane as a model tissue for surgical retinal research and simulation*, Retina. 2004 Jun;24(3):427-34

Leung DW, Cachianes G, Kuang WJ, Goeddel DV, Ferrara N, Vascular endothelial growth factor is a secreted angiogenic mitogen, Science. 1989 Dec 8;246(4935):1306-9, *

Mac Gabhann F, Ji JW, Popel AS, *Computational model of vascular endothelial growth factor spatial distribution in muscle and pro-angiogenic cell therapy*, PLoS Comput Biol. 2006 Sep 22;2(9):e127, Epub 2006 Aug 3

Magrane J, Christensen RA, Rosen KM, Veereshwarayya V, Querfurth HW, *Dissociation of ERK and Akt signaling in endothelial cell angiogenic responses to beta-amyloid*, Exp Cell Res. 2006 Apr 15;312(7):996-1010, Epub 2006 Jan 20

Maisonpierre PC, Suri C, Jones PF, Bartunkova S, Wiegand SJ, Radziejewski C, Compton D, McClain J, Aldrich TH, Papadopoulos N, Daly TJ, Davis S, Sato TN, Yancopoulos GD, *Angiopoietin-2, a natural antagonist for Tie2 that disrupts in vivo angiogenesis*, Science. 1997 Jul 4;277(5322):55-60

Man SM, Ma YR, Shang DS, Zhao WD, Li B, Guo DW, Fang WG, Zhu L, Chen YH, *Peripheral T cells overexpress MIP-1alpha to enhance its transendothelial migration in Alzheimer's disease*, Neurobiol Aging. 2007 Apr;28(4):485-96, Epub 2006 Apr 5

Mandriota SJ, Pepper MS, *Vascular endothelial growth factor-induced in vitro angiogenesis and plasminogen activator expression are dependent on endogenous basic fibroblast growth factor*, J Cell Sci. 1997 Sep;110 (Pt 18):2293-302

Marco S, Skaper SD, *Amyloid beta-peptide1-42 alters tight junction protein distribution and expression in brain microvessel endothelial cells*, Neurosci Lett. 2006 Jul 3;401(3):219-24, Epub 2006 Apr 27

McCarthy KD, de Vellis J, *Preparation of separate astroglial and oligodendroglial cell cultures from rat cerebral tissue*, J Cell Biol. 1980 Jun;85(3):890-902

McGeer EG, McGeer PL, *Inflammatory processes in Alzheimer's disease*, Prog Neuropsychopharmacol Biol Psychiatry. 2003 Aug;27(5):741-9, Review

Meyer EP, Ulmann-Schuler A, Staufenbiel M, Krucker T, *Altered morphology and 3D architecture of brain vasculature in a mouse model for Alzheimer's disease*, Proc Natl Acad Sci U S A. 2008 Mar 4;105(9):3587-92, Epub 2008 Feb 27

Milkiewicz M, Ispanovic E, Doyle JL, Haas TL, *Regulators of angiogenesis and strategies for their therapeutic manipulation*, Int J Biochem Cell Biol. 2006 Mar;38(3):333-57. Epub 2005 Nov 7, Review

Minuzzo S, Moserle L, Indraccolo S, Amadori A, *Angiogenesis meets immunology: cytokine gene therapy of cancer*, Mol Aspects Med. 2007 Feb;28(1):59-86. Epub 2007 Jan 11. Review

Molnár Z, Kovács P, Laczkó I, Soós K, Fülöp L, Penke B, Lengyel I, *Enhanced G-protein activation by a mixture of Abeta(25-35), Abeta(1-40/42) and zinc*, J Neurochem. 2004 Jun;89(5):1215-23

Mosmann T, *Rapid colorimetric assay for cellular growth and survival: application to proliferation and cytotoxicity assays*, J Immunol Methods. 1983 Dec 16;65(1-2):55-63, *

Murphy RM, *Kinetics of amyloid formation and membrane interaction with amyloidogenic proteins*, Biochim Biophys Acta. 2007 Aug;1768(8):1923-34, Epub 2007 Jan 3. Review

Nicosia RF, Ottinetti A, *Growth of microvessels in serum-free matrix culture of rat aorta. A quantitative assay of angiogenesis in vitro*, Lab Invest. 1990 Jul;63(1):115-22

Nolan K, Millet Y, Ricordi C, Stabler CL, *Tissue engineering and biomaterials in regenerative medicine*, Cell Transplant. 2008;17(3):241-3, Review

Noonan DM, De Lerma Barbaro A, Vannini N, Mortara L, Albini A, *Inflammation, inflammatory cells and angiogenesis: decisions and indecisions*, Cancer Metastasis Rev. 2008 Mar;27(1):31-40, Review

Otrock ZK, Mahfouz RA, Makarem JA, Shamseddine AI, *Understanding the biology of angiogenesis: review of the most important molecular mechanisms*, Blood Cells Mol Dis. 2007 Sep-Oct;39(2):212-20, Epub 2007 Jun 6, Review

Pandya NM, Dhalla NS, Santani DD, *Angiogenesis--a new target for future therapy*, Vascul Pharmacol. 2006 May;44(5):265-74, Epub 2006 Mar 20, Review

Papetti M, Herman IM, *Mechanisms of normal and tumor-derived angiogenesis*, Am J Physiol Cell Physiol. 2002 May;282(5):C947-70, Review

Paris D, Townsend K, Quadros A, Humphrey J, Sun J, Brem S, Wotoczek-Obadia M, DelleDonne A, Patel N, Obregon DF, Crescentini R, Abdullah L, Coppola D, Rojiani AM, Crawford F, Sebti SM, Mullan M, *Inhibition of angiogenesis by Abeta peptides*, Angiogenesis. 2004;7(1):75-85

Park SY, Chae CB, *Toxic levels of amyloid beta peptide do not induce VEGF synthesis*, Mol Cells. 2007 Aug 31;24(1):69-75

Pearson HA, Peers C, *Physiological roles for amyloid beta peptides*, J Physiol. 2006 Aug 15;575(Pt 1):5-10. Epub 2006 Jun 29, Review

Peichev M, Naiyer AJ, Pereira D, Zhu Z, Lane WJ, Williams M, Oz MC, Hicklin DJ, Witte L, Moore MA, Rafii S, *Expression of VEGFR-2 and AC133 by circulating human CD34(+) cells identifies a population of functional endothelial precursors*, Blood. 2000 Feb 1;95(3):952-8

Pfaffl MW, *A new mathematical model for relative quantification in real-time RT-PCR*, Nucleic Acids Res. 2001 May 1;29(9):e45

Pfaffl MW, Horgan GW, Dempfle L, *Relative expression software tool (REST) for group-wise comparison and statistical analysis of relative expression results in real-time PCR*, Nucleic Acids Res. 2002 May 1;30(9):e36

Phillips HJ, Terryberry JE, *Counting actively metabolizing tissue cultured cells*, Exp Cell Res. 1957 Oct;13(2):341-7

Pogue AI, Lukiw WJ, *Angiogenic signaling in Alzheimer's disease*, Neuroreport. 2004 Jun 28;15(9):1507-10

Post S, Peeters W, Busser E, Lamers D, Sluijter JP, Goumans MJ, de Weger RA, Moll FL, Doevendans PA, Pasterkamp G, Vink A, *Balance between angiopoietin-1 and angiopoietin-2 is in favor of angiopoietin-2 in atherosclerotic plaques with high microvessel density*, J Vasc Res. 2008;45(3):244-50. Epub 2008 Jan 10

Ribatti D, Gualandris A, Bastaki M, Vacca A, Iurlaro M, Roncali L, Presta M, *New model for the study of angiogenesis and antiangiogenesis in the chick embryo chorioallantoic membrane: the gelatin sponge/chorioallantoic membrane assay*, J Vasc Res. 1997 Nov-Dec;34(6):455-63

Ribatti D, Nico B, Vacca A, Roncali L, Burri PH, Djonov V, *Chorioallantoic membrane capillary bed: a useful target for studying angiogenesis and anti-angiogenesis in vivo*, Anat Rec. 2001 Dec 1;264(4):317-24, Review

Ribatti D, Urbinati C, Nico B, Rusnati M, Roncali L, Presta M, *Endogenous basic fibroblast growth factor is implicated in the vascularization of the chick embryo chorioallantoic membrane*, Dev Biol. 1995 Jul;170(1):39-49

Rieckmann P, Engelhardt B, *Building up the blood-brain barrier*, Nat Med. 2003 Jul;9(7):828-9

Rivron NC, Liu J J, Rouwkema J, de Boer J, van Blitterswijk CA, *Engineering vascularised tissues in vitro*, Eur Cell Mater. 2008 Feb 21;15:27-40, Review

Robertson LA, Moya KL, Breen KC, *The potential role of tau protein O-glycosylation in Alzheimer's disease*, J Alzheimers Dis. 2004 Oct;6(5):489-95

Sastre M, Klockgether T, Heneka MT, *Contribution of inflammatory processes to Alzheimer's disease: molecular mechanisms*, Int J Dev Neurosci. 2006 Apr-May;24(2-3):167-76, Epub 2006 Feb 10, Review

Sastre M, Walter J, Gentleman SM, *Interactions between APP secretases and inflammatory mediators*, J Neuroinflammation. 2008 Jun 18;5:25, Review

Staton CA, Stribbling SM, Tazzyman S, Hughes R, Brown NJ, Lewis CE, *Current methods for assaying angiogenesis in vitro and in vivo*, Int J Exp Pathol. 2004 Oct;85(5):233-48, Review

Suhara T, Magrané J, Rosen K, Christensen R, Kim HS, Zheng B, McPhie DL, Walsh K, Querfurth H, *Abeta42 generation is toxic to endothelial cells and inhibits eNOS function through an Akt/GSK-3beta signaling-dependent mechanism*, Neurobiol Aging. 2003 May-Jun;24(3):437-51

Tarkowski E, Issa R, Sjögren M, Wallin A, Blennow K, Tarkowski A, Kumar P, *Increased intrathecal levels of the angiogenic factors VEGF and TGF-beta in Alzheimer's disease and vascular dementia*, Neurobiol Aging. 2002 Mar-Apr;23(2):237-43

Thirumangalakudi L, Samany PG, Owoso A, Wiskar B, Grammas P, *Angiogenic proteins are expressed by brain blood vessels in Alzheimer's disease*, J Alzheimers Dis. 2006 Sep;10(1):111-8, Review

Urbich C, Dimmeler S, *Endothelial progenitor cells: characterization and role in vascular biology*, Circ Res. 2004 Aug 20;95(4):343-53, Review

Vagnucci AH Jr, Li WW, *Alzheimer's disease and angiogenesis*, Lancet. 2003 Feb 15;361(9357):605-8, Review

Verdier Y, Zarándi M, Penke B, *Amyloid beta-peptide interactions with neuronal and glial cell plasma membrane: binding sites and implications for Alzheimer's disease*, J Pept Sci. 2004 May;10(5):229-48, Review

Vinters HV, Wang ZZ, Secor DL, *Brain parenchymal and microvascular amyloid in Alzheimer's disease*, Brain Pathol. 1996 Apr;6(2):179-95, Review

Watson D, Castaño E, Kokjohn TA, Kuo YM, Lyubchenko Y, Pinsky D, Connolly ES Jr, Esh C, Luehrs DC, Stine WB, Rowse LM, Emmerling MR, Roher AE, *Physicochemical characteristics of soluble oligomeric Abeta and their pathologic role in Alzheimer's disease*, Neurol Res. 2005 Dec;27(8):869-81, Review

Yang SP, Bae DG, Kang HJ, Gwag BJ, Gho YS, Chae CB, *Co-accumulation of vascular endothelial growth factor with beta-amyloid in the brain of patients with Alzheimer's disease*, Neurobiol Aging. 2004 Mar;25(3):283-90

Yang SP, Kwon BO, Gho YS, Chae CB, *Specific interaction of VEGF165 with beta-amyloid, and its protective effect on beta-amyloid-induced neurotoxicity*, J Neurochem. 2005 Apr;93(1):118-27

Zand L, Ryu JK, McLarnon JG, *Induction of angiogenesis in the beta-amyloid peptide-injected rat hippocampus*, Neuroreport. 2005 Feb 8;16(2):129-32

Zangari M, Anaissie E, Stopeck A, Morimoto A, Tan N, Lancet J, Cooper M, Hannah A, Garcia-Manero G, Faderl S, Kantarjian H, Cherrington J, Albitar M, Giles FJ, *Phase II study of SU5416, a small molecule vascular endothelial growth factor tyrosine kinase receptor inhibitor, in patients with refractory multiple myeloma*, Clin Cancer Res. 2004 Jan 1;10(1 Pt 1):88-95

Zhao Y, Cui JG, Lukiw WJ, *Natural secretory products of human neural and microvessel endothelial cells: Implications in pathogenic "spreading" and Alzheimer's disease*, Mol Neurobiol. 2006 Dec;34(3):181-92, Review

Zlokovic BV, Neurovascular mechanisms of Alzheimer's neurodegeneration, Trends Neurosci. 2005 Apr;28(4):202-8, Review

* these articles were not directly consulted

Acknowledgements

First of all I would like to thank my Supervisor, prof.ssa Marcella Folin, for her help and all the possibilities she gave me during these three years of PhD that allow me to grow both by scientific and personal side.
I would like to thank all the people helped me during these years. Firstly my colleagues dr.ssa Elisa Boscolo and dr.ssa Silvia Baiguera for the experimental work and support. I learned that it is impossible to have a good research without a great group. Then I thank dr.ssa Giovanna Albertin and dr.ssa Raffaella Spinazzi (Department of Human Anatomy and Physiology, Section of Anatomy, University of Padua) for the realizization of Real Time-RT-PCR experiments. Moreover I would like to thank dr Diego Guidolin (Department of Human Anatomy and Physiology, Section of Anatomy, University of Padua) for the software to analyze Matrigel imagines. I would like to thank prof. Claudio Grandi (Department of Pharmaceutical Sciences, University of Padua) for the collaboration to determine cytokine levels by using Multilplex technique. Moreover I thank prof. Pier Paolo Parnigotto and prof.ssa Maria Teresa Conconi (Department of Pharmaceutical Sciences, University of Padua) for the collaboration to realize experiments by the disponibility of instruments.

A special thank to prof. Gastone G. Nussdorfer for his precious help and advices for the realization of experiments of Real Time RT-PCR.

I would like to thank my English teacher, Savio, for the proof-reading of this work.

Finally I would like to thank healtily all the PhD and final years students I met in these years and help me by discussion of the results and dubts. In particular I thank dr. Marco Venturini for his patience and help for the determination of cytokines by Multiplex technique.

Caspase-8 activation and oxidative stress are involved in the cytotoxic effect of ß-amyloid on rat brain microvascular endothelial cells

MARCELLA FOLIN[1], SILVIA BAIGUERA[1], LARA FIORAVANZO[1], MARIA TERESA CONCONI[2], CLAUDIO GRANDI[2], GASTONE G. NUSSDORFER[3] and PIER PAOLO PARNIGOTTO[2]

Departments of [1]Biology, [2]Pharmaceutical Sciences, and [3]Human Anatomy and Physiology, Section of Anatomy, University of Padua, I-35121 Padua, Italy

Received October 5, 2005; Accepted November 15, 2005

Abstract. Several studies have demonstrated that cerebrovascular dysfunction and damage play a significant role in the pathogenesis of Alzheimer disease (AD). In fact, ß-amyloid peptides (Aßs), the major component of the senile plaques and cerebrovascular amyloid deposits in AD, were shown to be cytotoxic to endothelial cells. We have recently observed that Aßs exert a toxic effect on neuromicrovascular endothelial cells (NECs) in a time- and concentration-dependent manner, apoptosis playing a pivotal role in this process. Hence, it seemed worthwhile to investigate the Aß-mediated apoptosis mechanism in NECs. Aßs were found to induce, after a short incubation period, apoptosis throughout caspase-8 activation. Moreover, Aßs elicited a highly significant ($p<0.001$) increase in superoxide dismutase (SOD) levels after a 3-h exposure period, while SOD concentration was not affected after a 24-h incubation. The time-dependent increase in SOD concentration is probably correlated with the production of an excess of reactive oxygen species. Collectively, our findings allow us to conclude that: i) Aßs may induce apoptosis via the activation of caspase-8, presumably by cross-linking and activating receptors of the death-receptor family; ii) oxidative stress is possibly involved in the Aß-induced cytotoxic effect; and iii) these two mechanisms do not act sequentially but, probably, are independent of each other.

Introduction

Evidence has been provided that, ß-amyloid peptides (Aßs) may accumulate not only in the brain parenchyma but also in the cerebral blood vessels (1,2) and that this is a major cause of hemorrhagic and ischemic strokes in elderly patients with or without Alzheimer disease (AD). *In vitro* studies demonstrated that Aßs exert, in a time- and concentration-dependent manner, a marked toxic effect on cerebral endothelial cells (ECs) (3-5). Moreover, Aßs have been shown to be neurotoxic, inducing cell death and oxidative stress in cultured neurons (6,7). Although the mechanism by which extracellular Aßs trigger endothelial and neuronal death has not yet been fully elucidated, the predominant hypothesis suggests the involvement of apoptotic cell death (8). Loo *et al* (9) reported that the exposure of cultured neurons to Aßs induces degeneration and cell death, which seems to occur via an apoptotic pathway. Neuronal cultures exposed to Aßs degenerate, exhibit nuclear chromatin condensation and plasma membrane blebbing. We have previously shown that also neuromicrovascular ECs (NECs) treated with Aßs undergo apoptosis (5).

At present, two major pathways of apoptosis are recognized: the death-receptor pathway in which caspase-8 plays a pivotal initiator role and the mitochondrial pathway involving oxidative stress and activation of caspase-9 (10). Caspase-8 is typically activated via ligand binding to death-receptors such as TNF-R1, Fas and others. Activation of caspase-8 triggers a proteolytic cascade, resulting in the activation of effector caspases, including caspase-3. In contrast, caspase-9 is activated through a complex pathway of mitochondrial dysfunction, mitochondrial-related oxidative stress and cytochrome c release, which eventually results in the activation of caspase-3 (11).

Recent studies provided evidence of the activation of caspase-8 in the AD brain, and suggested that this activation may occur through the stimulation of receptors in the death-receptor pathway (12). Moreover, *in vitro* investigations carried out on neurons and cerebral ECs, suggested that the Aß-induced apoptotic pathway requires caspase-8 activity (13,14). Mitochondrial dysfunction and mtDNA damage was also detected in ECs, probably caused by oxidative stress (14). However, it remains to be settled whether the two mechanisms mediating the Aß-induced EC death, i.e. caspase activation and oxidative stress, act sequentially or independently of each other.

In the frame of our current studies on AD and neurodegenerative dementia (5,15,16), we sought to investigate the role of caspase activation and oxidative stress in Aß-mediated NEC apoptosis.

Correspondence to: Professor Marcella Folin, Department of Biology, Via U. Bassi 58/b, I-35131 Padua, Italy
E-mail: folin@civ.bio.unipd.it

Key words: ß-amyloid, endothelial cells, apoptosis, caspase-8, superoxide dismutase, oxidative stress

Materials and methods

Animals and reagents. Sprague-Dawley male rats (350-400 g body weight) were purchased from Charles-River (Como, Italy), and the experiment protocol was approved by the local Ethics Committee for Animal Studies. Aß(1-40) and Aß(1-42), alkaline phosphatase conjugate anti-IgG, 5-bromo-4-chloro-3-indolyl phosphatase (BCIP) and p-nitroblue tetrazolium chloride (NBT) were provided by Calbiochem (La Jolla, CA). EC growth medium MV2 was obtained from PromoCell (Heidelberg, Germany) and the BCA protein assay kit was from Pierce (Rockford, IL). Polyvinylidene fluoride membrane (PVDF) was purchased from Gelman Science (Ann Arbor, MI) and benzyloxycarbonyl-IEDT-fluoromethylketone (Z-IEDT-FMK), rabbit anti-caspase-8 polyclonal antibody and a CaspaTag™ Caspase-8 *In Situ* assay kit were from Chemicon International (Temecula, CA). Bovine serum albumine (BSA), phosphatate-buffered saline (PBS) and all other chemicals and reagents were provided by Sigma-Aldrich Corp. (St. Louis, MO).

NEC culture and treatment. Rats were decapitated, and the brain was promptly removed. NECs were isolated and cultured according to the method of Abbot *et al* (17), with few modifications (5,18). NECs from the 3rd and 4th passage were plated ($1.5x10^4$ cells/cm^2) on fibronectin-coated Petri dishes, and cultured in MV2 medium, as previously described (19). After 24 h of culture, medium was replaced with a fresh one containing Aß(1-40) or Aß(1-42) (10^{-7} M).

Western blotting. NECs were treated for 1, 3, or 24 h, and then were washed with PBS and lysed for 30 min on ice using cell lysis buffer (50 mM Tris-HCl, 2 mM EDTA, aprotinin 10 μg/ml, leupeptin 10 μg/ml, phenylmethylsulfonylfluoride 1 mM). The protein concentration was measured using the BCA protein assay kit. Total 25 μg proteins were loaded onto a 12% sodium dodecyl sulfate-polyacrylamide electrophoresis gel and transferred to PVDF membrane. The membrane was then blocked overnight at 4˚C with Tris-buffered saline solution containing 2% BSA, followed by incubation with rabbit anti-caspase-8 polyclonal antibody (1:200 dilution). The membrane was then washed with the blocking solution prior to incubation with alkaline phosphatase conjugate anti-IgG (1:4000 dilution). Blots were developed using a solution containing 0.56 mM BCIP and 0.48 mM NBT in Tris-buffered saline solution (pH 9.5).

In vitro assay of caspase-8 activity. Caspase-8 activity was examined using a CaspaTag™ Caspase-8 *In Situ* assay kit (Chemicon International). The kit uses a carboxyfluorescein-labeled fluoromethyl ketone peptide inhibitor of caspase-8 (FAM-LETD-FMK), which produces a green fluorescence. Briefly, after a 3-h incubation period, fluorochome caspase-8 inhibitor reagent was added to the culture medium. Cells were observed under a fluorescence microscope using a bandpass filter (excitation 490 nm, emission 520 nm wavelength) to view the green fluorescence of caspase-8 positive cells.

Cell survival in the presence of caspase-8 inhibitor. For experiments using caspase-8 inhibitor, NECs ($2.5x10^4$ cells/cm^2) plated in 24-well dishes were pretreated with 20 μM Z-IETD-FMK for 1 h, followed by 10^{-7} M Aß peptides for up to 24 h. Cell survival was evaluated by trypan blue exclusion, by counting NECs which did not internalize the dye.

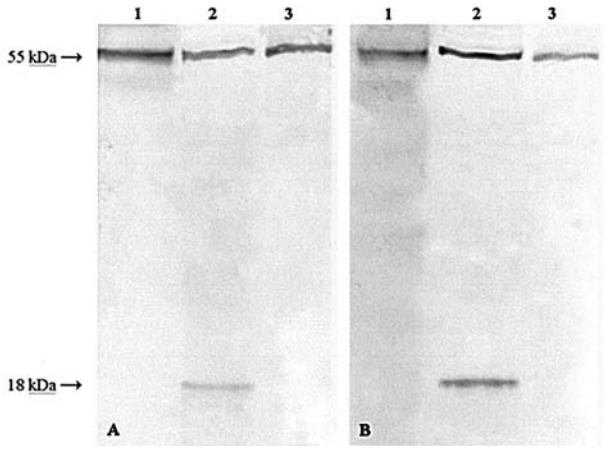

Figure 1. Western blot analysis showing caspase-8 activation in cultured rat NECs, after 1-h (lane 1), 3-h (lane 2) and 24-h incubation (lane 3) with Aß(1-40) (A) and Aß(1-42) (B).

Superoxide dismutase (SOD) assay. The superoxide radical is revealed by a reaction with luminol (5-amino-2,3-dihydro-1,4-ftalazinedione) which is oxidized in 3-amino-ftalic acid emitting light (maximum emission at 425 nm wavelength) measured using a Lumicon Hamilton Luminometer (20). The presence of superoxide dismutase (SOD) in the sample determines the subtraction of radicals through dismutation. At the end of the incubation time, cells were washed with PBS and lysed on ice by cell lysis buffer (0.5% v/v Triton X-100 in 0.154 M carbonate buffer pH 10.2). Two μl of xantine oxidase (1.35 mg/ml), 78 μl of EDTA (0.3 M) and luminol (0.03 mM) in carbonate buffer (0.154 M, pH 10.2), and 80 μl of hypoxantine (30 μM) were mixed with 80 μl of sample. The protein concentration was measured using the BCA protein assay kit. The calibration curve was constructed by using SOD from bovine erythrocyte (1 μg/ml) (ε=10300/cm^{-1}/mol^{-1}).

Statistics. Results were expressed as percent change from the control value, and were the mean ± SEM of four separate experiments. Statistical analysis was performed by ANOVA followed by t-test of Student-Newman-Keuls as a post-hoc test.

Results

Western blot assay performed on cell lysates prepared from NECs after 1-, 3- and 24-h treatment with Aß(1-40) and Aß(1-42) showed a time-dependent proteolytic cleavage of caspase-8. After a 1-h incubation period, a 55-kDa protein band was detected, corresponding to inactive procaspase-8. Two bands with molecular sizes of 55 and 18 kDa were detected after 3 h of incubation, the 18-kDa protein representing the fully processed active enzyme resulting from two-step proteolysis. After 24-h treatment, only the 55-kDa protein band was detected (Fig. 1).

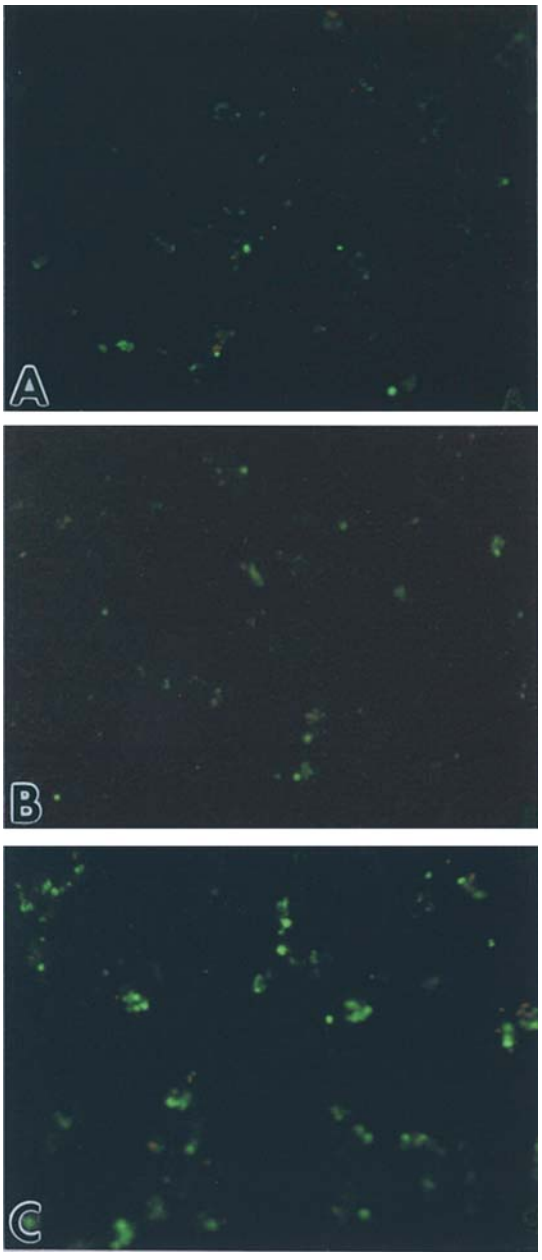

Figure 2. CaspaTag caspase-8-positive rat NECs in control cultures (A), and after incubation for 3 h with Aß(1-40) (B) or Aß(1-42) (C).

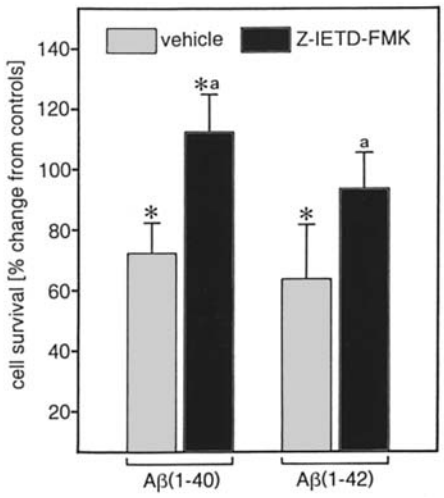

Figure 3. Trypan blue exclusion assay showing the effect of Z-IETD-FMK on the survival of cultured rat NECs treated for 3 h with Aß(1-40) or Aß(1-42). Bars are means ± SEM of four separate experiments. *p<0.05 from the respective control group; ap<0.05 from the respective vehicle group.

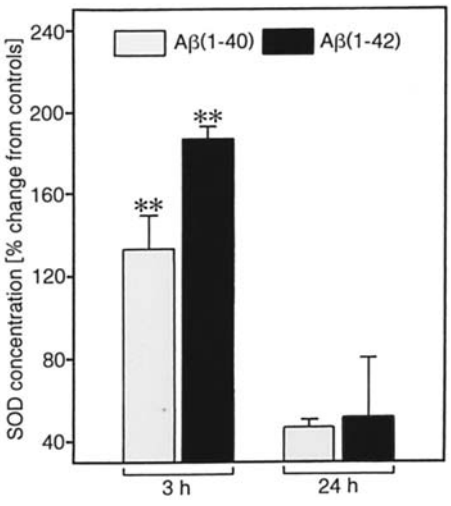

Figure 4. Luminol assay showing the effects of Aß(1-40) and Aß(1-42) on SOD concentration in cultured rat NECs. Bars are means ± SEM of four separate experiments. **p<0.001 from the respective control group.

CaspaTag Caspase-8 *In Situ* assay confirmed the activation of caspase-8 after 3 h of Aß(1-40) and Aß(1-42) treatment. As shown by fluorescence microscopy, NEC cultures treated with Aßs for 3 h displayed the presence of activated caspase-8. Moreover, the isoform, Aß(1-42), appeared to have a more toxic effect than Aß(1-40) (Fig. 2).

Trypan blue exclusion showed that, after a 3-h incubation period, both Aßs decreased NEC survival. Pretreatment with the caspase-8 specific and irreversible inhibitor, Z-IETD-FMK, significantly ($p<0.05$) protected NECs from Aß-induced cell death (Fig. 3).

In NEC cultures, both Aßs induced a highly significant ($p<0.001$) increase in SOD levels after a 3-h exposure period, Aß(1-42) being more effective than Aß(1-40) ($p<0.001$). SOD concentration levels were not affected by either Aß after a 24-h incubation period (Fig. 4).

Discussion

Aßs, the major component of senile plaques and of cerebrovascular amyloid deposits in Alzheimer disease (AD), have been shown to be cytotoxic to ECs (3,4,21-23). Specifically, amyloid fractions purified from AD brain inhibit EC replication *in vitro* and, therefore, could alter the ability of vessels to repair and regenerate after injury (24). Moreover, Aßs are directly toxic either to peripheral and cerebral vascular endothelium (3,4,25). Xu *et al* (14) confirmed the cytotoxic effect of Aßs on bovine and murine cerebral ECs. Their findings indicate that Aß-mediated EC death is an apoptotic process that is characterized by caspase activation, mitochondrial dysfunction and increased oxidative stress. We recently demonstrated that Aßs are toxic for rat NECs in a time- and concentration-dependent manner. Aßs were found to induce NEC death within 3 h and electron microscopy evidenced morphological

signs of cell degeneration after 24-h exposure. Moreover, our findings indicate that apoptosis seems to play a pivotal role in Aß-induced NEC death (5).

Our results show the activation of caspase-8 in NEC cultures treated with Aßs, as already observed in neuronal cultures (13). Particularly, Western blot analysis demonstrates the expression of the active form of caspase-8 within 3 h while, after 24 h, only the procaspase-8 form is expressed. Our findings obtained using CaspaTag assay and the selective caspase-8 inhibitor, Z-IETD-FMK, confirm those of the Western blot analysis and suggest that caspase-8 is likely to be the primary initiator caspase involved in Aß-mediated apoptosis of NECs. Our results accord well with that of Rohn *et al* (12) who, by means of *in vivo* immunohistochemical analysis, provided evidence for the activation of caspase-8 in the brain neurons of AD patients (12). Moreover, quantitative and statistically significant differences in the activation of caspase-8 in the peripheral blood mononuclear cells of AD patients have been recently observed (26). Our present findings support the possibility that Aß may induce apoptosis through the activation of caspase-8, presumably by cross-linking and activating receptors of the death-receptor family (12-14).

An important role in cell death seems to be played by oxidative stress. Thomas *et al* (3) demonstrated that Aß interacts with vascular EC to produce an ROS excess, which alters EC structure and function. In addition, free radical scavengers, such as SOD, have been shown to be protective against Aß cytotoxicity (3,28,29). We found that Aßs significantly increase SOD concentration as early as 3 h after incubation. The time-dependent increase of SOD concentration is probably correlated with production of an excess of ROS. Hence, this observation suggests a possible involvement of oxidative stress in the Aß-induced cytotoxic effect.

It seems reasonable to advance the hypothesis that the apoptotic effect induced by Aßs, at a concentration of 10^{-7} M, on rat NECs occurs through two different pathways: caspase-8 activation and increase of oxidative stress. Based on our findings and considering that both pathways are activated by Aßs after a short incubation time (3 h) and that, after a 24-h incubation period, SOD concentration is no longer affected by Aßs, we assume that the two mechanisms do not act sequentially but are probably independent of each other.

The present observations support our previous data demonstrating that the maximum cytotoxic effect of Aßs on NECs occurs within 3 h of exposure, followed by an NEC recovery at 24 h. Moreover, they are in agreement with other studies which showed that Aß(1-42) modulates the activation of glycogen synthase kinase-3ß (GSK-3ß), an enzyme involved in cell apoptosis regulation and tau abnormal phosphorylation, in a biphasic manner (29,30): Aß first activates GSK-3ß via both Ca^{2+}-dependent and Ca^{2+}-independent mechanisms and subsequently inhibits it, probably via the activation of kinases that inactivate GSK-3ß by phosphorylation.

References

1. Perlmutter LS: Microvascular pathology and vascular basement membrane components in Alzheimer's disease. Mol Neurobiol 9: 33-40, 1994.
2. Wisniewski HM, Wegiel J, Vorbrodt AW, Mazur-Kolecka B and Frackowiak J: Role of perivascular cells and monocytes in vascular amyloidosis. Ann NY Acad Sci 903: 6-18, 2000.
3. Thomas T, Thomas G, McLendon C, Sutton ET and Mullan M: ß-amyloid-mediated vasoactivity and vascular endothelial damage. Nature 380: 168-171, 1996.
4. Thomas T, McLendon C, Sutton ET and Thomas G: Cerebrovascular endothelial dysfunction mediated by beta-amyloid. Neuroreport 8: 1387-1391, 1997.
5. Folin M, Baiguera S, Tommasini M, Guidolin D, Conconi MT, De Carlo E, Nussdorfer GG and Parnigotto PP: Effects of ß-amyloid on rat neuromicrovascular endothelial cells cultured *in vitro*. Int J Mol Med 15: 929-935, 2005.
6. Yankner BA, Dawes LR, Fisher S, Villa-Komaroff L, Oster-Granite ML and Neve RL: Neurotoxicity of a fragment of the amyloid precursor associated with Alzheimer's disease. Science 25: 417-420, 1989.
7. Behl C, Davis JB, Lesley R and Schubert D: Hydrogen peroxide mediates amyloid beta protein toxicity. Cell 77: 817-827, 1994.
8. Troy CM, Rabacchi SA, Friedman WJ, Frappier TF, Brown K and Shelansky ML: Caspase-2 mediates neuronal cell death induced by ß-amyloid. J Neurosci 20: 1386-1392, 2000.
9. Loo DT, Copani A, Pike CJ, Whittemore ER, Walencewicz AJ and Cotman CW: Apoptosis is induced by beta-amyloid in cultured nervous system neurons. Proc Natl Acad Sci USA 90: 7951-7955, 1993.
10. Ashkenazi A and Dixit VM: Apoptosis control by death and decoy receptors. Curr Opin Cell Biol 11: 255-260, 1999.
11. Thornberry NA and Lazebnik Y: Caspases: enemies within. Science 281: 1312-1316, 1998.
12. Rohn TT, Head E, Nesse WH, Cotman CW and Cribbs DH: Activation of caspase-8 in Alzheimer's disease brain. Neurobiol Dis 8: 1006-1016, 2001.
13. Ivins KJ, Thornton PL, Rohn TT and Cotman CW: Neuronal apoptosis induced by ß-amyloid is mediated by caspase-8. Neurobiol Dis 6: 440-449, 1999.
14. Xu J, Chen S, Ku G, Ahmed SH, Xu J, Chen H and Hsu CY: Amyloid ß peptide-induced cerebral endothelial cell death involves mitochondrial dysfunction and caspase activation. J Cereb Blood Flow Metab 21: 702-710, 2001.
15. Folin M, Baiguera S, Conconi MT, Pati T, Grandi C, Parnigotto PP and Nussdorfer GG: The impact of risk factors of Alzheimer's disease in the Down syndrome. Int J Mol Med 11: 267-270, 2003.
16. Folin M, Baiguera S, Conconi MT, Di Liddo R, De Carlo E, Parnigotto PP and Nussdorfer GG: Apolipoprotein E as vascular risk factor in neurodegenerative dementia. Int J Mol Med 14: 609-613, 2004.
17. Abbot NJ, Hughes CCW, Revest PA and Greenwood J: Development and characterization of rat brain capillary endothelial culture: towards an *in vitro* blood-brain barrier. J Cell Sci 103: 23-27, 1992.
18. Conconi MT, Lora S, Baiguera S, Boscolo E, Scienza R, Folin M, Rebuffat P, Parnigotto PP and Nussdorfer GG: *In vitro* culture of rat neuromicrovascular endothelial cells on polymeric scaffolds. J Biomed Mat Res 71: 669-674, 2004.
19. Baiguera S, Conconi MT, Guidolin D, Mazzocchi G, Malendowicz LK, Parnigotto PP, Spinazzi R and Nussdorfer GG: Ghrelin inhibits *in vitro* angiogenic activity of rat brain microvascular endothelial cells. Int J Mol Med 14: 849-854, 2004.
20. Puget K and Michelson AM: Oxidation of luminol by xantine oxidase system in presence of carbonate anions. Photochem Photobiol 24: 499-501, 1976.
21. Blanc EM, Toborek M, Mark RJ, Hennig B and Mattson MP: Amyloid beta-peptide induces cell monolayer albumin permeability, impairs glucose transport, and induces apoptosis in vascular endothelial cells. J Neurochem 68: 1870-1881, 1997.
22. Suo Z, Fang C, Crawford F and Mullan M: Superoxide free radical and intracellular calcium mediate A beta(1-42) induced endothelial toxicity. Brain Res 762: 144-152, 1997.
23. Sutton ET, Hellermann GR and Thomas T: Beta-amyloid-induced endothelial necrosis and inhibition of nitric oxide production. Exp Cell Res 230: 368-376, 1997.
24. Grammas P, Botchlet T, Fugate R, Ball MJ and Roher AE: Alzheimer disease amyloid proteins inhibit brain endothelial cell proliferation *in vitro*. Dementia 6: 126-130, 1995.
25. Price JM, Sutton ET, Hellermann A and Thomas T: Beta-amyloid induces cerebrovascular endothelial dysfunction in the rat brain. Neurol Res 19: 534-538, 1997.
26. Tacconi S, Perri R, Balestrieri E, Grelli S, Bernardini S, Annichiarico R, Mastino A, Caltagirone C and Macchi B: Increased caspase activation in peripheral blood mononuclear cells of patients with Alzheimer's disease. Exp Neurol 19: 254-262, 2004.

27. Keller JN, Kindy MS, Holtsberg FW, St. Clair DK, Yen HC, Germeyer A, Steiner SM, Bruce-Keller AJ, Hutchins JB and Mattson MP: Mithocondrial MnSOD prevents neural apoptosis and reduces ischemic brain injury: suppression of peroxynitrite production, lipid peroxidation and mitochondrial dysfunction. J Neurosci 18: 687-697, 1998.
28. Preston JE, Hipkiss AR, Himsworth DT, Romero IA and Abbott JN: Toxic effects of beta-amyloid(25-35) on immortalised rat brain endothelial cell: protection by carnosine, homocarnosine and beta-alanine. Neurosci Lett 242: 105-108, 1998.
29. Takashima A, Noguchi K, Michel G, Mercken M, Hoshi M, Ishiguro K and Imahori K: Exposure of rat hippocampal neurons to amyloid beta peptide (25-35) induces the inactivation of phosphatidyl inositol-3 kinase and the activation of tau protein kinase I/glycogen synthase kinase-3 beta. Neurosci Lett 203: 33-36, 1996.
30. Cedazo-Minguez A, Popescu BO, Blanco-Millan JM, Akterin S, Pei JJ, Winblad B and Cowburn RF: Apolipoprotein E and beta-amyloid(1-42) regulation of glycogen synthase kinase-3beta. J Neurochem 87: 1152-1164, 2003.